

**DISTRIBUTED ADAPTATION TECHNIQUES
FOR CONNECTED VEHICLES**

Bengi Aygün

A Dissertation
Submitted to the Faculty
of the
WORCESTER POLYTECHNIC INSTITUTE
in partial fulfillment of the requirements for the
Degree of Doctor of Philosophy
in
Electrical and Computer Engineering

August 2016

APPROVED:

Professor Alexander M. Wyglinski
Primary Advisor
ECE Department
Worcester Polytechnic Institute

Professor Lifeng Lai
Committee Member
ECE Department
Worcester Polytechnic Institute

Professor K.C. Kerby-Patel
Committee Member
Engineering Department
University of Massachusetts Boston

Dr. Mate Boban
Committee Member
Huawei European Research Center

Abstract

In this PhD dissertation, we propose distributed adaptation mechanisms for connected vehicles to deal with the connectivity challenges. To understand the system behavior of the solutions for connected vehicles, we first need to characterize the operational environment. Therefore, we devised a large scale fading model for various link types, including point-to-point vehicular communications and multi-hop connected vehicles. We explored two small scale fading models to define the characteristics of multi-hop connected vehicles. Taking our research into multi-hop connected vehicles one step further, we propose selective information relaying to avoid message congestion due to redundant messages received by the relay vehicle. Results show that the proposed mechanism reduces messaging load by up to 75% without sacrificing environmental awareness.

Once we define the channel characteristics, we propose a distributed congestion control algorithm to solve the messaging overhead on the channels as the next research interest of this dissertation. We propose a combined transmit power and message rate adaptation for connected vehicles. The proposed algorithm increases the environmental awareness and achieves the application requirements by considering highly dynamic network characteristics. Both power and rate adaptation mechanisms are performed jointly to avoid one result affecting the other negatively. Results prove that the proposed algorithm can increase awareness by 20% while keeping the channel load and interference at almost the same level as well as improve the average message rate by 18%.

As the last step of this dissertation, distributed cooperative dynamic spectrum access technique is proposed to solve the channel overhead and the limited resources issues. The adaptive energy detection threshold, which is used to decide whether the channel is busy, is optimized in this work by using a computationally efficient numerical approach. Each vehicle evaluates the available channels by voting on the information received from one-hop neighbors. An interdisciplinary approach referred to as entropy-based weighting is used for defining the neighbor credibility. Once the vehicle accesses the channel, we propose a decision mechanism for channel switching that is inspired by the optimal flower selection process employed by bumblebees foraging. Experimental results show that by using the proposed distributed cooperative spectrum sensing mechanism, spectrum detection error converges to zero.

Acknowledgements

In my 4-year PhD adventure, I had a great number of individuals being my fellow travelers and helping me handle this challenging journey. I would like to express my deep appreciation and thanks to:

First, my PhD advisor Professor Alexander M. Wyglinski not only for his guidance but also for his great personality. Whenever I was stuck in my research or life, he was always there for me to advise and help. I am deeply grateful for his absolute support in any situation.

My PhD committee, Professor K.C Kerby-Patel, Professor Lifang Lai, and Doctor Mate Boban for agreeing to be my committee members, giving me key suggestions, and helping me improve my dissertation.

Doctor Mate Boban for being a fabulous supervisor during my internship in NEC Europe Labs, teaching me how to do research, opening my eyes on my research field, and being my role model. Doctor Chung-Wei Lin for being a great supervisor in my internship in Toyota InfoTech Center and making me be full of new research ideas in my future career. Joao P. Vilela and Mahni Shayganfar for helping me improve my writing skills. Tunay Cengiz for helping me have high-quality figures in my papers. The Turkish Ministry of Education for funding my PhD study.

The Wireless Innovation Laboratory (WiLab) family for their help in my research, making our lab a pleasant and sincere place in spite of its facility difficulties and impossibilities. Le Wang, Yuqing Yang, Zoe Fu Kobobel, Paulo Ferreira, Renato and Gizelle Iida, Travis Collins, Srikanth Pagadarai for listening to my complaints and bearing with my anxiety with an unbelievable patience, making me realize I have another family in this country very far from my homeland. My little prince Ricardo Iida for making me smile and reminding me nothing else matters but simple happiness. Captain-love, Wyglinskis' dog, for reminding me we do not need to have everything perfect to be happy.

Marc Green for being a window of light since the first moment I have met him, always blowing me away with his intelligence and his humble perfection, making me realize the differences of language and culture are not an obstacle to find bliss.

My family for their unconditional support and love. My mother Fatma Aygun for always giving a hand to stand me up whenever I fall down, making me realize my strengths, and teaching me to

trust myself. Asli Sakalli for being my precious friend, throughout the past and forever into the future, no matter the physical distance between us.

All the yoga I have done for helping me find my inner peace, all the books I have read for making me who I am, all the nature I have explored for inspiring me, and all the resistance against global injustice for ensuring the world is going to be a better place.

Finally, I would like to thank the acceptance of the different, because under the covers and labels, we are all one.

Contents

List of Figures	vii
List of Tables	xiii
List of Abbreviations	xiv
1 Introduction	1
1.1 Motivation	1
1.2 State-of-the-Art	5
1.3 Research Questions To Be Answered	10
1.4 Dissertation Contributions	10
1.5 Dissertation Outline	11
1.6 List of Publications	12
2 Literature Review	15
2.1 Channel Modeling on Connected Vehicles Networks	15
2.2 Distributed Congestion Control on Connected Vehicles Networks	19
2.3 Spectrum Sensing on Connected Vehicle Networks	22
2.4 Chapter Summary	25
3 Channel Characteristics and Relaying Optimization of Connected Vehicle Networks	26
3.1 Architecture Overview	27
3.2 Channel Models	29
3.2.1 Large Scale Attenuation Models	29
3.2.2 Small-Scale Fading Models: Geometry-based Channel Model for Multi-hopping Connected Vehicle Networks	36
3.2.3 Small-Scale Fading Models: Sum-of-Sinusoids Channel Model for Multi-hopping Connected Vehicle Networks	40
3.3 Derivation of Lower Bound on the Capacity for Relaying Connected Vehicles	44
3.3.1 SISO Relaying Connected Vehicles	45
3.3.2 MIMO Relaying Connected Vehicles	46
3.4 Selective Message Relaying Algorithm	47
3.4.1 Real-World Applications	49

3.4.2	Performance Metrics	50
3.4.3	Proposed Algorithm	51
3.5	Numerical Results	56
3.5.1	Simulation Results	58
3.6	Chapter Summary	66
4	Environment Aware Cooperative Distributed Congestion Control on Vehicular Network	67
4.1	Environment- and Application Context-aware Congestion Control	69
4.1.1	Design goals	69
4.1.2	Metrics	70
4.2	Proposed ECPR Algorithm	73
4.2.1	Power Adaptation for Awareness Control	74
4.2.2	Rate Adaptation	76
4.2.3	Combining power and rate control	77
4.3	Numerical Results	81
4.3.1	Simulation Results	83
4.4	Chapter Summary	92
5	Cooperative Spectrum Sensing and Bumblebee-Inspired Channel Switching Decision	94
5.1	A Voting Based Distributed Cooperative Spectrum Sensing Strategy	95
5.1.1	Connected Vehicle Environment Setup	96
5.1.2	Proposed Optimal Energy Detection	99
5.1.3	Proposed Entropy-Based Weighted Cooperative Spectrum Sensing	101
5.1.4	Proposed Switching Mechanism between Weighted and Equally Voting	104
5.2	Bumblebee-Inspired Channel Switching Decision	105
5.2.1	Why Bumblebees?	106
5.2.2	Translation Between Two Worlds	107
5.2.3	Foraging Theory	109
5.2.4	Proposed Switching Decision Mechanism	111
5.2.5	Memory Structures	112
5.3	Numerical Results	113
5.3.1	Simulation Results	114
5.4	Chapter Summary	129
6	Conclusion and Future Work	130
6.1	Research Achievements	130
6.2	Lessons Learned	131
6.3	Future Works	132
	Bibliography	134

List of Figures

1.1	Concept diagram of the connected vehicle concept employed in safety applications. Several statistics regarding safety enhancements resulting from connected vehicles is included in the diagram.	2
1.2	Interoperability on CVNs: Architecture and applications.	3
1.3	Investments to connected and autonomous vehicles.	4
1.4	General concept of autonomous and connected vehicle.	6
1.5	DSRC protocol stack and the correspond standards.	7
2.1	Taxonomy of distributed congestion control studies.	19
3.1	Large scale link attenuation greatly varies based on the link type: line-of-sight (LOS), non-line-of-sight by vehicles (NLOSv), non-line-of-sight by foliage (NLOSf), non-line-of-sight by buildings (NLOSb).	27
3.2	Network architecture of DF CVNs.	28
3.3	Locations of RSUs for selected scenarios representing different link types.	30
3.4	LOS V2I Links: OBU monotonically approaches the RSU at each time step for both measurements. Both results generated by the model and measured data have a pattern similar to free space path loss since the link type is LOS. Model vs Measurements: mean absolute error: 3.16 mean; standard deviation: 2.84.	31
3.5	NLOSv V2I links: comparison of field measurements and simulated results. OBU approaches to RSU at each time step while the heavy vehicle is driving right front of the OBU. Model vs Measurements: mean absolute error: 3.98 mean; standard deviation: 3.47.	33
3.6	NLOSf V2I links: comparison of field measurements and simulated results. Model vs Measurements: mean absolute error: 4.14 mean; standard deviation: 3.64.	34
3.7	NLOSb V2I links: comparison of field measurements and simulated results. Model vs Measurements: mean absolute error: 5.03 mean; standard deviation: 5.79.	35
3.8	System model of DF relaying vehicular communication with MIMO antenna arrays based on geometrical approach.	37
3.9	SISO relaying vehicular network architecture. The channel impulse responses, which consider both multipath propagation delay and time varying channel conditions, are defined as $h^{sr}(\tau, t)$, $h^{sd}(\tau, t)$, and $h^{rd}(\tau, t)$. The angle between scatterer and x -axis is α and the motion angle of vehicle is θ rad/s.	40

3.10	MIMO relaying vehicular network architecture. Channel impulse responses are defined as $\mathbf{H}^{sr}(\tau, t)$, $\mathbf{H}^{sd}(\tau, t)$, and $\mathbf{H}^{rd}(\tau, t)$. The distances between antennas on the top of vehicle is δ . The angle between antenna spacing and x -axis is γ	42
3.11	Autocorrelation of a CVN link. The channel is constant for 0.05 ms. Since a packet is transferred in $8 \mu s$ on DSRC architecture, capacity bounds are computed as block fading.	45
3.12	Relaying architecture. The source (blue) vehicles periodically broadcast the messages about environment status. The relay (red) vehicle receives these messages, performs the proposed algorithm, and then rebroadcasts the selected messages to the destination (green) vehicle.	48
3.13	Real-world applications that the proposed selective message relaying algorithm can be applied. S, R, and D represent the source, relay, and destination vehicles, respectively.	50
3.14	Distance between messages in the clustering space.	55
3.15	Hierarchical message clustering. The member of clusters are decided as the corresponding branches below the red line.	55
3.16	Experimental traffic data. The environment map is created using Open Street Map. The buildings in the chosen area are defined by white blocks. Vehicle traffic, illustrated as red vehicles, is created using SUMO based on the environmental map. The random traffic defined within the area is used as an input to the GEMV ² simulator. The link colors between vehicles show the link powers. If the link color is dark blue, the channel is noisy and experiencing strong fading. If the link color is red, the channel has little noise and fading.	57
3.17	Squared magnitude of the source to relay channel impulse response. Carrier frequency is 5.9 GHz; τ is excess delay; t is time variation.	59
3.18	Spreading function of the source to relay channel impulse response. τ is excess delay; ν is Doppler shift.	59
3.19	Impact of parameters to the lower bound on the capacity. (a) Lower bound depending on scatterer radii and initial distances. By increasing initial distance, the lower bound decreases. Conversely, lower bound increases by increasing scatterer radius. (b) Lower bound depending on antenna spacing (δ_s/λ) and maximum Doppler frequency ($f_{s_{max}}$). Lower bound increases by increasing antenna spacing since the effect of interference reduces. By increasing Doppler frequency, lower bound decreases since the scattering effect is increasing.	60
3.20	Comparison of lower bound on the network capacity given by two different models for both high and low speeds. SoS model has better rate performance since the excess delay (τ) is taken into account.	61
3.21	Comparison of normalized autocorrelation given by geometrical and SoS models. Although proposed SoS model and geometrical model use the same amount of resources, autocorrelation function of the SoS model matches with theoretical reference model.	62
3.22	Normalized Spreading functions for both SoS and geometrical model. The amplitude of geometrical model decreases slightly faster than the amplitude of SoS model by increasing Doppler shift.	62

3.23	Lower bound on the capacity of MIMO SoS model with LOS component and geometrical model for both cooperative and direct transmissions. For the same input parameters SoS model has higher achievable rate than geometrical model. Both models provide better performance by using relay-based approach rather than P2P transmission.	63
3.24	Message map. The points show the locations where the messages are created. The colors of messages are referred to the priorities of messages, and the messages with grey stars are selected to be rebroadcasted.	64
3.25	The number of rebroadcasted messages (rebroadcasting rate) with respect to the number of connected vehicles.	64
3.26	Processing delay with respect to the number of connected vehicles.	65
3.27	Vehicle coverage with respect to the number of connected vehicles.	65
4.1	An example of how environment shapes the awareness range. Due to the particular environment layout, with buildings surrounding the intersection, if it is using fixed transmit power, vehicle X is likely to inform the vehicles on the same road of its existence, with a limited awareness of vehicles on the perpendicular road, up until X is in the intersection, at which point vehicles on both roads are likely to be aware of it. However, for active safety applications, awareness of vehicles on perpendicular road is more valuable than that on the same road, since the drivers of those vehicles cannot see vehicle X. Thus, for most CVN applications, it is assumed that the target awareness/communication range is a circular shape (or as circular as possible) of certain radius. Achieving such range in different environments requires power control. Lower part of the figure shows an idealized transmit power profile to adapt to the intersection environment for vehicle X as it travels through the intersection.	71
4.2	Depending on the application context, which includes the speed of the vehicle, traffic context and the type of currently active application, vehicles can have different target awareness ranges. For example, vehicle Y can be going at a lower speed than vehicle Z, in which case it might require smaller awareness range. Similarly, vehicle Z might be executing a safety-critical application (e.g., emergency vehicle notification), in which case it requires larger awareness range	72
4.3	Measurements of NAR in Tampere, Finland. Measurements in both environments were collected using in the same measurement run based on the same vehicles, fixed transmit power, and 10 cooperative messages sent per second.	72
4.4	Regions used for highway and urban simulations (circled) on the topology of Newcastle, UK. Both regions have an area of approximately $1km^2$. White outlines represent buildings that were incorporated in simulations for realistic propagation modeling.	81
4.5	Target Awareness 85%, Target Awareness Distance = 150m, default Tx Power = 10 dBm. Urban Scenario. Power-only algorithm achieves awareness (NAR) comparable to ECPR; however, due to it not taking channel load (CBR) into account, it exceeds the target CBR.	84

4.6	Target Awareness 85%, Target Awareness Distance = 50m, default Tx Power = 23 dBm. Urban Scenario. In this application context, ECPR can reduce the average power while not jeopardizing awareness. This allows for increase of overall throughput in the system as visible through increased average rate, while at the same time keeping the average CBR lower than that of rate-only algorithm. . . .	85
4.7	Randomly selected 100 vehicles for Target Awareness Distance = 50 m, default Tx Power = 23 dBm.	86
4.8	The number of vehicles that can achieve the target awareness. The number of vehicles that can reach awareness target, 85%, and rate target, 10 Hz, for rate-only algorithm and ECPR. As a result of adaptation on transmission power on ECPR, frequency reuse is able to be used more actively, more vehicles reach the target message rate, and reaches target awareness more stably than rate-only adaptation.	87
4.9	Average transmit Power and beacon rate for highway and urban environments. The relationship between average message rate and average transmit power is reversely proportional on each environment.	88
4.10	Average difference between target and achieved message rate for highway and urban environments. Test 1 and 3 target the maximum message rate, the difference between target and current rate is higher than in Test 2 and Test 4. The target rate is on average less than maximum rate, thus the difference of achieved to target rate is less.	89
4.11	Standard deviation and mean of CBRs in highway and urban environments. The threshold CBR value is set as 0.6 with ± 0.05 tolerance. In urban scenario, average CBR is higher than in the highway scenario. The reason is that each ego node needs to communicate with a larger number of neighboring vehicles in urban environment than highway due to the vehicles being concentrated around intersections; combined with higher power to achieve the same awareness, this results in higher overall CBR.	90
4.12	Target Awareness 85%, Target Awareness Distance = 50m, default Tx Power = 23 dBm. Urban Scenario with MAC collisions.	91
5.1	Proposed concept diagram of connected vehicle environment: Each vehicle detects the available channels individually and shares the channel information with the one-hop neighbors in the next control message. Each vehicle decides the available channel list by using the information received from neighbors, if available.	97
5.2	The behavior of entropy function. Note how the Uncertainty converges to zero if the probability of random event occurring gets closer to the edges and at the peak value for $p = 0.5$	102
5.3	Flow chart of the cooperative voting algorithm at the receiver. If the vehicle receives an available channels list from nearby neighbor(s), it checks the number of neighbors. In case the number of vehicles is less than the threshold, it computes the weight functions of all the neighbors and itself when voting on the channel status. The channel that has the largest number of votes is chosen for the data transmission. In case the number of vehicles exceeds the threshold, an equally-weighted voting mechanism is employed. If the vehicle does not receive any available channel information from its neighbors, it trusts its own detection result.	105

5.4	Representation of mixed floral array used to assay learning, memory, and decision-making in foragers. Various patch colors present the nectar levels of flowers. Bumblebee uses the nectar levels to decide whether fly to the another flower with higher nectar level although it will spend energy to fly there.	109
5.5	The artificial vehicle traffic data in Worcester, MA for numerical results.	113
5.6	Probability of incorrect detection by changing the SNR and detection threshold. For each SNR value, there is only one minimum point since the function is convex.	115
5.7	Probability of incorrect detection by the optimizing detection threshold. Comparing to a fixed threshold, the probability of incorrect detection is decreased by approximately 20%. Both iterative methods give the correct probability values.	116
5.8	Optimum energy threshold for different SNR values. Both the Newton's method (as a reference numerical method) and the proposed Secant method are employed. The Secant method provides an accurate threshold value during a shorter process time.	116
5.9	Convergence time of the iterative methods the optimum threshold is detected in less time relative to the coherence time. Therefore, the proposed approach would be suitable for time varying CVN operating conditions.	117
5.10	Probability of incorrect detection for different fitness functions for spectrum detection at the individual vehicle. If the fitness function is defined with respect to only probability of missed detection to find the optimum energy threshold, the chosen threshold may not be optimum for the probability of false detection, or vice versa. On the other hand, the proposed mechanism finds the optimum energy detection threshold by considering both probability of missed and false detection. Therefore, the incorrect detection is minimized.	117
5.11	Receiver operating characteristics (ROC) curves for different numbers of attendees that join the cooperative channel sensing network. Notice how an increase in the number of neighbors provide a more robust sensing environment.	118
5.12	Comparison of only individual sensing, equally-weighted voting mechanism, and entropy-based weighted voting. Sparse traffic conditions of 150 vehicles were employed within the experiment region. Each vehicle senses the status of 10 channels at each time step.	119
5.13	Comparison of only individual sensing, equally voting mechanism, and entropy-based weighted voting. High dense traffic conditions of 1200 vehicles were employed within the selected region. Each vehicles sense the status of 20 channels at each time step.	120
5.14	The effect of the threshold on the number of neighbors in sparse traffic conditions. The switching scheme decides on using the entropy-based weighted voting if the number of neighbors are less than the neighbor threshold. Otherwise, equally-weighted voting is performed.	120
5.15	The effect of the threshold of number on the neighbors in dense traffic conditions. The cognitive scheme decides on using the entropy-based weighted voting if the number of neighbors are less than the threshold. Otherwise, equally-weighted voting is performed.	121
5.16	Detection performance changes with transmit power for sparse traffic conditions.	122

5.17	Normalized squared magnitude of the channel impulse response: t refers to the time variation on a channel. Three representative channels are visualized to indicate the environment changes on time.	124
5.18	Sparse highway traffic: The best number of vehicles that can access the best possible channel at the corresponding time step.	126
5.19	Sparse highway traffic: Switching cost at the corresponding time step.	126
5.20	Dense urban traffic: The number of vehicles that can access the best possible channel at the corresponding time step.	127
5.21	Dense urban traffic: Switching cost at the corresponding time step.	127
5.22	Sparse highway traffic: Benefit / Cost Rate for various memory lengths. For sparse highway traffic, 10 <i>sec</i> memory length provides the optimum point of trade-off while 5 <i>sec</i> is the best for dense urban traffic.	128
5.23	Benchmark on computation time: the proposed approach, optimal modified deflection coefficient (OPT-MDC), parallel artificial bee colony (PABC), genetic algorithms (GA), partial swarm optimization (PSO), memory enable genetic algorithms (MEGA). Since the proposed switching mechanism is based on individual decision process and uses the energy values in the memory without performing any complicated mathematical operation, the proposed approach possesses a low computation time.	128

List of Tables

1.1	OFDM Parameters in DSRC	8
1.2	Data Rates Options in DSRC	8
2.1	Spectrum Sensing Techniques in the Current State-of-the-Art.	23
3.1	The parameters that define channel coefficients based on angles and distances	39
3.2	A set of K received messages.	52
3.3	A set of K received messages after preprocessing.	54
3.4	System Parameter Setup.	58
4.1	Parameters used in the proposed algorithm	77
4.2	States that affect transmit power adaptation	80
4.3	System Parameters Setup for the Simulations.	82
4.4	Tests defined with different target awareness range and message rate combinations to stress-test ECPR.	83
4.5	Average percentage of potentially hidden nodes for ECPR and rate-only (LIMERIC) algorithm.	92
5.1	Vehicular Density for Traffic Classes.	104
5.2	Several Definitions in Connected Vehicular Communications and Their Equivalent Definitions in Bumblebees.	108
5.3	System Parameter Setup.	114
5.4	Computational complexity analysis based on the number of mathematical operations at each voting scheme.Total number of mathematical operations that are noted at the last two lines show that equally-weighted voting has relatively lower complexity than entropy-based weighted voting.	124
5.5	Caption for LOF	124

List of Abbreviations

AF	Amplify-and-Forward
AIMD	Additive Increase Multiplicative Decrease Method
AWGN	Additive White Gaussian Noise
BPSK	Binary Phase Shift Keying
BR	Beacon Rate
BSMs	Basic Safety Messages
CAMs	Cooperative Awareness Messages
CARS	Context-Aware Rate Selection
CBR	Channel Busy Ratio
CSI	Channel State Information
CVNs	Connected Vehicles Networks
DCC	Decentralized Congestion Control
DF	Decode-and-Forward
DSRC	Dedicated Short-Range Communications
DTV	Digital Television
ECPR	Environment- and Context-aware Combined Power and Rate
ECU	Electronic Control Unit
eNAR	Estimated Neighborhood Awareness Ratio
ETSI	European Telecommunications Standards Institute
FABRIC	Fair Adaptive Beaconing Rate for Inter-vehicular Communications
FCC	the United States Federal Communication Commission
FEC	Forward Error Correction

FHWA	Federal Highway Administration
GEMV	Geometry-Based Efficient Propagation Model for Vehicles
GPS	Global Positioning System
IPv6	Internet Protocol version 6
IETF	Internet Engineering Task Force
ITS	Intelligent Transportation System
LIMERIC	Linear Message Rate Integrated Control
LOS	Line-of-Sight
MAC	Medium Access Control Layer
MIMO	Multi-Input-Multi-Output
NAR	Neighborhood Awareness Ratio
NHTSA	U.S. Department of Transportation National Highway Traffic Safety Administration
NLOS	Non Line-of-Sight
OFDM	Orthogonal Frequency Division Multiplexing
OPRAM	Opportunistic-Driven Adaptive Radio Resource Management
OSM	Open Street Map
P2P	Point-to-Point
PHY	Physical Layer
PLCP	Physical Layer Convergence Procedure
PMD	Physical Medium Dependent
PLE	Path Loss Exponent
PULSAR	Periodically Updated Load Sensitive Adaptive Rate
PU	Primary Users
QAM	Quadrature Amplitude Modulation
QPSK	Quadrature Phase Shift Keying
QoS	Quality of Service
RFCs	Request for Comments
RNAR	Ratio of Neighbors Above Range
ROC	Receiver Operating Characteristics

RSUs	Road Side Units
SI	Self Interference
SISO	Single-Input-Single-Output
SNR	Signal-to-Noise Ratio
SoS	Sum-of-Sinusoids
SUMO	Simulation of Urban Mobility
SUs	Secondary Users
TCP	Transmission Control Protocol
UDP	User Datagram Protocol
V2X	Vehicle-to-X
V2I	Vehicle-to-Infrastructure
V2V	Vehicle-to-Vehicle
VDSA	Vehicular Dynamic Spectrum Access
WAVE	Wireless Access in Vehicular Environments
WSMP	WAVE Short Message Protocol

Chapter 1

Introduction

1.1 Motivation

Connected vehicles networks (CVNs) describe the connectivity of vehicles and roadside access points or base stations within a given vicinity. In February 2014, the National Highway Traffic Safety Administration (NHTSA) announced that Intelligent Transportation Systems (ITS), including connected vehicles technology, will be required in all cars by 2019 [1]. To serve this purpose, the United States Federal Communication Commission (FCC) reserved 75 MHz of spectrum in the 5.9 GHz band for dedicated short-range communications (DSRC) for CVNs [2]. Potential applications of CVNs are based upon having reliable connectivity over the dedicated spectrum band. Recent wireless research activities enable the realization of CVNs with the help of novel and reliable solutions.

There are numerous benefits of CVNs [3]. First, the communication links between source and destination are more robust although the link can potentially be non line-of-sight (NLOS). Second, the information sharing increases environmental awareness and enables applications, designed to improve traffic safety and efficiency. Third, the cost of positioning and communication hardware is significantly less than the equivalent autonomous sensing equipment needed to cover the 360-degree envelope around the vehicle. Finally, communications allow vehicles to coordinate maneuvers for safety goals as well as reduce the severity of the maneuvers required by each vehicle to avoid a collision as shown in Figure 1.1 (diagram adapted from [4]).

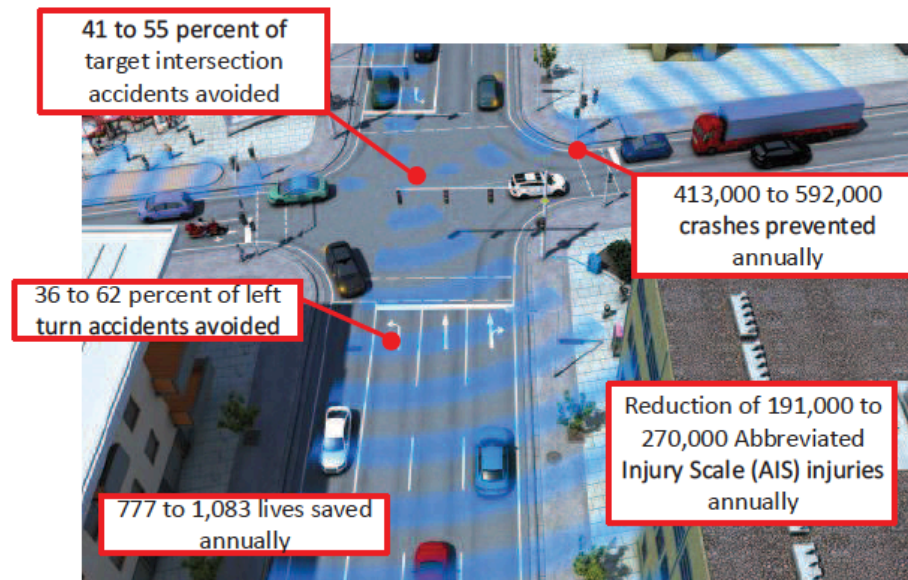


Figure 1.1: Concept diagram of the connected vehicle concept employed in safety applications. Several statistics regarding safety enhancements resulting from connected vehicles is included in the diagram.

CVN applications are summarized in two main categories: safety and mobility applications [5]. Mobility and traffic efficiency applications include transmitting information about the road coefficient of friction, road weather conditions, parking management and payment solutions, enhanced route guidance and navigation, green light optimal speed advisory, and lane merging assistants [4]. For safety-related applications, NHTSA identified eight high potential applications [6]: traffic signal violation warning, curve speed warning, emergency electronic brake light, pre-crash sensing, cooperative forward collision warning, left turn assistant, lane-change warning, and stop sign movement assistant. NHTSA reported that CVN systems would help drivers avoid 41 – 55% of intersection crashes and 36 – 62% of left turn crashes [5]. NHTSA highlighted the significance of connected vehicles in technical report as [7]:

“ Connected vehicle safety applications are designed to increase situational awareness and reduce or eliminate crashes through V2V and V2I data transmission that supports: driver advisories, driver warnings, and vehicle and/or infrastructure controls. These technologies may potentially address up to 82 percent of crash scenarios with unimpaired drivers, preventing tens of thousands of automobile crashes every year. ”

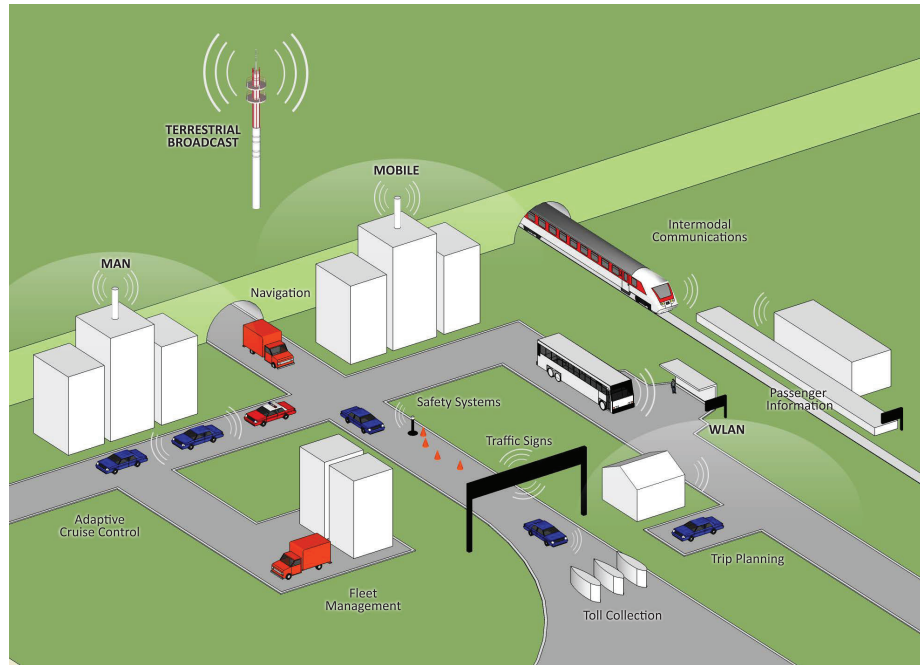


Figure 1.2: Interoperability on CVNs: Architecture and applications.

CVNs, also referred as Vehicle-to-X (V2X) communications as shown in Figure 1.2 [8], have slightly different dynamics based on the transmitter and receiver types. In Vehicle-to-infrastructure (V2I) architectures, messages are transmitted between vehicles and roadside units (RSUs) located on nearby arterial road intersections or highway on-ramps. In Vehicle-to-vehicle (V2V) communication, messages are transmitted between neighboring vehicles. The information dissemination can be point-to-point (P2P) or multi-hop (relaying) messaging scenarios in which vehicles communicate directly with other vehicles or through intermediary vehicles, respectively. In the other type of V2X links, messages are transmitted between vehicles and various receivers such as vehicle-to-pedestrians, vehicle-to-bicycle, and vehicle-to-home, vehicle-to-device [9–11].

The US Federal Highway Administration (FHWA) released the 2015 FHWA Vehicle to Infrastructure Deployment Guidance and Products", a document assisting operators in adapting traffic signals and other roadside devices so that they are capable of communicating with the new connected vehicles [12]. V2I systems include RSUs, which collect data about the vehicular activity and inform nearby vehicles, signal phase and timing traffic signal enabled traffic signal controllers,

Organization	Research Investment	Research Field
 Obama Administration	\$3.9 billion	Driverless Cars on US
 General Motors	\$1 billion	Autonomous Cars
 Mobileye	\$9 billion	Connected Vehicles
 Kia Motors	\$2 billion	Autonomous Driving
 Toyota Motor Corporation	\$1 billion	Self-driving Cars

Figure 1.3: Investments to connected and autonomous vehicles.

which control the synchronization of the intelligent traffic lights with the current traffic situation, and traffic management centers. V2I communication is envisioned as a key building block for enabling safety and traffic efficiency applications in Europe as well [13, 14]. DSRC infrastructures enable anticipatory and safe driving, as drivers are informed about the current traffic situation and danger zones. Furthermore, traffic centers receive precise and comprehensive information on the traffic situation from vehicles. In this way, it is possible to control the traffic flow more intelligently, efficiently, and quickly, resulting in an improved flow of traffic. As a result, transportation systems can potentially have less accidents, improve the use of the road network, experience less vehicle traffic congestion, and reduce the production of CO_2 emissions.

V2V networks are more challenging to design than V2I architectures since the connection architecture is a decentralized mesh network instead of being supported by a centralized control unit. This unique topology has the benefit that vehicles can provide to each other the most updated situation, thereby increasing the current environmental awareness. The vehicle's adaptation mechanisms can thus use this updated information to provide reliable decisions. This is especially true for traffic safety applications and information security protocols, which require the most current situational information. V2V communications provide the input data for substantial solutions

to these time-critical requirements. The recent fatal accident of Tesla autopilot system, that the Tesla driver and a truck could not have detected each other and crashed while the advanced driving assistant system was active, urges the V2V systems to improve environmental awareness particularly when the sensors cannot detect the other vehicles due to the obstacles [15].

The motivation for connected vehicle networks, which is explained above, makes research and development in this industry very active. The leading companies of the automotive industry invest substantial amount of resources for CVN research as shown in Figure 1.3 [16–19]. For example, Google and Ford are performing actual road trials of autonomous vehicles while Volvo and Honda are working on increasing vehicular awareness by providing robust connectivity in vehicular environments [20]. Moreover, Toyota recently announced that it is investing \$50 million to design and produce artificial intelligence within vehicular networks [21]. A quote of Tim Cook, Apple CEO, from an interview on the Apple Car summarizes the enthusiasm on the ITS world [22]:

“ – *Tim Cook, Apple CEO: Auto industry is at an inflection point for massive change. Not just an evolutionary change.* ”

1.2 State-of-the-Art

CVNs improve traffic safety by preventing mistakes caused by human drivers. In order to enable information sharing, connected vehicles use periodic broadcast message exchanges to make vehicles aware of their surrounding environments. Those are referred to as Basic Safety Messages (BSMs) in the United States and Cooperative Awareness Messages (CAMs) in Europe.

Vehicular communications consist of two types of messages: safety messages and certificate exchange messages. The safety messages are used to support the safety applications, and the certificate exchange messages ensure that the safety messages are from a trusted source. The safety messages include information about the vehicles' behavior such as the vehicles' Global Positioning System (GPS) location, speed, transmission power, predicted path, lateral and vertical acceleration, and yaw rate. The messages are time-stamped so the receiving vehicle knows when the message was sent. This information can be used by other vehicles for a variety of crash avoidance applications [5].

The intra-vehicle components, which are categorized in three main blocks, are shown in Fig-

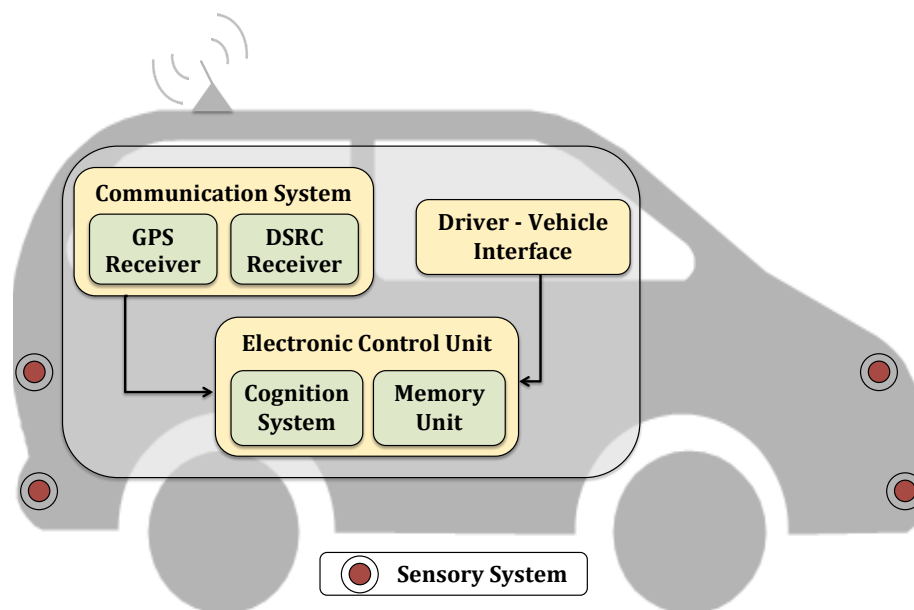


Figure 1.4: General concept of autonomous and connected vehicle.

Figure 1.4. The internal vehicle components include two DSRC radios, whose standardization is still under development [5]. According to current vision, the internal vehicle components include two DSRC radios. One of the radios can potentially be assigned handling safety messages, or both radios could be used to support a multi-channel hopping algorithm. These radios provide information sharing with other ITS platforms in order to increase awareness on the roads. Another important component for enabling cognition in vehicles is GPS receiver for gathering position and timekeeping information. The onboard computer uses this information with the data generated from its sensors, such as heading, speed, and acceleration, in order to provide information to intra- and inter- vehicle intelligence systems. The safety electronic control unit (ECU) prepares BSMs to periodically broadcast in order to run safety applications. The memory unit satisfies the needs of the data acquisition system, records the historical data from itself as well as other vehicles, and stores security certificates. Finally, a driver-vehicle interface provides a mechanism for issuing warnings to the driver. Such warnings could be audible, visual, or haptic, e.g., any type of audio-visual alarm, tightening of the seat belt, or vibrating the driver's seat.

The main topology of the connected vehicles standard is released besides the standardiza-

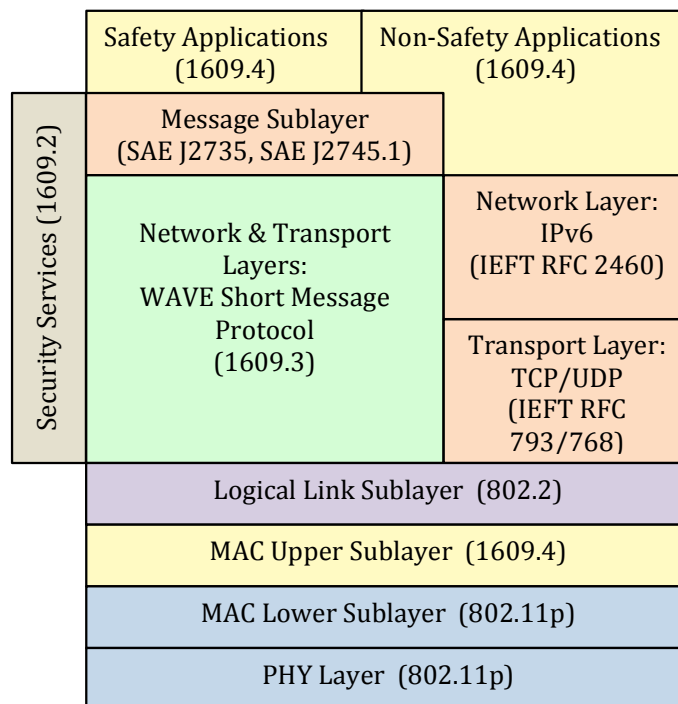


Figure 1.5: DSRC protocol stack and the correspond standards.

tion activities are not finalized yet. The wireless access in vehicular environments (WAVE) protocol stack, which is defined in the IEEE 1609 standards, describes the higher layers while IEEE 802.11p [23] explains the physical (PHY) and low level medium access control (MAC) layers. In Figure 1.5, the protocol stack for CVNs and corresponding standard of each layer are illustrated [24]. IEEE 1609 standards are specified for the tasks as follows: 1609.4 for Channel Switching [25], 1609.3 for Network Services and WAVE short message protocol (WSMP) [26], and 1609.2 for Security Services [27]. DSRC is capable of using all internet protocols for the Network and Transport layers, *i.e.*, Internet Protocol version 6 (IPv6), User Datagram Protocol (UDP) and Transmission Control Protocol (TCP). These protocols are defined by the Internet Engineering Task Force (IETF) Request for Comments (RFCs). Single-hop messages, *e.g.*, collision avoidance messages, use WSMP since it is bandwidth-efficient, and multi-hop messages use IPv6 for its routing capability. At the top of the stack, the SAE J2735 Message Set Dictionary standard specifies a set of message formats that support a variety of CVNs applications [24].

Table 1.1: OFDM Parameters in DSRC

Parameter	Value
Number of data subcarriers	48
Number of pilot subcarriers	4
Subcarrier frequency spacing	156.25 KHz
Guard interval	1.6 μ sec
Symbol interval	8 μ sec

Table 1.2: Data Rates Options in DSRC

Modulation Technique	Coded Bit Rate (Mbps)	Coding Rate	Data Rate (Mbps)	Data Bits per OFDM Symbol
BPSK	6	1/2	3	24
BPSK	6	3/4	4.5	36
QPSK	12	1/2	6	48
QPSK	12	3/4	9	72
16-QAM	24	1/2	12	96
16-QAM	24	3/4	18	144
64-QAM	36	2/3	24	192
64-QAM	36	3/4	27	216

The PHY layer is divided into two layers: the physical medium dependent (PMD) sublayer, which directly interfaces with the wireless medium, and the physical layer convergence procedure (PLCP) sublayer, which converts the MAC frames and PMD messages between each other. PMD uses orthogonal frequency division multiplexing (OFDM) with a 10 MHz bandwidth, with its specifications are shown in Table 1.1 [24]. Four modulation techniques are available for use on each subcarrier, which correspond to a different number of bits encoded per subcarrier symbol. Forward error correction (FEC) coding is applied to the user bits, which reduces the effective user bit rate but also improves the probability of successful decoding. Eight combinations of these specifications are shown in Table 1.2 [24].

There exists several technical challenges when operating wireless networks within a vehicular environment in spite of the advantages associated with CVNs. The major challenge is the highly time-varying characteristics of the vehicle environment, which significantly impacts network reliability and efficiency [28, 29]. DSRC offers a convenient solution to this highly dynamic architecture, whereas cellular networks may possess latency and time synchronization issues due to the large coverage area and how the infrastructure is configured. Other technical challenges associated with CVNs include the following [3]:

- Dynamic vehicular environments include obstacles that vary with time, a changing number of vehicles, and varying road topology;
- Relative motion due to neighbor vehicles will yield Doppler spreads across the frequency spectrum, which makes it more difficult to lock onto the target center frequency;
- Multipath fading due to the relative motion of the roadside structures is much more dynamic within a CVN operating environment relative to a static wireless network;
- Error by human drivers with unexpected situations make predefined decision mechanisms insufficient;
- Decision making mechanisms in ITS are not delay tolerant since the network environment changes rapidly;
- Frequently broadcasting between connected vehicles cause a messaging overhead on the processing unit at each vehicle;
- Diverse interference caused by the other networks decreases vehicles' communication efficiency;
- Each vehicle can have its own target awareness distance and target message rate based on application context and environment;
- The limited capability on information sharing, *i.e.*, process time and bandwidth capacity limitations, makes network organization challenging.

1.3 Research Questions To Be Answered

The main objective of this dissertation is to develop practical decision and adaptation techniques to make the V2X communications reliable. The proposed solutions include realistic assumptions and are time-efficient in order to handle the dynamic characteristics of connected vehicle networks. Therefore, several research questions must be answered, namely:

- What are the characteristics of the connected vehicle channels? What are the limitations and strengths of point-to-point and multi-hop V2X links?
- Is it necessary to rebroadcast all information, received from any source, with other vehicles?
- How can we increase the environmental awareness and achieve the context requirements by adjusting transmission parameters?
- How can we realistically solve the spectrum scarcity issue by considering the connected vehicle dynamics?

1.4 Dissertation Contributions

Compared to the current state-of-the-art, this dissertation presents several novel and practical adaptive solutions for connected vehicles. The contributions of this dissertation are the following:

- **Channel models, limitations, and optimization of message relaying on multi-hopping connected vehicles (Chapter 3):** Modeled of large and small scale fading channels for CVN systems; derived the capacity limitations for both single-input-single-output (SISO) and multi-input-multi-output (MIMO) networks; proposed a selective information relaying mechanism for multi-hop relaying vehicles. Compared to the current state-of-the-art, the proposed mechanism decreases the message congestion due to the redundant messages received by relay vehicles without any assumption on network architecture.
- **Distributed congestion control for connected vehicles (Chapter 4):** Proposed a combined transmission power and rate adaptation algorithm for decentralized V2V communications. Although the existing literature possesses techniques that separately adapts the

transmission power and rate, the proposed algorithm jointly controls the message rate and transmission power as well as achieves the target awareness rate, target message rate, and target awareness distance requirements of each vehicle for any environment and context.

- **Distributed cooperative channel sensing mechanism for connected vehicles (Chapter 5):** Proposed an adaptive optimization of the energy detection threshold by considering process time limits; a cooperative channel access mechanism to decide the available channels for unlicensed users based on a novel voting scheme. The optimum point of the trade-off between the computational cost and robust spectrum sensing is achieved. The proposed mechanism outperforms existing works by converging spectrum detection error to zero in any environmental condition without violating process time constraints.
- **Bumblebee behavior from foraging theory to channel switching decision for connected vehicles (Chapter 5):** Proposed a distributed adaptive mechanism to decide if the unlicensed user should stay in the same channel or switch to better channel; implemented memory structure to obtain the optimum point between switching to the better quality channel and the switching cost. While the current-state-of-the-art does not consider the switching cost, the proposed switching decision mechanism increases the *Benefit/Cost* rate.

1.5 Dissertation Outline

The rest of this dissertation is organized as follows:

Chapter 2 provides an extensive literature survey on connected vehicles. Existing works for channel models for vehicular communications are explained. A comprehensive review of existing distributed congestion control mechanisms is discussed. Finally, dynamic spectrum access (DSA) mechanisms for vehicular communications are presented.

Chapter 3 starts with introducing the large and small scale fading channel models of CVN systems. Lower bound on the capacity is studied for multi-hopping CVNs by using SISO and MIMO antenna sets. Lastly, a selective message relaying mechanism is proposed to avoid relaying the redundant messages and decrease messaging load.

In Chapter 4, a novel algorithm is presented for decentralized congestion control (DCC) on V2V systems. The proposed combined rate and power control algorithm efficiently achieves the target awareness and rate requirements given by the application context in varying propagation environments. The proposed algorithm adapts the transmit power to reach the target awareness range while controlling the channel load by adjusting the rate and power according to the current channel load, awareness range, and rate information.

In Chapter 5, a novel distributed cooperative DSA technique for connected vehicles is proposed. The adaptive energy detection threshold, which is used to decide whether the channel is busy, is optimized in this work by using a computationally efficient numerical approach. Each vehicle evaluates the available channels by voting on the information received from one-hop neighbors, where the credibility of each neighbor is weighted during the voting process. An interdisciplinary approach referred to as entropy-based weighting is used for defining the neighbor as well as the vehicle's own credibility. The voting mechanism is switched between the proposed voting mechanism and the traditional voting approach obtained from the current-state-of-the-art in order to maintain a balance between the computational cost/latency and robust spectrum sensing. As the last block of channel access strategy, we propose an individual decision mechanism that decides whether to switch to a better quality channel while accepting a switching cost or stay in the same channel assuming it is already of sufficient quality. To enable vehicles to effectively meet this challenge, we devised a bumblebee-inspired decision-making algorithm. In proposed approach, channel energy information is stored and updated in memory to estimate qualities of channel options and then weighed against switch costs to determine optimal (benefit/cost) channel selection. We found that an individual adaptive switching decision mechanism provides shorter computation times and obtains an optimal point between switching benefit and cost.

1.6 List of Publications

Over the past several years, the following publications resulting from this dissertation research have appeared or will appear in the open literature:

List of Patents

[P1] **B. Aygun**, M. Boban. ECPR: Environment-aware Combined Power and Rate Distributed

Congestion Control for Vehicular Communication, *European Patent Office*, NLE-581-14 (Filed), 2014

List of Journal Papers

- [J6] **B. Aygun**, M. Boban, and A.M. Wyglinski. ECPR: Environment- and Context-aware Combined Power and Rate Distributed Congestion Control for Vehicular Communications, *Elsevier Computer Communications*, Accepted, May 2016 [30]
- [J5] **B. Aygun**, Robert J. Gegear Elizabeth F. Ryder, and Alexander M. Wyglinski. Adaptive Behavioral Responses for Dynamic Spectrum Access-Based Connected Vehicle Networks, *IEEE Vehicular Technology Magazine*, Under Review, May 2016
- [J4] **B. Aygun**, M. Shayganfar, and A.M. Wyglinski. Connected Vehicles & Cognition: Technologies That Can Save Lives, *IEEE Vehicular Technology Magazine*, Under Review, April 2016
- [J3] **B. Aygun** and A.M. Wyglinski. A Voting Based Distributed Cooperative Spectrum Sensing Strategy for Connected Vehicles, *IEEE Transactions on Vehicular Technology*, Under 2nd Review, May 2016
- [J2] D. Pu. **B. Aygun**, and A.M. Wyglinski. Primary User Emulation Detection Algorithm Based on Distributed Sensor Networks, *Springer International Journal of Wireless Information Networks*, Under Review, February 2016
- [J1] **B. Aygun**, Robert J. Gegear, Elizabeth F. Ryder, and Alexander M. Wyglinski. Adaptive Behavioral Responses for Dynamic Spectrum Access-Based Connected Vehicle Networks, *IEEE COMSOC Technical Committee on Cognitive Networks*, Vol. 1, No. 1, pp. 45 - 48, December 2015 [31]

List of Conference Papers

- [C5] **B. Aygun**, CW. Lin, S. Shiraishi, and A.M. Wyglinski. Selective Message Relaying for Multi-Hopping Vehicular Networks, *IEEE Vehicular Networking Conference (VNC)*, Under Preparation, Aug. 2016

- [C4] **B. Aygun**, M. Boban, J.P. Vilela, and A.M. Wyglinski. Geometry-Based Propagation Modeling and Simulation of Vehicle-to-Infrastructure Links, *IEEE 83rd Vehicular Technology Conference*, pp. 1-5, May 2016
- [C3] **B. Aygun**, M. El Gamal, and A.M. Wyglinski. Performance Analysis for High-Velocity Connected Vehicles, *IEEE 81st Vehicular Technology Conference*, pp. 1-5, May 2015 [32]
- [C2] **B. Aygun** and A.M. Wyglinski. Channel Modeling of Decode-and-Forward Relaying VANETs, *IEEE 80th Vehicular Technology Conference*, pp. 1-5, Sept. 2014 [33]
- [C1] **B. Aygun**, A. Soysal, and A.M. Wyglinski. Short Paper: Performance Analysis of MIMO-Based Decode-and-Forward Relaying VANETs, *IEEE Vehicular Networking Conference (VNC)*, pp. 1-4, 2013 [34]

My role with the aforementioned publications except for [P1] and [J2] were to define the research problems, devise the solutions, and implement the computer simulations in order to run the experiments. My role with respect to [J2] was to document and organize the publication, while my contribution to publication [P1] was filed as 20% inventor.

Chapter 2

Literature Review

This chapter provides an overview on several subjects that are relevant to this dissertation. In Section 2.1, we present the research efforts on channel modeling CVNs. We discuss both the analysis of V2V channel models and V2I link models. By realizing the benefits of multi-hopping communications, we extend the review of P2P channel models to multi-hop channel models. Finally, we describe existing multi-hopping strategies to make the relaying operation more efficient. In Section 2.2, we explain congestion control approaches as a solution to overhead on channel utilization load. We classified congestion control mechanisms in three main titles and analyzed the existing works under these categories. In Section 2.3, we present existing solutions for handling the current spectrum scarcity issue. Since the understanding of system behavior is the first step of conducting research, we first denote the field experiments that demonstrate the system behavior of vehicular dynamic spectrum access (VDSA). Then, we discussed the cognitive learning approaches implemented for VDSA for different system behaviors. Finally, we narrow down the literature review to focus on cognitive learning approaches for cognitive spectrum access techniques to give a detail survey on one of the main focus on this dissertation.

2.1 Channel Modeling on Connected Vehicles Networks

Channel characterization is a fundamental step for CVNs since all design approaches are based on knowing the channel behavior. While the modeling of V2V channels has been a steadily growing research interest over the past several years, V2I channel modeling has been increasing over

the past couple of years since V2I systems are essential for reliable ITS connectivity [28, 35]. V2V and V2I communications have multipath propagation with the characteristics of fading channels. One frequently used small scale channel modeling approach for multipath propagation is Jakes model, which defines the channel as a Rayleigh fading sum-of-sinusoids (SoS) for non line-of-sight (NLOS) scenarios [36]. Since Jakes model is a deterministic approach, it has some difficulty in creating multiple uncorrelated fading waveforms for frequency-selective fading channels and MIMO channels. Hence, this model has been extended to statistical models for Rayleigh fading in [37–40] and Rician fading in [41, 42].

While small scale fading defines the channel impulse response behavior, large scale fading models provide the loss between transmit and received power values. In [43], large scale channel fading characteristics of V2V communications are mathematically modeled for LOS and NLOS links due to the different obstacles on the links. In [44], various propagation environments are measured for MIMO antennas, and the parameter values that should be used in mathematically models are provided. In [45], the accuracy of proposed models are proved by real-world measurements and the effect of the adjacent lane traffic on the vehicular channel is discovered empirically.

V2I links differ from V2V links, in terms of antenna height, relative speed, and the scatterer density at the infrastructure end of the link, resulting in significantly different communication performance [46]. It is assumed that the infrastructure component of the link will be located near the roads (e.g., at intersections in cities or on gantries on highways) with antennas configured for DSRC. These characteristics distinguish V2I communication from other mobile-to-base station (“cellular”) communication, where the base station is located farther away from the road, typically mounted on the tops of buildings or hills. As such, V2I links do not have the same characteristics as the well studied mobile-to-base station links used in cellular networks, for which models are readily available [47].

Field tests are crucial for the study and evaluation of V2I communications. Gozalvez *et al.* [48] performed comprehensive measurements for different antenna heights, vehicle driving directions, and locations in Bologna, Italy. Measurement results on highways involving an infrastructure near the road such as Roadside Units (RSUs) and onboard units (OBUs) inside of cars with omnidirectional antennas show that environment conditions significantly affect communication performance [49]. Shivaldova *et al.* [50] evaluate the performance of omnidirectional antennas, as

well as different types of directional antennas, and showed that directional antennas possess better performance than omnidirectional antennas if the RSUs with directional antennas are deployed properly so as to not cause interference. The propagation behavior of V2I communications in a highway scenario was measured by Maier *et al.* [51] for multi-antenna systems whereas Shivaldova *et al.* [52] analyzed the performance of single-antenna systems in tunnels.

While field tests provide realistic insights for specific scenarios, simulations are better suited for repeatable, low cost evaluations of protocols and applications for vehicular communications. Current state-of-the-art simulators focus mainly on V2V communications or V2I communications operating in the cellular sense (*e.g.*, LTE communication between mobile terminal and base station). Existing V2I studies either utilize simplified OBU-RSU link behavior (*e.g.*, Paulin *et al.* [53] used NS-3 [54] to regulate the data flow and collection between the OBU and RSUs) or focus on LTE communication (*e.g.*, Altintas *et al.* [55] explored the use of cellular communication to enable “cars as an ICT resource” in the context of future smart cities).

CVNs structure could potentially employ a relay-based architecture that leverages spatial diversity techniques [56]. Furthermore, multi-hop relaying vehicular communications ensure more reliable and robust links relative to direct P2P transmissions since the transmission distance is shortened in the case of multi-hop communications [57]. Finally, depending on the type of information communicated by the vehicle hops, the awareness of all vehicles can be enhanced while simultaneously relaying this information to its final destination. In [58], half duplex mode V2I single antenna CVNs were studied given an amplify-and-forward (AF) operating scenario, which the received message at the relay node is amplified and transmitted to the another node. Although amplify-and-forward scenarios are desirable for low latency networks, they also amplify channel noise and significantly affect the reliability of the overall transmission. Another half duplex approach proposes a link scheduling scheme and investigates the maximum throughput problem [56]. Decode-and-forward (DF) system, as an alternative to AF approach, decodes the received message at the relay vehicle, recodes it, and transmits to the other vehicle.

MIMO-based CVNs are used to increase capacity, data rates, and transmission robustness [59]. In [60], MIMO channel characteristics are measured for collision avoidance application. The simulation models for MIMO mobile channels are denoted in [61]. In [62], the reference geometry-based channel model between MIMO mobile nodes is presented and the simulation model whose charac-

teristic matches with the reference model is discussed in [63]. This work is extended to wideband systems in [64] and relaying systems in [65]. The channel capacity is evaluated in [66] for the perfect channel state information (CSI) at the transmitters that is not realistic since it does not consider the feedback error and delay.

A geometrical model for MIMO-based relaying CVNs was proposed in [65], with a channel capacity analysis for a geometrical model presented in [34]. This model defines the channel matrices based on the scatterers' angles and distances between vehicles within the network. However, estimating the angles and distances can incur a latency penalty, which can affect time-sensitive applications supported by CVNs. In addition, geometrical models derive the channel model as a time-varying random variable. However, the transmission channel for network applications is actually a random process that depends on the time-variations occurring within the environments, as well as the excess delay that exists between multipath components. Therefore, geometric isotropic models are better suited for cellular networks rather than for V2V channel characteristics.

As an alternative to the ring-model, [67] proposes an elliptical model which denotes the ring model with a large number of scatterers that is not valid in urban areas. Also, this work highlights the case when several scatterers are also in a motion. Another work on moving scatterers is built into [68]. In this reference and also in this research, the maximum Doppler shift is given as [36]:

$$f_n = (v_n - v_i)\cos(\alpha_n)/\lambda, \quad (2.1)$$

where λ is wavelength, v_n is the speed of considered vehicle, n is s , r , and d for source, relay, and destination nodes, respectively. The angle between x -axis and the corresponding scatterer is α_n . The speed of the scatterers v_i changes between zero (*i.e.*, fixed scatterer case) and a maximum speed limit.

It is possible to increase the benefits of multi-hop relaying CVNs even more by optimizing the message transmission at the relay vehicle. Message optimization primarily focuses on decreasing the network load by dropping the redundant or expired messages instead of re-transmitting them at the relay vehicle. Barradi *et al.* [69] proposed a MAC layer strategy to avoid broadcast storm by adjusting the backoff time in highway scenarios. Hoque and Kwon [70] proposed to choose the packets in order to rebroadcast based on packet directions. Although this technique helps decrease the network load, a relay vehicle needs to know the types of applications that destination vehicles

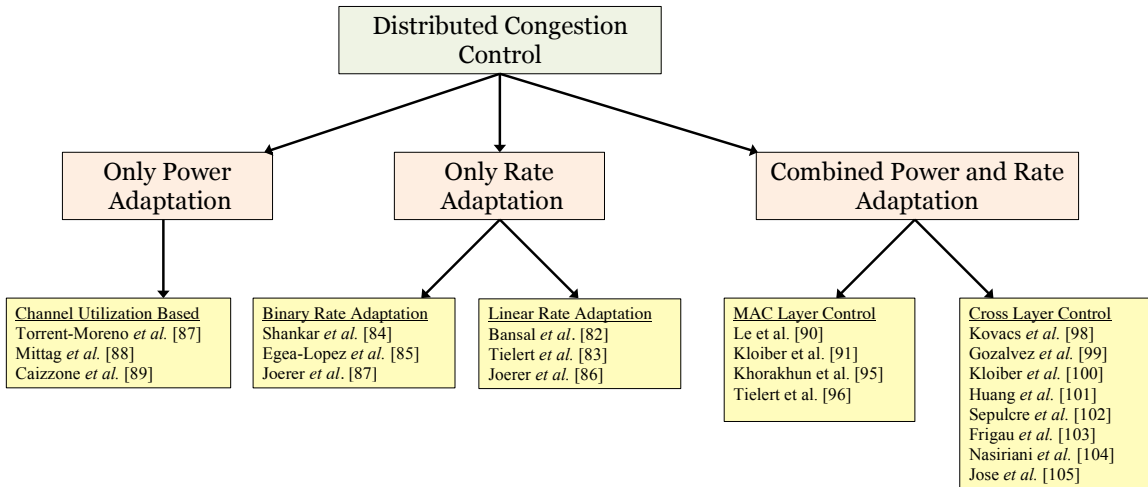


Figure 2.1: Taxonomy of distributed congestion control studies.

use. For instance, intersection warning messages from a relay vehicle need to be received by the vehicles behind the relay vehicle. On the other hand, ambulance warning messages from a relay vehicle usually need to be received by the vehicles ahead of the relay vehicle. Xiang *et al.* [71] chose the rebroadcast messages based on their packet values. The data preference is a promising idea, although the messages are checked one-by-one, which causes processing delay.

2.2 Distributed Congestion Control on Connected Vehicles Networks

The main goal for enabling many safety applications in CVNs is cooperative awareness. The main premise for cooperative awareness is that by knowing their operating environment, vehicles and their drivers are going to be better equipped for decision-making in hazardous situations (*e.g.*, emergency braking) and more adept at finding better routes to their destination (*e.g.*, avoiding congested roads). To enable cooperative awareness, vehicles use periodic message exchanges (also referred to as “beaconing”) in order to exchange position, speed, heading, and other vital information that makes the vehicles aware of their surroundings. Such cooperative awareness is used to enable safety applications, such as intersection collision warning, accident warning, and

emergency braking [72]. Since they are sent periodically by all vehicles, beacons are envisioned to occupy a large proportion of the channel time [73]. Decentralized Congestion Control (DCC) algorithms can be used to control the number of beacons and other messages transmitted across the channel. Typically, DCC approaches in CVNs are classified as shown in Figure 2.1: 1) rate control; 2) power control; and 3) combined rate and power control. Rate control algorithms adapt the message rate, *i.e.*, number of packets per unit time that a vehicle can transmit, where the rate is often adapted based on the channel load information. Power adaptation algorithms use transmit power control to limit the range over which a message is broadcast, thus effectively controlling the channel load. Hybrid algorithms employ the previous two types of control by applying both rate control to reduce the number of messages and power control to limit their range.

In recent years, there have been a number of works on DCC approaches proposed for CVNs. Since the standardization of DCC is vital for interoperability and performance of vehicle-to-X (V2X)¹ communications, there continues to be ongoing research on DCC in various standardization bodies and special interests consortia (*e.g.*, within European Telecommunications Standards Institute (ETSI) and as part of the Car-to-Car Communications Consortium) aimed at performance evaluation and providing a unified cross-layer DCC framework [73–77]. One example of a metric that is often used is the channel busy ratio (CBR), defined as the proportion of channel time that is deemed occupied by an ongoing transmission. Bansal *et al.* devised an algorithm called the LInear MESSage Rate Integrated Control (LIMERIC) [78], a rate control algorithm that adapts the message rate by using CBR measurements in a linear manner (*e.g.*, proportional to the change of CBR). The authors prove that the convergence of LIMERIC yields fair and efficient channel utilization. Tielert *et al.* [79] proposed an algorithm called PULSAR (Periodically Updated Load Sensitive Adaptive Rate control), which uses piggybacked two-hop CBR information and additive increase multiplicative decrease method (AIMD) in order to achieve better channel utilization and max-min fairness. The approaches described above used linear rate adaptation. A simpler approach to rate control is to increase/decrease the rate based on, for example, the CBR being above or below a preset threshold. This approach is frequently referred to as binary rate control. One example of a binary rate control algorithm is Context-Aware Rate Selection (CARS) by Shankar *et al.* [80]. Egea-Lopez and Pavon-Marino [81] reformulated the congestion control problem as a network

¹V2X is referred as the common name of all type of communication links such as V2V, V2I, V2D, V2P.

utility maximization problem and design fair adaptive beaconing rate for intervehicular communications (FABRIC), a proportionally fair binary rate control algorithm. The required message rate may change depending on the situation. To deal with these differences, Joerer *et al.* [82] perform rate adaptation by considering the context.

Power adaptation algorithms use transmit power control to limit the range over which a message is broadcast, thus effectively controlling the channel load. Torrent-Moreno *et al.* [83] designed a power control algorithm aimed at ensuring bandwidth allocation for high-priority event-based messages (*e.g.*, for safety applications), whereas Mittag *et al.* [84] elaborated on the same algorithm by introducing segment-based power control with the goal of reducing overhead. By testing the solution on homogeneous vehicular traffic densities and imperfect channel information, the authors demonstrated the effectiveness of their algorithm. Caizzone *et al.* [85] proposed an algorithm that adapts transmit power depending on the number of neighbors, where the transmit power is increased in case the number of neighbors is under the threshold or *vice versa*. Regarding combined power and rate adaptation algorithms, Le *et al.* [86] evaluated rate-only, power-only, and combined rate and power control algorithms. By performing extensive simulations, the authors identified which of the algorithms is preferable for a specific scenario and application requirement. Kloiber *et al.* [87] introduced a random transmission power assignment in order to make correlated packet collisions more uncorrelated in space. Authors in [88–90] define the DCC problem as a state machine to perform transmission power control. Khorakhun *et al.* [91] combined the binary rate adaptation with transmit power control, where the increase/decrease of transmit power is defined with a parameter chosen based on CBR. Tielert *et al.* [92] adapted the transmit power and rate with respect to the target transmission distance and channel conditions by using Pareto optimal parameter combinations. The authors point out that there is a need for further study involving variable channel conditions, including dynamic transitions between line-of-sight (LOS) and non-LOS conditions, which was experimentally shown to have a profound impact on communication performance, and with significant real-world effect on congestion control algorithms [93].

Since congestion control is inherently a cross-layer issue, with the need for implicit or explicit coordination between applications, transport-, network-, and access-layer algorithms, there have been studies looking at the cross-layer congestion control (*e.g.*, Kovacs *et al.* [94] and ETSI specialist task force work on cross-layer DCC [73]). In terms of using awareness to adjust the parameters

(power and rate) of congestion control algorithms, Gozalvez and Sepulcre propose OPRAM [95], an opportunistic transmission power control algorithm that increases the transmit power of messages in critical situations (*e.g.*, before intersections). However, in order to function properly, apart from precise location information, such as from GPS transmissions, OPRAM requires *a priori* knowledge about geographical regions that are accident-prone. Kloiber *et al.* [87, 96] used awareness quality as a metric and employ a random transmit power for messages with a goal of reducing interference. Huang *et al.* [97] perform power and rate adaptation mechanisms independently as well as based on potential tracking error resulting from the difference between actual and estimated states. This approach might be challenging to use in practice since it is hard to precisely obtain the actual state at each algorithm step. Sepulcre *et al.* [98] proposes the integration of congestion and awareness control (INTERN), which adjusts transmit power based on the prevailing application context (target dissemination distance set by applications) alone, without considering the surrounding environment. Numerous measurement studies have shown that the surroundings and vehicle traffic significantly affect the range, thus making it difficult to separate the target application range from the propagation environment restrictions. Frigau *et al.* [99] control the transmission range using the transmission power as well as beacon generation range based on beacon reception rate. Nasiriani *et al.* [100] perform similar power control mechanism and combine it with rate control based on channel utilization. Jose *et al.* [101] defines power adaptation as a joint Lagrangian optimization and rate adaptation. These approaches as well as [102] combine power and rate adaptation without their combined operation. However, the value that power control decides may cause a negative effect on message rate control mechanism, and vice versa.

2.3 Spectrum Sensing on Connected Vehicle Networks

The issue of wireless spectrum scarcity caused by increasing connectivity demand impacts the automotive industry. It is predicted that the currently allocated 6 channels of DSRC spectrum band will be insufficient for meeting all connectivity needs of the emerging ITS architecture [103]. Consequently, in many of the envisioned scenarios, the use of other wireless spectrum band such as TV white space (TVWS) is viewed as a potential solution of the spectrum challenges faced by connected vehicles [104–109].

Table 2.1: Spectrum Sensing Techniques in the Current State-of-the-Art.

Technique	Benefit	Drawback	Reference
Genetic Algorithm	Finds global optimum	Converges slow	[114–118]
Queuing Theory	Gives priority to safety messages	Large number of switching operation	[119–121]
Game Theory	Finds the optimum of benefit and cost	Needs a centralized control mechanism	[122–125]

As the idea of VDSA evolves, connected vehicles use available non-DSRC channels as unlicensed users (*i.e.*, secondary users or SUs) while not interfering with the licensed users (*i.e.*, primary users or PUs) of the specific frequency bands [110]. The viability of VDSA is based on the successful classification of channel available [107,111]. As an alternative to using Digital Television (DTV) band, Ghandour *et al.* proposed the usage of the 5.8 GHz ISM band for secondary connected vehicle users in [112]. Although this idea has the benefit of not requiring to perform primary user detection and the hardware configuration is similar to DSRC standards, it also has several drawbacks such as other users utilizing the ISM band and the CSMA/CA mechanism causing extra process latency [113].

Field experiments have provided several insights on the practical limitations of VDSA designs [111,126–128]. While these experiments have demonstrated the characteristics of highway and urban environments, parameter settings for secondary user (SU) vehicles that fit into these characteristics have been obtained in [129–132]. The field measurement data also has led to the development of realistic testbed implementations. In [133], a testbed employing the Microsoft Software Radio was used to create a realistic test scheme, while a software defined radio implementing the IEEE 802.11p standard was used to observe the out-of-band spectral leakage in [134]. Another testbed was implemented using multi-radio access technologies (GSM/GPRS, CDMA, Wi-Fi) in order to demonstrate V2V communication in [135,136].

There have been numerous approaches for implementing different parts of the cognitive learning cycle of VDSA as listed in Table 2.1. Genetic algorithm has been one of the most common techniques to cognitive network parameter adaptation [114–118]. Although the genetic algorithm is robust to various environmental characteristics, the convergence time is relatively slow, which is not practical for a dynamic CVNs environment. As an alternative to genetic algorithms, queuing theory has been considered for the adaptation of cognitive network parameter settings [119–121].

Queuing solves the problem of successful reception of urgent safety messages. However, this approach may cause a large number of channel switching operations in some scenarios. Game theory has also been considered for channel access strategies, since game theory optimizes sensing time and sensing benefits [122–125].

Detecting the current environment conditions is key for cognitive network parameters adaptation as well as sensing the channel status, *i.e.*, busy or available. Energy detection is the most common spectrum sensing technique since it does not have any initial assumption and its computation complexity is lower than the alternatives such as cyclostationary detection and action recognition [137]. In [138], spectrum detection schemes were described for Additive White Gaussian Noise (AWGN) channels. Although this study provides a generic idea about spectrum sensing, an AWGN channel is not a realistic assumption for CVNs. In [139], an optimization of resources was performed for the empirical Okumura-Hata Model. In [140], blind spectrum sensing was performed for cognitive CVNs in Nakagami fading. Since vehicular channels are Rayleigh fading for non-line-of-sight (NLOS) and Rician fading for line-of-sight (LOS) links in reality, energy detection for fading channels is viewed as more practical for several scenarios derived in [141–145]. The approaches are derived for general wireless communications perspective without considering specific features of CVNs.

The success of spectrum sensing is directly affected by the choice of the threshold used during the binary decision. It was proven that minor interruptions in the PU data traffic may cause serious traffic jams under highway conditions [146]. Due to the highly mobile environment of vehicles, the energy detection threshold may vary significantly in time. In [147], the optimum detection threshold is derived for AWGN channels for a stable network. However, adaptive energy detection threshold in a dynamic fading network was still an open research question in the current state-of-the-art. In addition to the spectrum sensing with energy detection threshold, likelihood detection operations were described in [148–151]. The likelihood ratio is not a realistic solution for highly time varying CVN environments since their likelihood thresholds need to be defined, which is an additional unknown variable that causes extra computational cost and time. The existing literature on the spectrum sensing was not considered the process timing which is critical for dynamic VDSA applications. Process time of the proposed approach should not take more time than the channel coherence time, *i.e.*, the duration that the channel is fixed. To define the process time limits, the

channel coherence time has been derived based on the vehicle speed and environmental conditions in [152].

Cooperative sensing is one of the most promising applications for VDSA [153, 154] since the detection errors made by the vehicles can be fixed with the help of neighbor vehicles. The current state-of-the-art shows that cooperative sensing makes the detection operation more robust and reliable [144, 155–157]. Once the available channels are detected by secondary users, this information is shared between neighbor nodes. When the vehicle receives the available channels list from its neighbors, it votes on the received available channels. With respect to distributed channel sensing studies, [158, 159] proposed a voting algorithm where the channel was deemed to be available if half of the neighbors have the same decision on corresponding channel availability. However, this voting mechanism assumes that all neighbors are at the same credibility level although they might not be. In [160], belief propagation was performed with few iterations which causes delay. In [161], a weighing function was defined to evaluate a neighbor's credibility and operate the voting based on the weight function which depends on only the distance between the vehicles. In reality, the distance may not be consistent with the neighbor's credibility. For example, in an urban area, the closer neighbor may misinform the vehicle as there might be obstacles between the vehicles. Alternatively, a more distant neighbor may inform correctly the availability of channels to the vehicle if there is a LOS component.

2.4 Chapter Summary

This chapter summarizes the literature review related this dissertation. The main topics are channel modeling, congestion control mechanisms, and dynamic spectrum access techniques for CVNs. While they are separated topics by themselves, CVNs possess the potential to combine them, and it is the cross-discipline efforts that revolutionize ITS applications. In the following chapters, this background material is referenced to explain the contribution to the current state-of-the-art. The proposed approaches in the dissertation address the open research problems discussed in this chapter.

Chapter 3

Channel Characteristics and Relaying Optimization of Connected Vehicle Networks

Understanding and modeling channel behavior is the first step in devising CVN solutions. Although the literature includes many propagation models and channel simulators for point-to-point (P2P) V2V systems, there is a noticeable lack of studies focused on multi-hopping vehicular communications. In this chapter, we explore limitations and strengths of multi-hopping CVNs. We first define the channel propagation models with large and small scale fading. Large scale fading is analyzed for different link types. Small scale channel models are presented for Decode-and-Forward (DF) relaying MIMO antennas since MIMO systems are generalized version of all type of antenna arrays, *i.e.*, SISO, SIMO, MISO, MIMO. Next, we analyzed the lower bound on the channel capacity of multi-hopping CVNs by using the channel models. Lastly, we proposed a selective message relaying algorithm to solve message overhead on rebroadcasting operation at the relay vehicle.

The work presented in this chapter has been published in parts at [C5], [C4], [C3], [C2], and [C1].

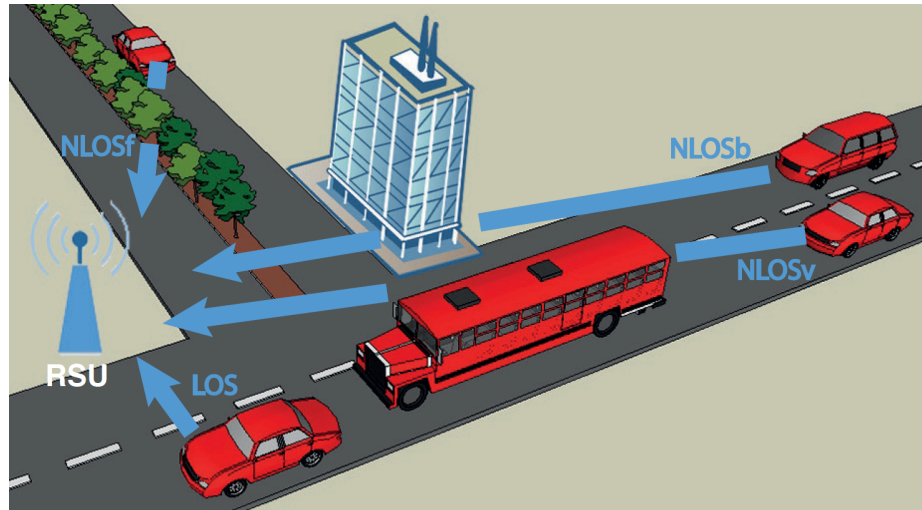


Figure 3.1: Large scale link attenuation greatly varies based on the link type: line-of-sight (LOS), non-line-of-sight by vehicles (NLOSv), non-line-of-sight by foliage (NLOSf), non-line-of-sight by buildings (NLOSb).

3.1 Architecture Overview

Line-of-Sight (LOS) links can be affected by different objects, from which we classify link types into non-line-of-sight (NLOS) links, with the latter being further classified as NLOS due to obstruction by vehicles (NLOSv), buildings (NLOSb), and foliage (NLOSf). These three main object types affecting propagation are shown for V2I architecture in Figure 3.1. In V2I architecture, road side units (RSUs) and vehicles, *i.e.*, on board units (OBU), exchange information to enable safety and mobility applications.

In the DF multi-hopping architecture, the source vehicle transmits data \mathbf{x}_s to both the relay and destination vehicles. In turn, the relay vehicle receives \mathbf{x}_s , decodes it, re-encodes it as the relay data \mathbf{x}_r , and sends it to destination vehicle. The main benefit of DF relaying is that the coding scheme at the relay vehicle helps to correct for any corruption on transmitted data.

In the full-duplex relaying architecture, the relay can act as both a transmitter and a receiver at the same time. The transmission from the source to the relay, as well as the relay to the destination, uses the same carrier frequency (Figure 3.2). A significant challenge for full-duplex relaying systems is *self interference (SI)*, which refers to the situation where each transmission pollutes its own signal at the transmitter by producing receiver noise, thus reducing the signal-to-noise-ratio (SNR)

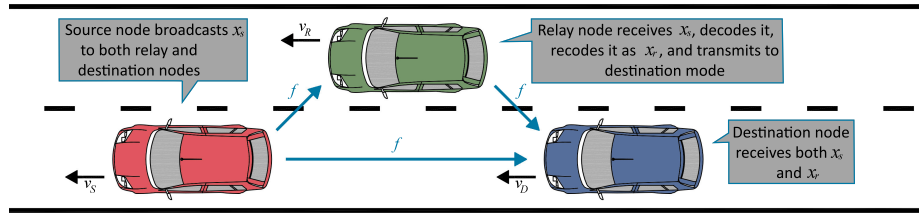


Figure 3.2: Network architecture of DF CVNs.

and ultimately the throughput [162]. In order to realize the advantages of full-duplex relaying with respect to throughput and bandwidth utilization, the SI problem is a topic of extensive research activities [163]. Although passive suppression techniques such as natural isolation, orthogonal polarization, orthogonal polarization, and antenna selection are not practical for connected vehicles network, active (digital/analog) cancellation schemes are successfully mitigates the interference effect [164, 165]. Given that several SI cancellation techniques applied to the RF front-end have been proposed in the literature, this work does not consider the impact of untreated SI on the channel capacity [166–168].

In addition to the relay transmission, a direct transmission is also performed since it increases the network capacity and reliability. The source-to-relay and source-to-destination links are called the Broadcast Channel (BC). Similarly, source-to-destination and relay-to-destination links are collectively called the Multiple Access Channel (MAC). The DF mode enables the use of the same frequency bandwidth for all three links due to a special decoding scheme [169]. The scatterers are not affected by the other vehicles since the distance between the vehicles are assumed to be sufficiently large. This frequency architecture shows DF architecture provides more reliable transmission than single link by using same frequency band.

A highly dynamic CVN topology does not lend itself to standard channel models. The effects of Doppler spread with respect to relative velocities between nodes need to be detected and fixed. Furthermore, a successful implementation must take into account of safety application at the application layer. This issue causes limits on latency and reliability of packet delivery which are strong challenges to designer.

3.2 Channel Models

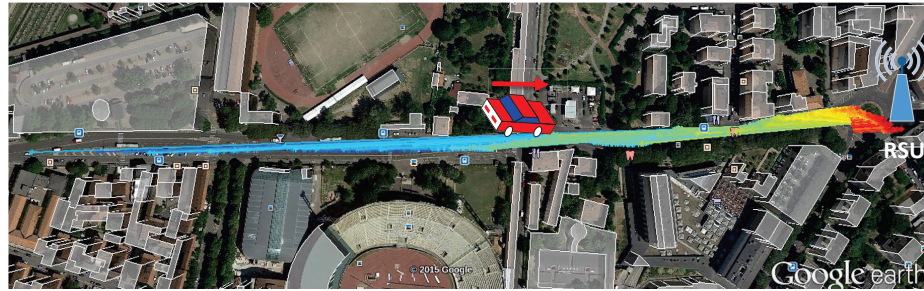
In this section, we define both large and small scale fading models for CVNs [170]. We consider different link types for large scale fading. We apply two different small scale statistical channel models to DF relaying vehicular communication: geometrical-based model, sum-of-sinusoids (SoS) model. The small scale fading is analyzed for both non-line-of-sight (NLOS) and line-of-sight (LOS) conditions, and both multipath propagation and time varying channel conditions are considered. In this chapter, we consider block fading and explain this is a realistic assumption in Section 3.3. Therefore, Doppler effect on fading channel is stable on a block.

Notations: Upper (lower) boldface letters are used to denote matrices (column vectors). The conjugate-transpose operation is shown as $(\cdot)^\dagger$ and $E[\cdot]$ to express expectation with respect to all random variables within the brackets. The matrix trace and determinant are denoted as $tr(\cdot)$ and $|\cdot|$, respectively.

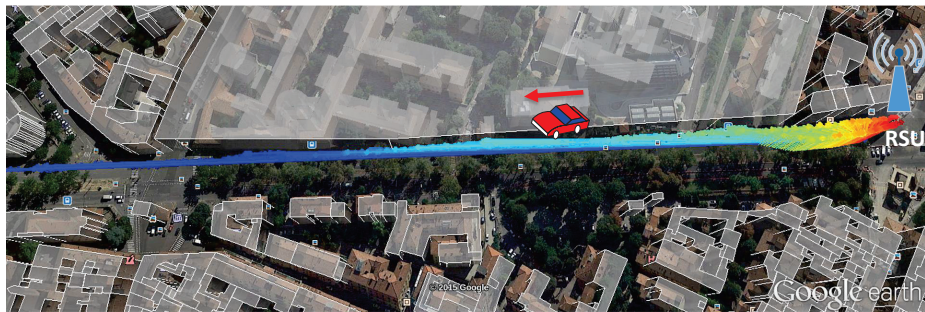
3.2.1 Large Scale Attenuation Models

We derive the large scale attenuation characteristics based on the V2I architecture since there is a freely available data from a V2I measurement campaign in 5.9 GHz frequency band performed in the city center of Bologna, Italy [48]. We employ real world measurements to : i) extract the large scale received power variation parameters; and ii) validate the accuracy of proposed model. Although the link types are explored for V2I links to be able compare with open source measurement results, the models are valid for also V2V links. The only difference between V2V and V2I links is that V2I has fewer scatterers that are also distributed more isotropically than in case of V2V, thus resulting in less variation due to multipath since the antenna height of the RSU is higher than the OBU. We also depict free space path loss as a reference point for the reader (*i.e.*, not as a representative model for all of the link types).

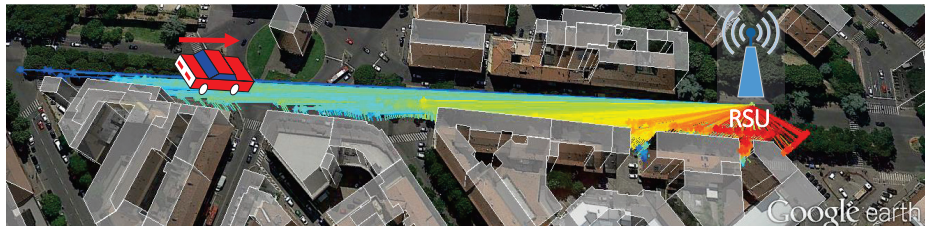
In the referenced V2I measurement campaign [48], 10 RSUs are deployed throughout the city so as to encompass different conditions in an urban environment. In Figure 3.3, the RSUs that are used in this section and corresponding propagation power levels are depicted. In Figure 3.3(a), the OBU approaches the RSU in a straight street which is 500 m long. At each time step, the received power is recorded. The levels of received power are shown with colors varying from red



(a) LOS and NLOSv experiment region



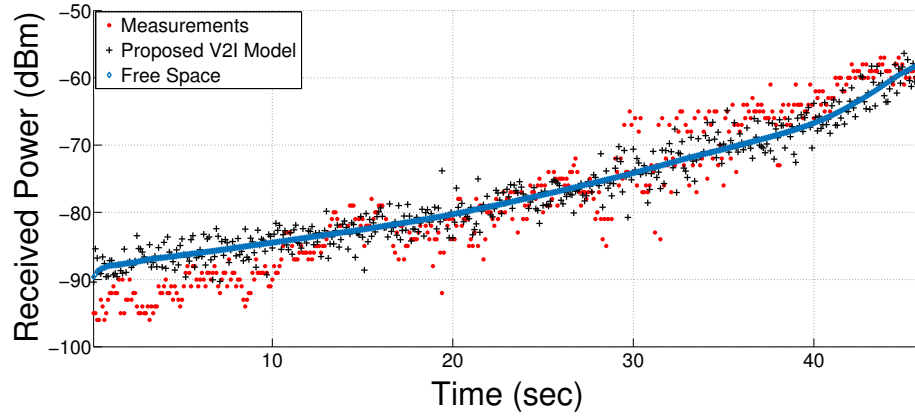
(b) NLOSf experiment region



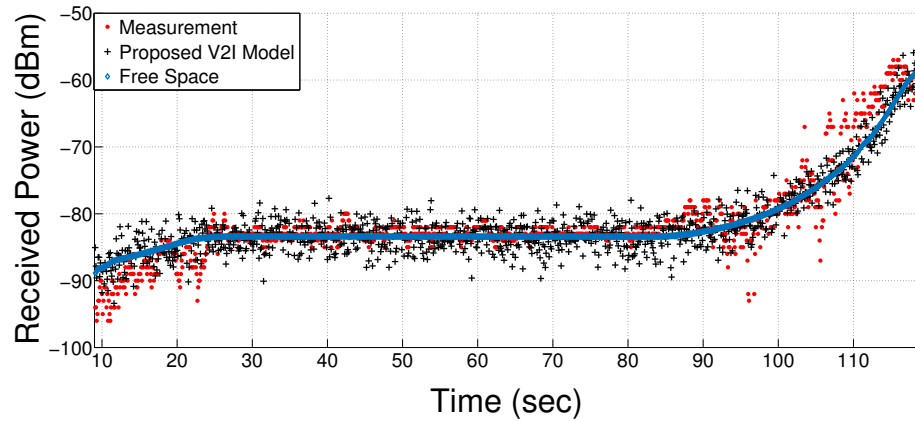
(c) NLOSb experiment region

Figure 3.3: Locations of RSUs for selected scenarios representing different link types.

to blue, respectively corresponding to high and low received power. The same setup is also used for NLOS due to heavy vehicle obstacles. In this experiment, the vehicle with OBU approaches the RSU while a heavy vehicle drives right in front of the OBU, thus breaking the direct LOS link. In Figure 3.3(b), the RSU is located in a region surrounded by foliage. The street is curve-shaped right in front of the RSU, which is itself surrounded by trees. Hence, the vegetation limits the reception of signals from the RSU, causing extra attenuation. In Figure 3.3(c), the RSU is located near a building and the OBU approaches the RSU on the road in front of the building, so that the



(a) LOS V2I Links: Measurement 1



(b) LOS V2I Links: Measurement 2

Figure 3.4: LOS V2I Links: OBU monotonically approaches the RSU at each time step for both measurements. Both results generated by the model and measured data have a pattern similar to free space path loss since the link type is LOS. Model vs Measurements: mean absolute error: 3.16 mean; standard deviation: 2.84.

building breaks the direct link. We propose a model that separately models all these link types and evaluate it against real-world measurements depicted in Figure 3.3. For each link type, we define large-scale attenuation effects through a characterization of its unique link properties.

Line-of-Sight Links (LOS): To characterize LOS links, we resort to a two-ray ground reflec-

tion model described as follows [171]:

$$E_{\text{TOT}} = \frac{E_0 d_0}{d_{\text{LOS}}} \cos \left(w_c \left(t - \frac{d_{\text{LOS}}}{c} \right) \right) R_{\text{ground}} \frac{E_0 d_0}{d_{\text{ground}}} \cos \left(w_c \left(t - \frac{d_{\text{ground}}}{c} \right) \right), \quad (3.1)$$

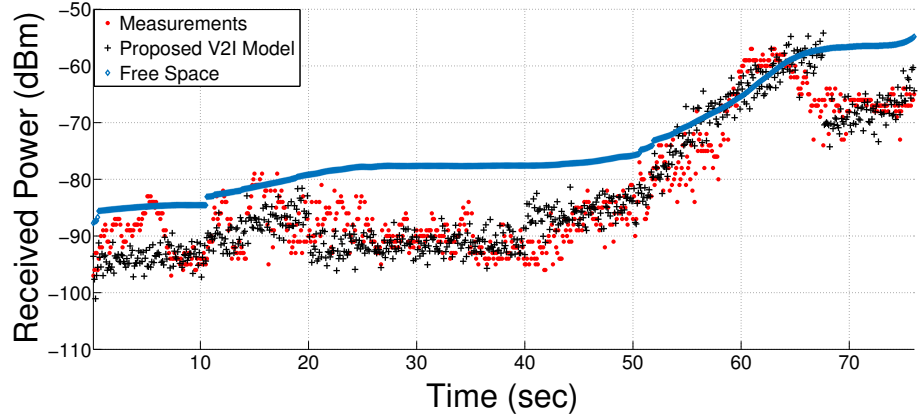
where the reflection coefficient R_{ground} and distance d_{ground} for the ground-reflected ray are calculated according to the exact antenna heights, w_c is the carrier frequency in radian. In Figure 3.4, the OBU approaches the RSU as shown in 3.3(a). The same experiment is performed two times. In the first measurement, the OBU approaches the RSU during 450 time steps, so that received power monotonically increases (Figure 3.4(a)). In the second measurement, the OBU moves around the RSU by keeping a steady distance throughout 500 time steps and then approaching the RSU, thus leading to increased received power (Figure 3.4(b)). As expected, both model and measured data follow a pattern similar to the free space path loss model.

Non-Line-of-Sight Links due to Vehicles (NLOSv): Vehicles – particularly large ones like buses and trucks – have a strong impact on CVN links. When a link is blocked by one or more vehicles, additional attenuation can be modeled as (multiple) knife-edge diffraction [172]. According to the knife-edge model, the additional attenuation A can be computed as follows:

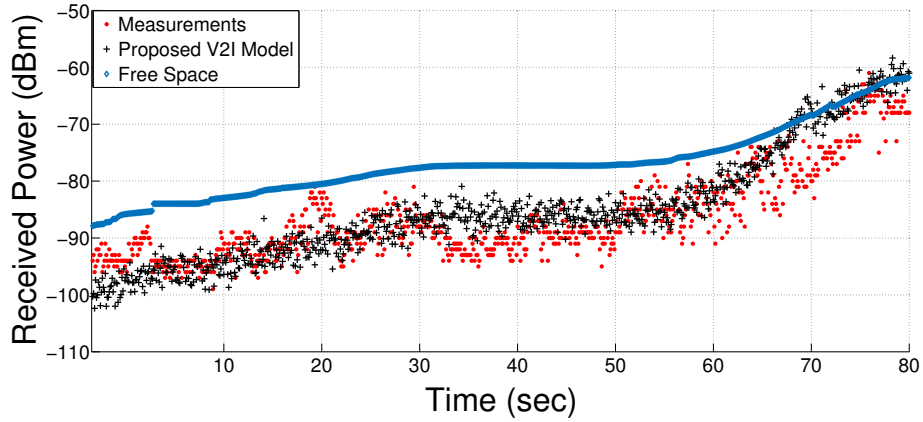
$$A = \begin{cases} 6.9 + 20 \log_{10} \left[\sqrt{(v - 0.1)^2 + 1} + v - 0.1 \right] & v > 0.7 \\ 0 & \text{otherwise} \end{cases}, \quad (3.2)$$

where $v = \sqrt{2}H/r_f$, H is the height difference between obstacle and OBU antenna, r_f is the Fresnel ellipsoid radius. In Figure 3.5, field measurements for the RSU deployed in Bologna are compared with the considered NLOSv model. During the measurement, there is a heavy vehicle in front of the OBU as it approaches the RSU as shown in 3.3(a). The same experiment is performed twice, with the first lasting 700 (Figure 3.5(a)) and the other one 800 time steps (Figure 3.5(b)). The distance between the heavy vehicle and the OBU varies between 5 and 25 m during the measurements. We can observe that the proposed model matches measured data well, with mean absolute error of 3.98 and standard deviation of 3.47 over the two experiments. The good match shows the flexibility of the knife-edge model, which, unlike stochastic models, takes into account the heights of antennas and obstructing objects to calculate the link attenuation.

Non-Line-of-Sight Links due to Foliage (NLOSf): NLOSf links are modeled by using the empirical derivation given by Goldhirsh *et al.* [173], where the attenuation caused by foliage is



(a) NLOSv V2I: Measurement 1



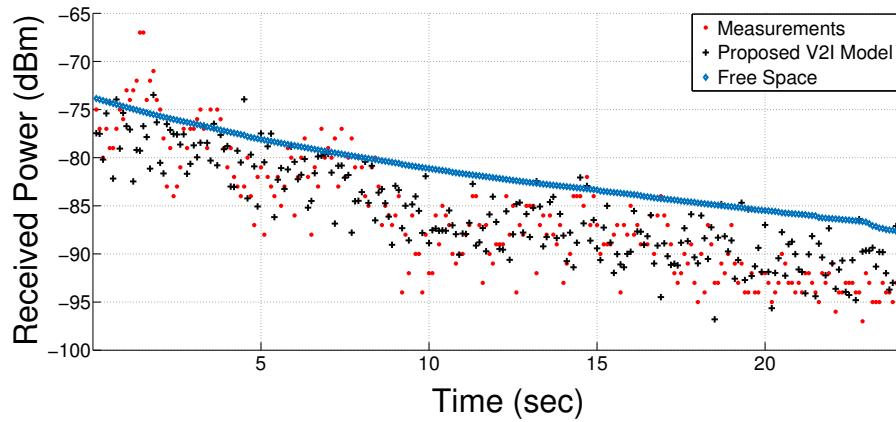
(b) NLOSv V2I: Measurement 2

Figure 3.5: NLOSv V2I links: comparison of field measurements and simulated results. OBU approaches to RSU at each time step while the heavy vehicle is driving right front of the OBU. Model vs Measurements: mean absolute error: 3.98 mean; standard deviation: 3.47.

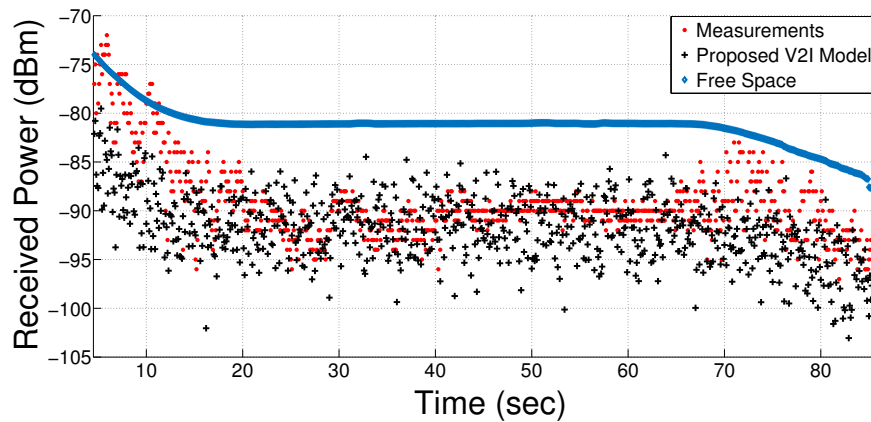
defined as mean excess loss (MEL) per meter as follows:

$$\text{MEL} = 0.79 f^{0.61} \quad (3.3)$$

where f is the carrier frequency, *i.e.*, 5.9 GHz for 802.11p-based communication. MEL is multiplied with the length of propagation through foliage. In Figure 3.6, field measurements for the RSU deployed in Bologna are compared with the proposed model. In this experiment, the RSU is located on a road that has a curve surrounded by trees; once the OBU moves behind the curve, the direct



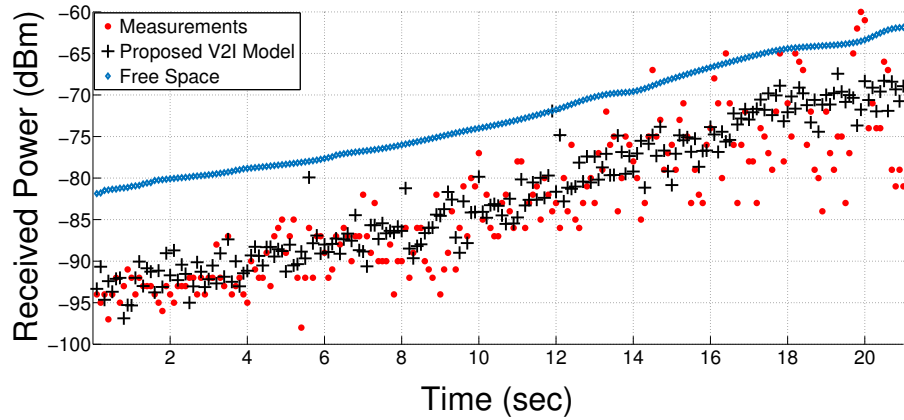
(a) NLOSf V2I links: Measurement 1



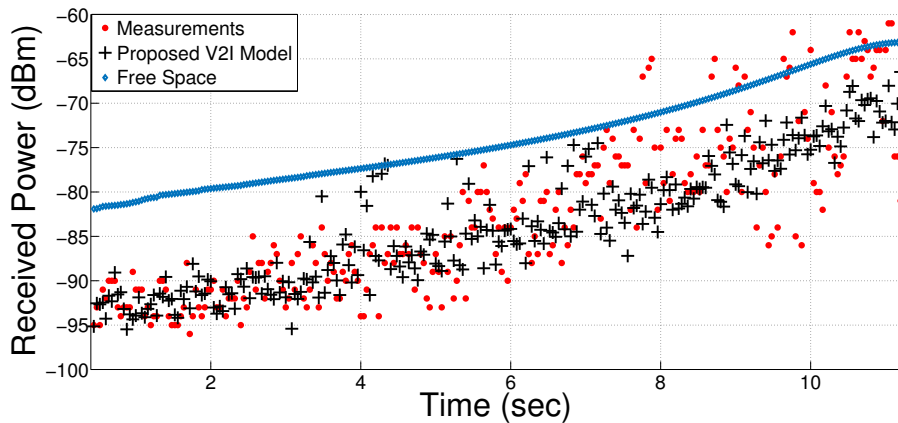
(b) NLOSf V2I links: Measurement 2

Figure 3.6: NLOSf V2I links: comparison of field measurements and simulated results. Model vs Measurements: mean absolute error: 4.14 mean; standard deviation: 3.64.

link becomes obstructed by trees. The measurement in the location shown in Figure 3.3(b) is performed two times. In the first measurement, the OBU drives away from the RSU during 350 time steps, so that the received power decreases largely monotonically (Figure 3.6(a)). In the second measurement (Figure 3.6(b)), the OBU moves away from RSU; between time step 200 and 700, the speed is very low (under 1 km/h), which is reflected in almost stable received power. The transmission distance through foliage (and thus the attenuation) gradually increases in the first measurement, while it remains stable in the second measurement, as evidenced relative to the free



(a) NLOSb V2I: Measurement 1



(b) NLOSb V2I: Measurement 2

Figure 3.7: NLOSb V2I links: comparison of field measurements and simulated results. Model vs Measurements: mean absolute error: 5.03 mean; standard deviation: 5.79.

space path loss. Figure 3.6 shows that the proposed model can model the foliage-obstructed V2I links well.

Non-Line-of-Sight V2I links due to Buildings Obstacles (NLOSb): Since the large scale effect of buildings is similar for V2V and V2I links, for the attenuation on V2I NLOSb link, we used the model for V2V NLOSb from GEMV² simulator [43], with modified small scale signal variation parameters, which were extracted from V2I measurements [48]. In the model, the attenuation due to buildings is estimated as the maximum received power between: i) the joint effect of

single-interaction diffractions and reflections; and ii) the log distance path loss model with a comparatively high path loss exponent (for details, see [43]). In Fig. 3.7, the field measurements for the RSU deployed in Bologna (shown in Figure 3.3(c)) are compared with the proposed model. In this measurement, the RSU is located near a building and the OBU approaches it through the street in front of the building. Therefore, the nearby building slightly breaks the direct link between OBU and RSU, resulting in a moderate attenuation due to the building. The same experiment is performed two times. We can observe that the proposed model result matches measured data with mean absolute error of 5.03 and standard deviation of error of 5.79.

3.2.2 Small-Scale Fading Models: Geometry-based Channel Model for Multi-hopping Connected Vehicle Networks

In this channel model, channel coefficients for small scale fading are computed based on geometrical parameters such as distances and angles. We present the channel model for MIMO antenna arrays. However, it is also used for SISO systems by setting the antenna number to one.

3.2.2.1 Geometrical Framework

The source, relay, and destination vehicles are assumed to possess instantaneous speeds of v_s , v_r , and v_d , with angles to x-axis labeled as α_s , α_r , and α_d , respectively (Figure 3.8). We extend the geometrical model, which was proposed in [65], to DF relaying LOS conditions. The proposed three rings scattering model is based on only local scattering since high path loss dilutes the effects of remote scatterers. The scatterers of source (relay and destination, respectively) are S_s^m , $m = 1, \dots, M$ (S_r^k , $k = 1, \dots, K$ and S_d^l , $l = 1, \dots, L$). The random phase shift for the source (relay and destination) is $\theta_s^{(m)}$ ($\theta_r^{(k)}$ and $\theta_d^{(l)}$) which is i.i.d. random variable with a uniform distribution over the interval $[0, 2\pi)$.

Distances between the mobiles are D_{xy} where the subscript x and y refer the transmitter and receiver nodes, respectively. The angle of source to relay link and x-axis is γ_s and the angle of relay to destination link and x-axis is γ_d . The radii of the scatterers of transmitters and receivers, R_s , R_r , and R_d , are significantly smaller than the distances between the corresponding nodes. The antenna spacing for each node are defined as δ_s , δ_r , and δ_d , which are less than radii of the scatterers. The angles between antenna arrays and x-axis are defined as β_s , β_r , and β_d .

the channel model can be extended to any number of antenna array elements. Considering a three ring MIMO model for CVNs, the first channel element of $\mathbf{H}_{xy}(t)$ for the finite number of scatterers is defined in NLOS channel components are obtained as [65]:

$$z_{sr}^{(11)}(t) = \frac{1}{\sqrt{MK}} \sum_{m,k=1}^{M,K} g_{sr}^{(mk)} e^{j[2\pi(f_s^{(m)} + f_{sr}^{(k)})t + (\theta_{sr}^{(mk)} + \theta_{sr})]}, \quad (3.6)$$

$$z_{rd}^{(11)}(t) = \frac{1}{\sqrt{KN}} \sum_{k,n=1}^{K,N} g_{rd}^{(kn)} e^{j[2\pi(f_{rd}^{(k)} + f_d^{(n)})t + (\theta_{rd}^{(kn)} + \theta_{rd})]}, \quad (3.7)$$

$$z_{sd}^{(11)}(t) = \frac{1}{\sqrt{MN}} \sum_{m,n=1}^{M,N} g_{sd}^{(mn)} e^{j[2\pi(f_s^{(m)} + f_d^{(n)})t + (\theta_{sd}^{(mn)} + \theta_{sd})]}, \quad (3.8)$$

where $f_{x_{max}} = v_x/\lambda$ is maximum Doppler frequency and λ is the carrier's wavelength [65]. The angle of departure of the m th and k th transmitted waves are $\phi_s^{(m)}$ and $\phi_{sr}^{(k)}$ at the source and the relay. The angle of arrival of the k^{th} and l^{th} received waves are $\phi_{rd}^{(k)}$ and $\phi_d^{(l)}$ at the relay and the destination. The parameters in these equations are defined in Table 3.1. NLOS path loss components are added to the direct link to obtain LOS channel envelope:

$$h_{sr}^{(11)}(t) = \frac{z_{sr}^{(11)}(t) + \sqrt{K^{sr}} \exp(j2\pi f_0^{sr} t + \Phi_0^{sr})}{\sqrt{1 + K^{sr}}}, \quad (3.9)$$

$$h_{rd}^{(11)}(t) = \frac{z_{rd}^{(11)}(t) + \sqrt{K^{rd}} \exp(j2\pi f_0^{rd} t + \Phi_0^{rd})}{\sqrt{1 + K^{rd}}}, \quad (3.10)$$

$$h_{sd}^{(11)}(t) = \frac{z_{sd}^{(11)}(t) + \sqrt{K^{sd}} \exp(j2\pi f_0^{sd} t + \Phi_0^{sd})}{\sqrt{1 + K^{sd}}}, \quad (3.11)$$

$$(3.12)$$

where K^{xy} is the Rician coefficient, Φ_0^{xy} is the random phase in the interval $[-\pi, \pi]$, and Doppler frequency of the LOS component is derived as:

$$f_0^{xy} = (|v_y| \cos(\alpha_y - \beta_y) - |v_x| \cos(\alpha_x - \beta_x)) / \lambda. \quad (3.13)$$

The other channel elements are obtained by replacing $a_x^{(p)}$ and $b_y^{(p)}$ with the complex conjugates $a_x^{(p)\dagger}$ and $b_y^{(p)\dagger}$ for $h_{xy}^{(22)}(t)$, $a_x^{(p)}$ with $a_x^{(p)\dagger}$ for $h_{xy}^{(12)}(t)$, $b_y^{(p)}$ with $b_x^{(p)\dagger}$ for $h_{xy}^{(21)}(t)$ where p is m for source, k for relay, and l for destination.

Table 3.1: The parameters that define channel coefficients based on angles and distances

$h_{sr}^{(11)}(t)$	$h_{rd}^{(11)}(t)$	$h_{sd}^{(11)}(t)$
$g_{sr}^{(mk)} = a_s^{(m)} b_r^{(k)} c_{sr}^{(mk)}$	$g_{rd}^{(kl)} = a_r^{(k)} b_d^{(l)} c_{rd}^{(kl)}$	$g_{sd}^{(ml)} = a_s^{(m)} b_d^{(l)} c_{sd}^{(ml)}$
$\phi_s^{(m)} = (2\pi/M)(m - 1/2) + \alpha_s, m = 1, \dots, M$	$\phi_{rd}^{(k)} = (2\pi/K)(k - 1/2) + \alpha_r, k = 1, \dots, K$	$\phi_s^{(m)} = (2\pi/M)(m - 1/2) + \alpha_s, m = 1, \dots, M$
$\phi_{sr}^{(k)} = (2\pi/K)(k - 1/2) + \alpha_r, k = 1, \dots, K$	$\phi_d^{(l)} = (2\pi/L)(l - 1/2) + \alpha_d, l = 1, \dots, L$	$\phi_d^{(l)} = (2\pi/L)(l - 1/2) + \alpha_d, l = 1, \dots, L$
$a_s^{(m)} = e^{j(\pi/\lambda)\delta_s \cos(\phi_s^{(m)} - \beta_s)}$	$a_r^{(k)} = e^{j(\pi/\lambda)\delta_r \cos(\phi_r^{(k)} - \beta_r)}$	$a_s^{(m)} = e^{j(\pi/\lambda)\delta_s \cos(\phi_s^{(m)} - \beta_s)}$
$b_r^{(k)} = e^{j(\pi/\lambda)\delta_r \cos(\phi_{sr}^{(k)} - \beta_r)}$	$b_d^{(l)} = e^{j(\pi/\lambda)\delta_d \cos(\phi_{rd}^{(l)} - \beta_d)}$	$b_d^{(l)} = e^{j(\pi/\lambda)\delta_d \cos(\phi_d^{(l)} - \beta_d)}$
$c_{sr}^{(mk)} = e^{j(2\pi/\lambda)\{R_s \cos(\phi_s^{(m)} - \gamma_s) - R_r \cos(\phi_{sr}^{(k)} - \gamma_r)\}}$	$c_{rd}^{(kl)} = e^{j(2\pi/\lambda)\{R_r \cos(\phi_{rd}^{(k)} - \gamma_r) - R_d \cos(\phi_d^{(l)} - \gamma_d)\}}$	$c_{sd}^{(ml)} = e^{j(2\pi/\lambda)\{R_s \cos(\phi_s^{(m)}) - R_d \cos(\phi_d^{(l)})\}}$
$\theta_{sr} = (-2\pi/\lambda)(R_s + D_{sr} + R_r)$	$\theta_{rd} = (-2\pi/\lambda)(R_r + D_{rd} + R_d)$	$\theta_{sd} = (-2\pi/\lambda)(R_s + D_{sd} + R_d)$
$f_s^{(m)} = f_{smax} \cos(\phi_s^{(m)} - \alpha_s)$	$f_{rd}^{(k)} = f_{rmax} \cos(\phi_{rd}^{(k)} - \alpha_r)$	$f_s^{(m)} = f_{smax} \cos(\phi_s^{(m)} - \alpha_s)$
$f_{sr}^{(k)} = f_{rmax} \cos(\phi_{sr}^{(k)} - \alpha_r)$	$f_d^{(l)} = f_{dmax} \cos(\phi_d^{(l)} - \alpha_d)$	$f_d^{(l)} = f_{dmax} \cos(\phi_d^{(l)} - \alpha_d)$

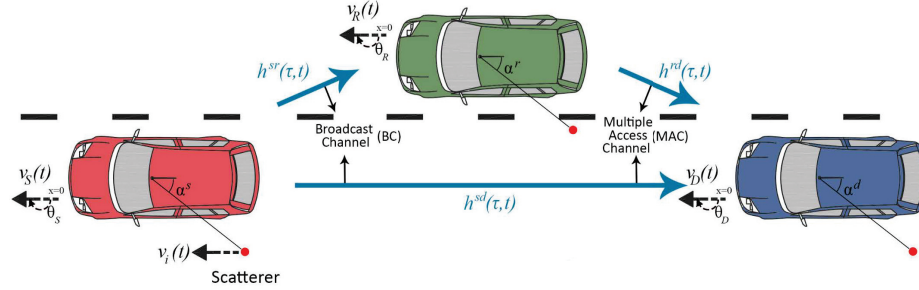


Figure 3.9: SISO relaying vehicular network architecture. The channel impulse responses, which consider both multipath propagation delay and time varying channel conditions, are defined as $h^{sr}(\tau, t)$, $h^{sd}(\tau, t)$, and $h^{rd}(\tau, t)$. The angle between scatterer and x -axis is α and the motion angle of vehicle is θ rad/s.

3.2.3 Small-Scale Fading Models: Sum-of-Sinusoids Channel Model for Multi-hopping Connected Vehicle Networks

In this section, a sum-of-sinusoids (SoS) model [39, 42] for small scale fading is derived for relaying CVNs. The model is presented for both SISO and MIMO cases. The applied SoS model is independent from parameters such as distance/angles between vehicles, which changes continuously in time. Therefore, it is more suitable to use for real-time CVNs applications than geometrical model. Furthermore, SoS relaying channel model that takes into account excess delay of multipath contributions besides time variation. Therefore, it potentially provides a more reliable channel model relative to those that consider only time variation.

3.2.3.1 SISO Sum-of-Sinusoids Model with LOS Component

We start with the channel model proposed for P2P networks in [40] by extending it to DF relaying CVNs. In Figure 3.9, the channel architecture is illustrated, where the speed of the source (resp. relay, destination) node is v_s (resp. v_r, v_d) and the angle between the movement direction of the source (resp. relay, destination) and x - axis is θ_s (resp. θ_r, θ_d). The angles between the uniformly distributed random scatterers, occurring as a result of the mobility, and the x -axis are defined as α_s, α_r , and α_d for the source, relay, and destination, respectively.

The complex envelope of the Rayleigh distribution on source to relay link is given as [42, Ch 9]:

$$g_k^{sr}(t) = g_{ik}^{sr}(t) + jg_{qk}^{sr}(t), \quad (3.14)$$

$$g_{ik}^{sr}(t) = \frac{1}{\sqrt{NM}} \sum_{m,n=1}^{M,N} \cos(2\pi f_r \cos(\alpha_k^r)) \cos(2\pi f_s \cos(\alpha_k^s) + \Phi_{nmk}), \quad (3.15)$$

$$g_{qk}^{sr}(t) = \frac{1}{\sqrt{NM}} \sum_{n,m=1}^{M,N} \sin(2\pi f_r \cos(\alpha_k^r)) \cos(2\pi f_s \cos(\alpha_k^s) + \Phi_{nmk}), \quad (3.16)$$

where N is the number of scatterers of source node and M is the number of scatterers of relay node. The random phase, Φ_{nmk} , is uniformly distributed on the interval $[-\pi, \pi)$. Maximum Doppler shifts occurring at source and relay nodes (f_s and f_r) are computed as shown in Equation (2.1). The angles of the scatterers at the source (α_k^s) and the relay (α_k^r) are given as:

$$\alpha_k^s = \frac{2\pi n}{4N} + \frac{2\pi k}{4PN} + \frac{\Omega - \pi}{4N}, \quad (3.17)$$

$$\alpha_k^r = 0.5 \left(\frac{2\pi m}{M} + \frac{2\pi k}{PM} + \frac{\Psi - \pi}{M} \right), \quad (3.18)$$

where $k = 0 \dots P - 1$ is the number of complex envelopes, Ω and Ψ are random variables that possess identical and independently distributed (i.i.d.) uniform random variables across the interval $[-\pi, \pi)$. The complex envelope of the vehicular networks with LOS component is obtained by:

$$z_k^{sr}(t) = \frac{g^{sr}(t) + \sqrt{K} \exp(j2\pi f_0 t + \Phi_0)}{\sqrt{1 + K}}, \quad (3.19)$$

where Φ_0 is an independent and identically distributed (i.i.d.) random variable across the interval $[-\pi, \pi)$ and K is the Rician coefficient. The Doppler shift caused by relative speeds of vehicles on LOS path is defined as [42, Ch 9]:

$$f_0 = (|v_r| \cos \theta_r - |v_s| \cos \theta_s) / \lambda, \quad (3.20)$$

where λ is wavelength. A multipath channel impulse response function of time (t) and excess delay (τ) is defined as [175, pg 760]:

$$h^{sr}(\tau, t) = \sum_{k=0}^{P-1} h_k^{sr}(t) e^{-j2\pi f_c \tau_k(t)} \delta[\tau - \tau_k(t)], \quad (3.21)$$

where $h_k^{sr}(t)$ is k^{th} independent channel envelope, and f_c is carrier frequency, which is defined as 5.9 GHz for the vehicular networks analyzed in this work. The channel impulse response for all three links are obtained by using the same method.

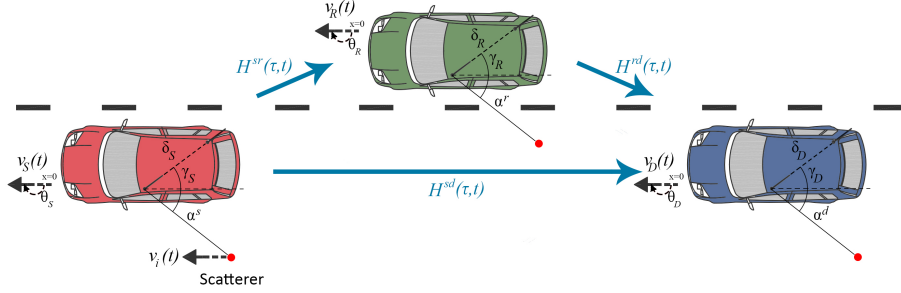


Figure 3.10: MIMO relaying vehicular network architecture. Channel impulse responses are defined as $\mathbf{H}^{sr}(\tau, t)$, $\mathbf{H}^{sd}(\tau, t)$, and $\mathbf{H}^{rd}(\tau, t)$. The distances between antennas on the top of vehicle is δ . The angle between antenna spacing and x -axis is γ .

The autocorrelation, or second order statistics, of the channel impulse response, which defines the duration channel stays stable, is given as [42, Ch 9]:

$$R_{sr}(\tau) = \frac{2J_0(2\pi f_s \tau)J_0(2\pi f_r \tau) + K e^{-j2\pi f_0 \tau}}{1 + K}, \quad (3.22)$$

while the received signals at the relay and destination are given for the DF relaying time varying channels as:

$$r(t) = \int_{-\infty}^{\infty} h^{sr}(\tau, t) x_s(t - \tau) dx_s + n_r, \quad (3.23)$$

$$y(t) = \int_{-\infty}^{\infty} h^{sd}(\tau, t) x_s(t - \tau) dx_s + h^{rd}(\tau, t) x_r(t - \tau) dx_r + n_y. \quad (3.24)$$

3.2.3.2 MIMO SoS Model with LOS Component

Spatial diversity provides a communication system with a higher reliability at MIMO systems [176]. However, MIMO technology has not been extensively deployed in CVNs due to its complexity [59]. In this section, a reliable channel model for MIMO-based DF relaying vehicular communication is obtained with LOS component. The applied relaying model is extended from point-to-point model proposed in [61]. The envelope matrix of a Rayleigh MIMO model is given in Equations (3.20) – (3.22) for $N_t \times N_r$ antenna arrays.

In these derivations, $w_s = 2\pi f_s$ and $w_r = 2\pi f_r$, $R_x = 3 - 2N_t/\lambda$ and $R_y = 3 - N_r/\lambda$, where N_t and N_r are number of antennas at the transmitter and receiver vehicles, δ_s and δ_r are the distances between two antennas at the source and relay vehicles, respectively (see Figure 3.10). The angle between antenna spacing and x -axis are γ_s at the source node and γ_r at the relay node.

$$\mathbf{G}^{sr}(t) = \begin{bmatrix} \mathbf{g}_{11i}^{sr}(t) + j\mathbf{g}_{11q}^{sr}(t) & \cdots & \mathbf{g}_{1N_r i}^{sr}(t) + j\mathbf{g}_{1N_r q}^{sr}(t) \\ \cdots & \cdots & \cdots \\ \mathbf{g}_{N_t 1i}^{sr}(t) + j\mathbf{g}_{N_t 1q}^{sr}(t) & \cdots & \mathbf{g}_{N_t N_r i}^{sr}(t) + j\mathbf{g}_{N_t N_r q}^{sr}(t) \end{bmatrix}, \quad (3.20)$$

$$\mathbf{g}_{xyi}^{sr}(t) = \frac{1}{\sqrt{NM}} \sum_{n,m=1}^{N,M} \cos(R_x \delta_s \cos(\alpha_s - \gamma_s) + w_s t \cos(\alpha_s - \theta_s)) \cdot \cos(R_y \delta_r \cos(\alpha_r - \gamma_r) + w_r t \cos(\alpha_r - \theta_r) + \Phi_{nm}), \quad (3.21)$$

$$\mathbf{g}_{xyq}^{sr}(t) = \frac{1}{\sqrt{NM}} \sum_{n,m=1}^{N,M} \sin(R_x \delta_s \cos(\alpha_s - \gamma_s) + w_s t \cos(\alpha_s - \theta_s)) \cdot \sin(R_y \delta_r \sin(\alpha_r - \gamma_r) + w_r t \sin(\alpha_r - \theta_r) + \Phi_{nm}). \quad (3.22)$$

The source node moves towards the direction with the angle of θ_s to x -axis, similarly θ_r for relay node and θ_d for destination node. The uniform random phase Φ_{nm} is in interval of $[-\pi, \pi]$. The angles of the random scatterers are similar to the SISO case, yielding:

$$\alpha_s = \frac{2\pi n}{4N} + \frac{\Omega - \pi}{4N}, \quad (3.23)$$

$$\alpha_r = 0.5 \left(\frac{2\pi m}{M} + \frac{\Psi - \pi}{M} \right). \quad (3.24)$$

By using a Rayleigh complex envelope, the Rician envelope is obtained using:

$$z^{sr}(t) = \frac{g_{xy}^{sr}(t) + \sqrt{K} \exp(j2\pi f_0 t + \Phi_0)}{\sqrt{1 + K}}, \quad (3.25)$$

where K is the Rician coefficient, Φ_0 is the random phase in the interval $[-\pi, \pi]$, and Doppler frequency of the LOS component is derived as:

$$f_0 = (|v_r| \cos(\theta_r - \gamma_r) - |v_s| \cos(\theta_s - \gamma_s)) / \lambda. \quad (3.26)$$

The multipath channel impulse response function of time (t) and excess delay (τ) is computed by using Equation (3.21). By determining all of the elements of the channel matrix, the Rician

channel impulse response for the $N_t \times N_r$ MIMO links matrix is given as:

$$\mathbf{H}^{sr}(\tau, t) = \begin{bmatrix} h_{11}^{sr}(\tau, t) & \dots & h_{1N_r}^{sr}(\tau, t) \\ \dots & \dots & \dots \\ h_{N_t1}^{sr}(\tau, t) & \dots & h_{N_tN_r}^{sr}(\tau, t) \end{bmatrix}. \quad (3.27)$$

This method is used for computing all channel links. The received signals at the relay and destination for DF MIMO relaying time varying channels are:

$$\mathbf{r}(t) = \int_{-\infty}^{\infty} \mathbf{H}^{sr}(\tau, t) \mathbf{x}_s(t - \tau) dx_s + \mathbf{n}_r, \quad (3.28)$$

$$\mathbf{y}(t) = \int_{-\infty}^{\infty} \mathbf{H}^{sd}(\tau, t) \mathbf{x}_s(t - \tau) dx_s + \int_{-\infty}^{\infty} \mathbf{H}^{rd}(\tau, t) \mathbf{x}_r(t - \tau) dx_r + \mathbf{n}_y. \quad (3.29)$$

As a result, both geometrical and SoS models take each scatterer around the vehicle as one path and sums the multipath contributions to find the channel impulse responses. Geometrical model assumes the number and the location of the scatterers are exactly known and uses the geometrical parameters of this given information. However, this assumption may not be realistic since estimation of the location of the scatterers in the dynamic vehicular environment is challenging. On the other hand, the SoS model assigns the location of scatterers statistically. Furthermore, it considers the time delay between the multipaths. These features make SoS model more realistic and more accurate than geometrical model.

3.3 Derivation of Lower Bound on the Capacity for Relaying Connected Vehicles

The channel capacity of the relay network, which is provider a limit within information flow on the network in the presence of noise and interference, is analyzed in order to demonstrate the efficiency of the proposed models. For the relay network, we cannot define the exact capacity since BC and MAC are vector channels. However, we can derive the upper and lower bounds of the capacity. In this chapter, we derive only lower bounds of the channels for SISO and MIMO cases since lower and upper bounds are very close numbers to each other, *i.e.*, 0 – 1 bit/sec/Hz difference [169, 174, 177].

In the analysis, the receivers have perfect channel state information (CSI) and the transmitters have only covariance feedback. This case provides more realistic perspective than perfect CSI at

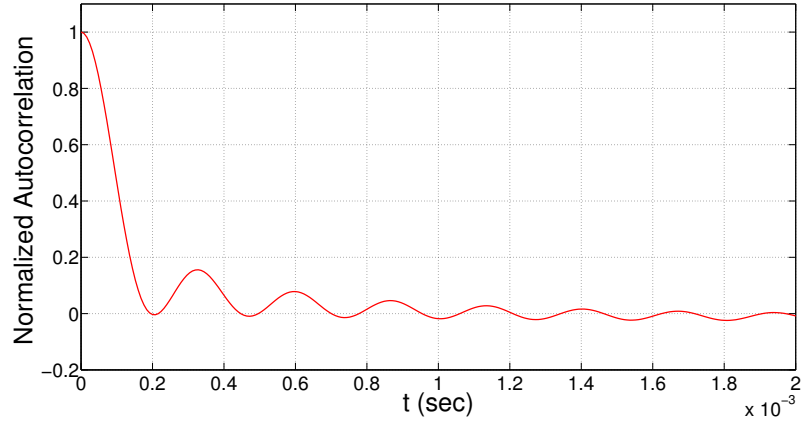


Figure 3.11: Autocorrelation of a CVN link. The channel is constant for 0.05 ms. Since a packet is transferred in 8 μ s on DSRC architecture, capacity bounds are computed as block fading.

the transmitters. We perform full duplex mode communications with individual power constraints at the source and relay.

The relay channel DF lower bound presented in [169] is valid for block fading channels where the channel remains the same during a transmission block and jumps to another realization for the next block. CVN links remain stable during approximately 0.05 ms, as shown in Figure 3.11. The block fading assumption makes sense since the time interval of the DSRC channel is 8 μ s. Under a block fading assumption, we can define discrete channel random processes $(c_i^{sr}, c_i^{sd}, c_i^{rd})$ from the channel impulse responses, where i is the running index of successive blocks. Note that random variables corresponding to successive blocks are correlated, although this does not violate the achievability proof of [169].

3.3.1 SISO Relaying Connected Vehicles

The channel impulse responses $(h^{sr}(\tau, t), h^{sd}(\tau, t), h^{rd}(\tau, t))$ for the SISO relaying connected vehicles are defined in Equation (3.21). The channel envelopes that fit to SoS model define the discrete channel random processes $(c_i^{sr}, c_i^{sd}, c_i^{rd})$. The lower bound on the capacity of a SISO

relay-based CVNs is given as [177]:

$$R_{SISO} = \max(I_{sd}, \min(I_{mac}, I_{sr})), \quad (3.30)$$

$$I_{sr} = E \left[\log \left(1 + P_{sr} |c^{sr}|^2 \right) \right], \quad (3.31)$$

$$I_{sd} = E \left[\log \left(1 + P_{sd} |c^{sd}|^2 \right) \right], \quad (3.32)$$

$$I_{mac} = E \left[\log \left(1 + P_{sd} |c^{sd}|^2 + P_{rd} |c^{rd}|^2 \right) \right], \quad (3.33)$$

where the signal-to-noise ratio (SNR) of the source-to-relay, source-to-destination, and relay-to-destination links are P_{sr} , P_{sd} , and P_{rd} , respectively.

It is important to note that using the ergodicity of the channel random process, we can calculate the above capacity as an average over time instead of finding the probability distribution functions of the channel random processes. By using SoS model for fading relaying vehicular network, lower bound on the capacity is computed with the consideration of vehicular propagation characteristics such as Doppler shift, scatterers.

3.3.2 MIMO Relaying Connected Vehicles

Similar to the SISO case, we can assume block fading and define the block fading channel random processes \mathbf{C}_i^{sr} , \mathbf{C}_i^{sd} and \mathbf{C}_i^{rd} from the channel impulse responses ($\mathbf{H}^{sr}(\tau, t)$, $\mathbf{H}^{sd}(\tau, t)$, and $\mathbf{H}^{rd}(\tau, t)$). Then, the lower bound on the capacity of MIMO relay vehicular communication is given as [174, 177]:

$$R_{MIMO} = \max_{\text{tr}(\mathbf{Q}_s) \leq P_s, \text{tr}(\mathbf{Q}_r) \leq P_r} \max(\mathbf{I}_{sd}, \min(\mathbf{I}_{mac}, \mathbf{I}_{sr})), \quad (3.34)$$

$$\mathbf{I}_{sr} = E \left[\log \left| \mathbf{I} + \mathbf{C}^{sr} \mathbf{Q}_s \mathbf{C}^{sr\dagger} \right| \right], \quad (3.35)$$

$$\mathbf{I}_{sd} = E \left[\log \left| \mathbf{I} + \mathbf{C}^{sd} \mathbf{Q}_s \mathbf{C}^{sd\dagger} \right| \right], \quad (3.36)$$

$$\mathbf{I}_{mac} = E \left[\log \left| \mathbf{I} + \mathbf{C}^{mac} \mathbf{Q}_{mac} \mathbf{C}^{mac\dagger} \right| \right], \quad (3.37)$$

where:

$$\mathbf{C}^{mac} = \begin{bmatrix} \mathbf{C}^{sd} & \mathbf{C}^{rd} \end{bmatrix}, \quad (3.38)$$

$$\mathbf{Q}_{mac} = [\mathbf{Q}_s, \mathbf{Q}_r], \quad (3.39)$$

with L_s and L_r being the number of antennas at the source and relay. The covariance matrices of the transmitted signals at the source and relay are $\mathbf{Q}_s = E[\mathbf{x}_s \mathbf{x}_s^\dagger]$ and $\mathbf{Q}_r = E[\mathbf{x}_r \mathbf{x}_r^\dagger]$, respectively and the power constraints at the transmitters are $\text{tr}(\mathbf{Q}_s) \leq P_s$ and $\text{tr}(\mathbf{Q}_r) \leq P_r$.

3.4 Selective Message Relaying Algorithm

The advantages of multi-hopping vehicular communications are explained in the previous sections. To enable safe and efficient multi-hopping vehicular communications, there are several technical challenges associated with CVNs. The periodic broadcasting at the source vehicles and the rebroadcasting the same information at the relay vehicles result in a significant number of messages. However, most of the rebroadcast messages are redundant or not useful information for the destination vehicles. With the large number of messages, high network and processing loads cause significant message delays and message losses. The existing works require specific information in messages such as message directions.

In this section, we present a selective message relaying algorithm that relays information and only rebroadcasts a few non-redundant messages that are useful for other vehicles. To the best of our knowledge, selective message relaying in V2V networks without contextual knowledge of the destination vehicles has not been proposed before. The proposed algorithm rebroadcasts urgent safety messages immediately without any selection. For the rest of the received messages, the proposed algorithm utilizes a hierarchical clustering mechanism to identify similar information among those received messages. The number of clusters is decided by a technique considering the proximity of the messages, and only a few messages from each cluster are selected and rebroadcast. It is important to note that the proposed algorithm selects messages and *rebroadcasts* them. It is a completely different approach from traditional routing techniques, such as Position Based Forwarding (PBF) [178], Contention-Based Forwarding (CBF) [179], and Ad hoc On-Demand Distance Vector (AODV) [180], which choose destination vehicles and forward messages. The proposed clustering mechanism detects redundant the information, and selects messages to rebroadcast without sacrificing environmental awareness. Therefore, network and processing loads are decreased since only a few messages from each cluster are rebroadcast. Moreover, the proposed algorithm uses only general information in messages such as time stamp, location, and message

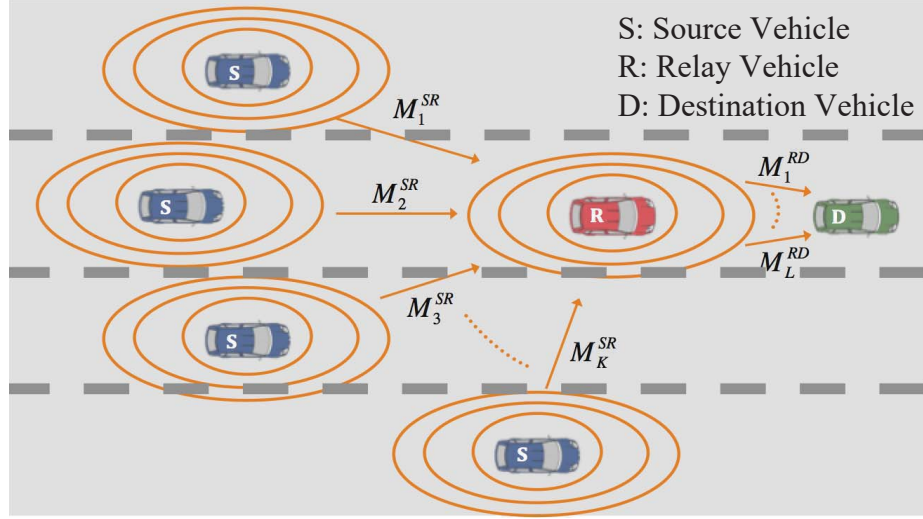


Figure 3.12: Relaying architecture. The source (blue) vehicles periodically broadcast the messages about environment status. The relay (red) vehicle receives these messages, performs the proposed algorithm, and then rebroadcasts the selected messages to the destination (green) vehicle.

priority so that it can be applied to many real-world applications.

Vehicles between the *source* and *destination* vehicles¹ play the roles of *relay* vehicles to propagate information. Figure 3.12 shows an example. The relay vehicle receives the messages broadcast by source vehicles near the event region. The received messages are denoted as M_i^{SR} where $i = 1, 2, \dots, K$ and K is the number of received messages. The relay vehicle decides which information is crucial or worth rebroadcasting and rebroadcasts the selected messages. The rebroadcast messages are denoted as M_j^{RD} where $j = 1, 2, \dots, L$ and L is the number of rebroadcast messages. We assume that relay vehicle has sufficient computing ability or the computation can be supported by other devices such as laptops. We also assume that all vehicles have dedicated short-range communications (DSRC) devices [23], and there are one transmitting and one receiving omnidirectional antennas at each vehicle.

The standardized broadcast scheme is used [23]. The MAC layer performs the traditional Request to Send/Clear to Send (RTS/CTS) mechanism in order to avoid the hidden node problem and broadcast collisions. Additionally, the exponential backoff time is utilized based on the wireless access in vehicular environments (WAVE) standard [26]. The network architecture utilizes

¹Source and destination here are conceptual terms. In practical, all messages are broadcast without specifying destinations.

the BSM format, as defined in IEEE 802.11p [23], which includes core state information such as location, speed, and brake status, as well as path history and prediction. These messages are typically on the order of 300–400 bytes [46] with a 6 Mbps data rate and a 10 Hz message rate, and transmitted over 300–500 meters. Usually, a vehicle can handle up to 2,000 messages per second, so some works adjust the message rates to avoid congestion. Rather than decreasing the message rates to solve the network congestion problem, our goal is to let the relay vehicle select crucial or representative messages and rebroadcast them to the destination vehicle(s), so we will focus on the selection algorithm in Section 3.4.3.

3.4.1 Real-World Applications

In this part, we present several real-world applications that the proposed selective message relaying algorithm can be applied. The first application is intersection awareness, as shown in Figure 3.13(a). The source vehicles near the intersection broadcast the environmental situation. The relay vehicle eliminates the redundant messages and rebroadcasts useful information to the destination vehicle which is approaching the intersection. The second application is emergency vehicle warning, as shown in Figure 3.13(b). The source vehicles create the messages indicating the presence of the approaching emergency vehicle. The relay vehicle eliminates the redundant messages and rebroadcasts useful information to the destination vehicle ahead so that it can yield the emergency vehicle. The other two applications are side road merging and sharp curve assistant as shown in Figure 3.13(c) and Figure 3.13(d). They have several common features. The destination vehicle does not have a direct line-of-sight to the environment where the source vehicles are located. Furthermore, similar (or even redundant) messages are created from different source vehicles so that a relay vehicle should perform message selection. The application list can be extended to cover collision warning, parking lot assistance, traffic jam warning, and so on.

These application can be performed more efficiently by using the proposed selective message relaying algorithm. The proposed mechanism detects the redundant information and rebroadcast only the unique information. Therefore, the same environmental awareness is provided by relaying a smaller number of messages. Hence, message delay and congestion in the message buffer are avoided.

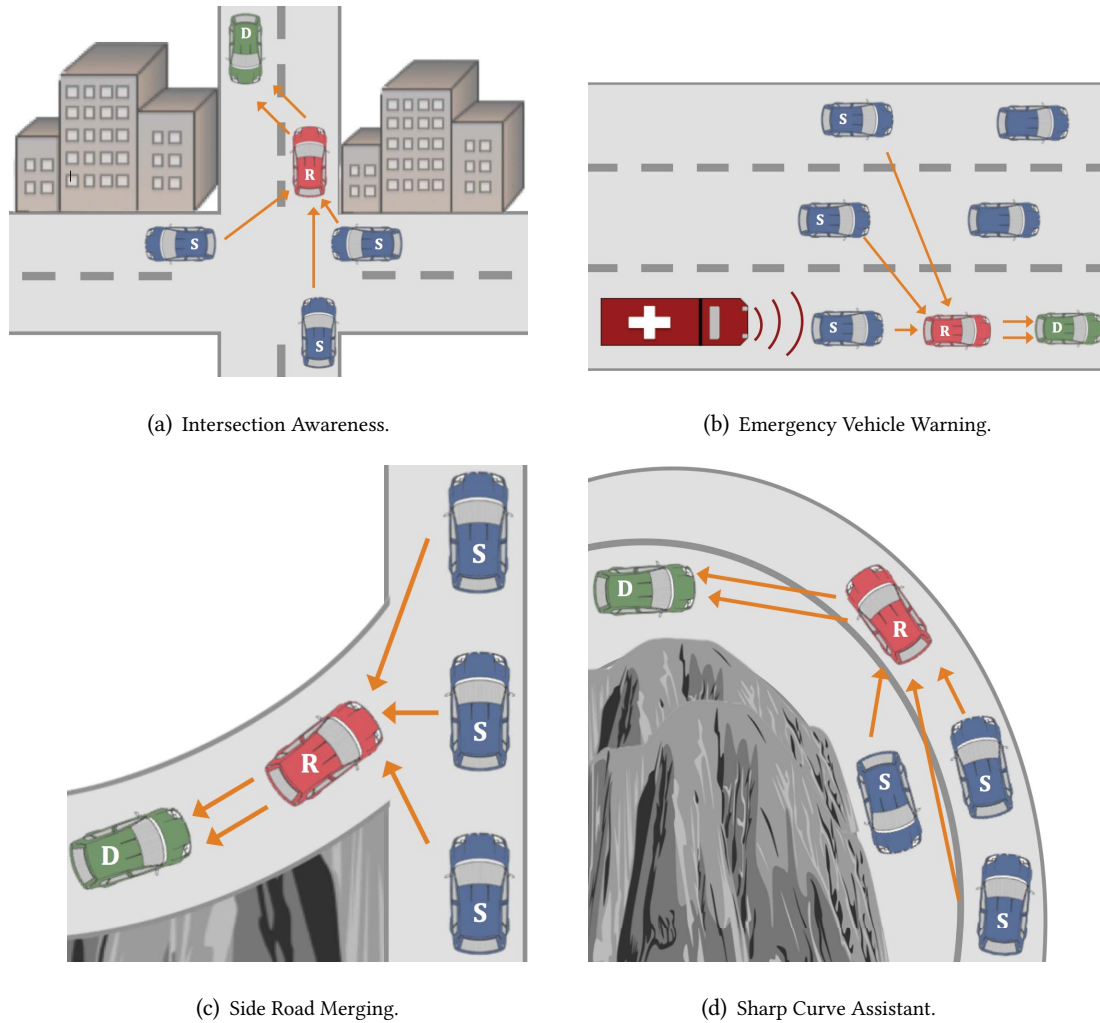


Figure 3.13: Real-world applications that the proposed selective message relaying algorithm can be applied. S, R, and D represent the source, relay, and destination vehicles, respectively.

3.4.2 Performance Metrics

To evaluate cooperative awareness in vehicular environments, we use the following three metrics:

- **Rebroadcasting Rate:** The number of messages that are rebroadcasted to the destination vehicle(s). This metric is highly related to processing delay and system efficiency.
- **Processing Delay:** The summation of computing delay and queuing delay. The computing

delay is measured directly, and the processing delay is calculated by the M/M/1 queuing model [181]. Assuming a Poisson arrival rate and exponential service time, the expected response time for broadcast messages is defined as [182]:

$$E[T_r] = \frac{1}{\mu} \left(1 + \frac{\rho}{1 - \rho} \right), \quad (3.40)$$

where μ is the service rate of the relay vehicle, which is set to 2,000 messages per second, and ρ is the traffic intensity for first-come-first-serve behavior, which is defined as:

$$\rho = \frac{V\lambda}{\mu}, \quad (3.41)$$

where V is the number of source vehicles, and λ is the message rate, which is set to 10 Hz (as defined in the standard). Processing delay measures the system efficiency.

- **Vehicle Coverage:** The number of vehicles that receive the message of corresponding events. This metric measures the level of environmental awareness.

3.4.3 Proposed Algorithm

The goal of the proposed algorithm is to identify crucial or representative messages received by a relay vehicle and only rebroadcast them for the destination vehicles. Due to different environments and traffic conditions, the relay vehicle will receive various numbers of messages at different broadcast periods, so the proposed algorithm uses an adaptive clustering mechanism which can be used in different environments and traffic conditions.

3.4.3.1 Message Clustering

Clustering mechanisms find the set of objects that are more similar to each other than the other sets of objects² [183]. There are three main clustering methods that are commonly used: K -means [184], density-based [185], and hierarchical [186]. K -means clustering associates each cluster with its centroid. K -means clustering is not the best for the selective message relaying problem since its performance is very dependent on initial cluster centroids. Furthermore, outlier data points, *i.e.*, those very different messages from the others, can cause K -means clustering

²Objects are referred to received messages of a relay vehicle in our case.

Table 3.2: A set of K received messages.

Received Messages	Features					
	f_1	f_2	\cdots	f_j	\cdots	f_N
M_1^{SR}	x_{11}	x_{12}	\cdots	x_{1j}	\cdots	x_{1N}
M_i^{SR}	x_{i1}	x_{i2}	\cdots	x_{ij}	\cdots	x_{iN}
\cdots	\cdots	\cdots	\cdots	\cdots	\cdots	\cdots
M_K^{SR}	x_{K1}	x_{K2}	\cdots	x_{Kj}	\cdots	x_{KN}

to be nonfunctional. Regarding density-based clustering, the data set is evaluated by clustering high-density data points and leaving the low-density data points out of the clusters as outliers. This does not fit our problem since message clustering considers the similarities of the messages instead of how they are distributed. On the other hand, hierarchical clustering is independent of the initial centroids and capable of adapting to various information sets. Therefore, we use the agglomerative hierarchical clustering as our clustering mechanism.

In hierarchical clustering, each object is initially a cluster and then the closest two clusters are merged until a single cluster remains. The main paradigm of hierarchical clustering is the proximity matrix. Different approaches are proposed to define the distance between clusters such as the minimum or maximum distance between clusters. In this work, we use the average distance between clusters since it is more robust to outliers and noise. The Euclidean distance between message i and message j can be computed as:

$$d_{ij} = \sqrt{\sum_{n=1}^N (x_{in} - x_{jn})^2}, \quad (3.42)$$

where N is the number of features of a message and x_{in} is the n -th feature of message i . A set of K received messages is illustrated in Table 3.2.

We consider three features to define the location of a message in the clustering space: *message type*, *time stamp*, and *location* that the message is created. Although these three features are sufficient to define the similarity of messages, the interval (difference between the maximum and minimum values) of these features are relatively different from each other. For example, the distance between the source and relay vehicles is between $[0, 300]$ meters, while the time stamp is

between $[0, 60]$ seconds. To develop a reliable clustering mechanism, we need to process the received messages first and model the features in similar intervals. The modeling approach of each feature is addressed below. Note that we define the proposed algorithm with these three features to demonstrate the general idea. Besides them, any information in BSM can be utilized as a feature.

Message Type: The events that the broadcast message include have different priority levels. In IEEE 802.11p standard [23], four different access categories (AC), *i.e.*, message priorities, are defined. The first category, AC_0 , is assigned to the lowest priority messages, which are non-safety and non-urgent applications. The second category, AC_1 , is assigned to non-urgent events. The third category, AC_2 , is for environmental awareness or presence of other vehicles, especially when drivers have limited vision abilities. The highest priority, AC_3 , defines urgent safety messages [187].

With the message types, we assign the weight for message i with AC_0, AC_1, AC_2 to $P_i = 0.125, 0.25, 0.5$, respectively. All urgent safety messages, *i.e.*, AC_3 , are broadcast by default, so they do not need any message selection or weight assignment.

Temporal Feature: Each broadcast message includes the time stamp defined in Coordinated Universal Time (UTC) format. A relay vehicle computes the difference between the times that a message is created and the current time. We assign the temporal feature for message i as [71]:

$$T_i = e^{-\frac{1}{\alpha_i}(t_c - t_i)}, \quad (3.43)$$

where t_c is the current time, t_i is the time that message i is created, and α_i is the mean of exponential, which is defined based on message type. Here, we assign the means of AC_0, AC_1, AC_2 to 4, 8, 16, respectively. Again, AC_3 does not need this assignment.

Exponential modeling provides the property that a newer message has a higher value and an older one has a lower but never non-zero value (a message may still be useful for the destination vehicle although it gets older). A unique mean value is defined for each message type since a message with higher priority should decay slower as time goes. On the other hand, a message with lower priority should decay faster. For example, if two messages are created at the same time, one with AC_0 decays faster than the other with AC_3 .

Spatial Feature: The relevance of messages received by a relay vehicle intuitively has a neg-

Table 3.3: A set of K received messages after preprocessing.

Received Messages	Features		
	P	T	S
M_1^{SR}	P_1	T_1	S_1
M_i^{SR}	P_i	T_i	S_i
...
M_K^{SR}	P_K	T_K	S_K

ative correlation to the distance. We assign the spatial feature for message i as:

$$S_i = \begin{cases} 1 - \frac{D_i}{AR} & \text{if } D_i \leq AR; \\ 0 & \text{otherwise,} \end{cases} \quad (3.44)$$

where D_i is distance between the source and relay vehicles and AR is the awareness range that is pre-defined.

The preprocessing above provides the value of each feature needed for clustering message, and each feature is in the interval of $[0, 1]$. As an example, the raw data shown in Table 3.2 is transformed to the version as shown in Table 3.3. The hierarchical clustering is then performed on the features after preprocessing. Once the hierarchy is obtained, the next step is to decide the number of clusters on which the number of rebroadcast messages depends.

3.4.3.2 Number of Clusters

We use the L -method to obtain the number of clusters [188]. The method to obtain the adaptive number of clusters is based on the distance between messages in the clustering space [189]. The distance set is divided into two subsets, and the curve fitting is performed for these two subsets. The intersection of the extensions of the two fitting lines is decided as the number of clusters. In Figure 3.14, the method is illustrated, and the number of clusters is detected as 9. This number is used in hierarchy of messages as shown in Figure 3.15. As a result, the member of clusters are decided as the corresponding branches below the red line.

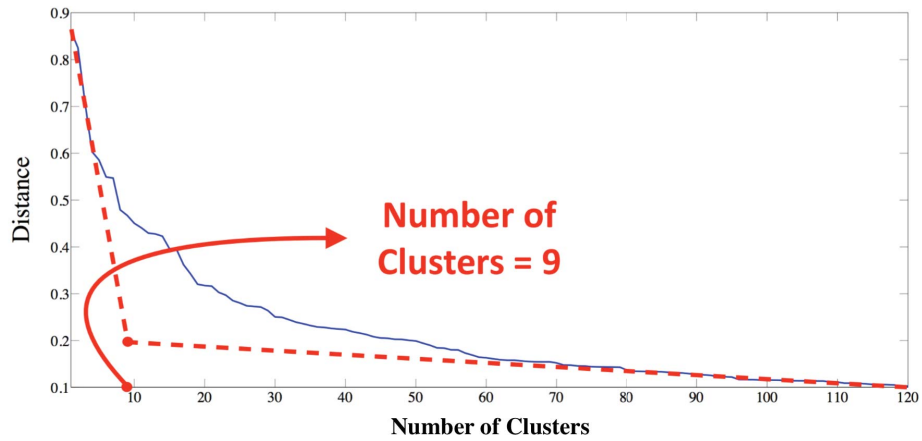


Figure 3.14: Distance between messages in the clustering space.

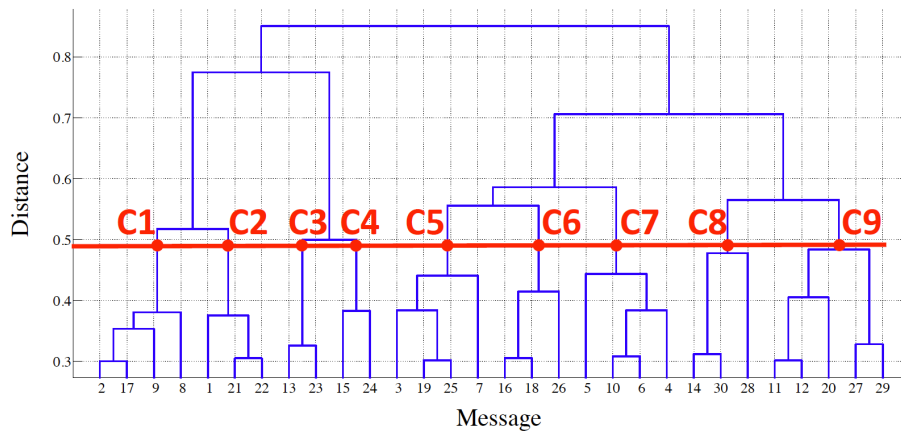


Figure 3.15: Hierarchical message clustering. The member of clusters are decided as the corresponding branches below the red line.

3.4.3.3 Message Selection for Rebroadcasting

The received messages at a relay vehicle are clustered based on their distances to each other in the clustering space. We use the centroids of clusters to represent the corresponding clusters, and the closest messages to the centroids are selected to be rebroadcast. Depending on the requirement of application context, multiple messages from each cluster can be selected to be rebroadcast. The proposed selective message relaying algorithm is summarized in Algorithm 1.

Algorithm 1 Selective Message Relaying Algorithm

```

1: /*preprocessing */
2: for Each message  $M_i^{SR}$  do
3:   if Message Type =  $AC_3$  then
4:     Rebroadcast;
5:   else
6:      $P_i = 0.125, 0.25, 0.5$  for  $AC_0, AC_1, AC_2$ , resp.;
7:      $T_i = e^{-\frac{1}{\alpha_i}(t_c - t_i)}$ ;
8:     if  $D_i \leq AR$  then
9:        $S_i = 1 - \frac{D_i}{AR}$ ;
10:    else
11:       $S_i = 0$ ;
12:    end if
13:  end if
14: end for
15: /*clustering */
16: Compute the distances between messages;
17: Build hierarchy;
18: Decide the number of clusters;
19: Decide the members of clusters;
20: Rebroadcast the closest messages to the centroids of clusters;

```

3.5 Numerical Results

We analyze the performance of the selective message relaying algorithm within a CVN environment using the GEMV² Vehicle-to-X (V2X) propagation simulator and MATLAB [43]. GEMV² is a computationally efficient propagation model for V2X communications, which explicitly accounts for surrounding objects. The environment map is created using Open Street Map [190]. The experimental traffic data is created in SUMO for a 1 km² region (shown in Figure 3.16) and used as an input to GEMV² [191]. The link colors between vehicles highlight the link powers. The experiment setup is summarized in Table 4.3.

By increasing number of scatterers, the accuracy of channel model also increases. However, higher number of scatterers means higher computational complexity. In this section, the numbers



Figure 3.16: Experimental traffic data. The environment map is created using Open Street Map. The buildings in the chosen area are defined by white blocks. Vehicle traffic, illustrated as red vehicles, is created using SUMO based on the environmental map. The random traffic defined within the area is used as an input to the GEMV² simulator. The link colors between vehicles show the link powers. If the link color is dark blue, the channel is noisy and experiencing strong fading. If the link color is red, the channel has little noise and fading.

of scatterers change between 6 and 12, and are located within the geographical vicinity of each node. These numbers are preferred for scatterers since more than these numbers does not make any change on the channel impulse response result.

The two-lanes highway scenario is considered, with traffic in each lane traveling in the same direction. The speeds of the vehicles have uniform random distribution in an interval of [40, 80] km/h and changes ± 10 km/h every time. The motion angle is chosen as $\theta_s = \theta_r = \theta_d = \pi$, which means the nodes move towards the negative x -axis. The wavelength is $\lambda = c/f_c = 3 \times 10^8 / 5.9 \times 10^9 = 0.0508$ 2m, where c is speed of light in m/s and carrier frequency of DSRC is $f_c = 5.9$ GHz.

The MIMO channel models are derived for 2×2 antenna arrays, but the model can be readily extended to $N_t \times N_r$ MIMO models. The antenna spacing of each vehicle is chosen as $\delta_s = \delta_r = \delta_d = 10\lambda$. Thus, it can be assumed that the antennas are uncorrelated. The angle between the antenna spacing and x -axis for each vehicle is $\gamma_s = \gamma_r = \gamma_d = \pi/2$.

Since the geometrical model depends on the radius of scatterer and the angles/distance between vehicles, we denote these parameters setup as well. The radii of the isotropic scatterers are $R_s =$

Table 3.4: System Parameter Setup.

Parameter	Value
Message Size (Byte)	375
Message Rate (Hz)	10
Transmission Power (dBm)	23
Carrier Sense Threshold (dBm)	-90
Noise Floor (dBm)	-113
Max Transmission Range (m)	300
Message Period (msec)	100

$R_r = R_d = 50$ m, and the initial distance between each two nodes is $D_s = D_r = D_d = 200$ m. Since the initial distance is same for each node pair, the initial angle between vehicles are $\pi/3$ radians. Changing the vehicles speeds, the distances and angles are computed by the algorithm for each time constant.

3.5.1 Simulation Results

We start with an analysis of the proposed framework for the SISO DF relaying CVNs. The channel impulse response is a random process, which depends on time (t) and excess delay (τ) for time varying multipath channels. In Figure 3.17, the changing on power of channel impulse response ($|h_{sr}^2(\tau, t)|$) is shown for source to relay link (h_{sr}). The channel impulse response changes for each time constant. In addition, channel impulse response is non-zero only for some excess delays. This result matches with the real data measurements shown in [192, pg 108].

The characteristics of the channel model are provided below such that they can be used in order to help to understand the propagation characteristics. The spreading function, which is also referred to as the delay Doppler spreading function, of a random process channel model demonstrates the channel behavior by changing the Doppler shift and excess delay [193]:

$$S_{sr}(v, \tau) = \int_{-\infty}^{\infty} h_{sr}(\tau, t) e^{-j2\pi vt} dt. \quad (3.45)$$

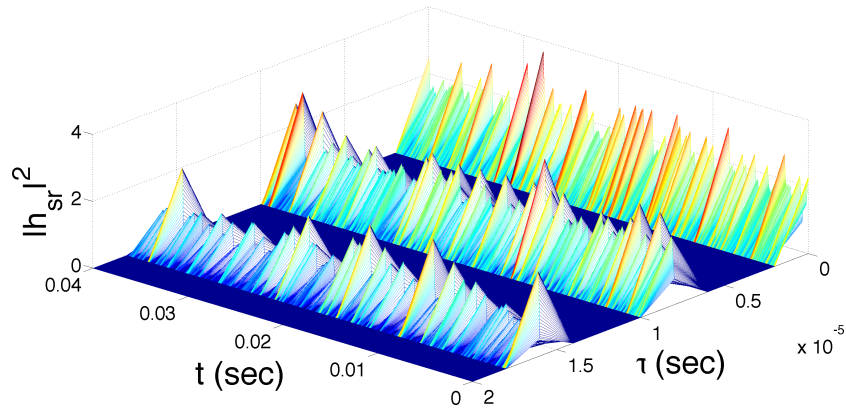


Figure 3.17: Squared magnitude of the source to relay channel impulse response. Carrier frequency is 5.9 GHz; τ is excess delay; t is time variation.

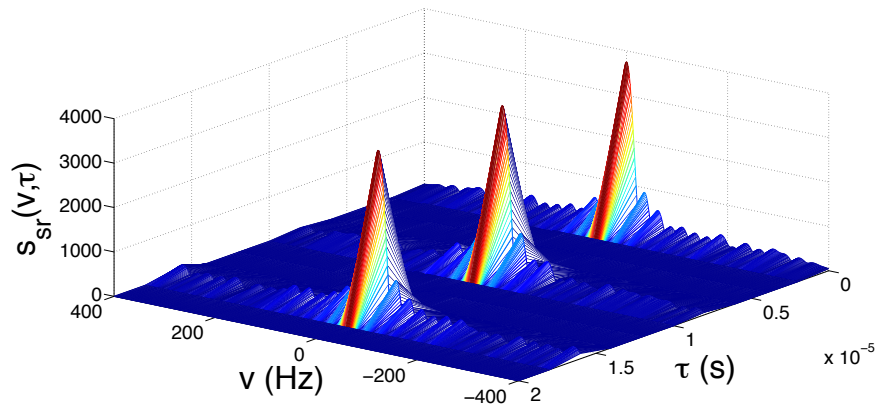
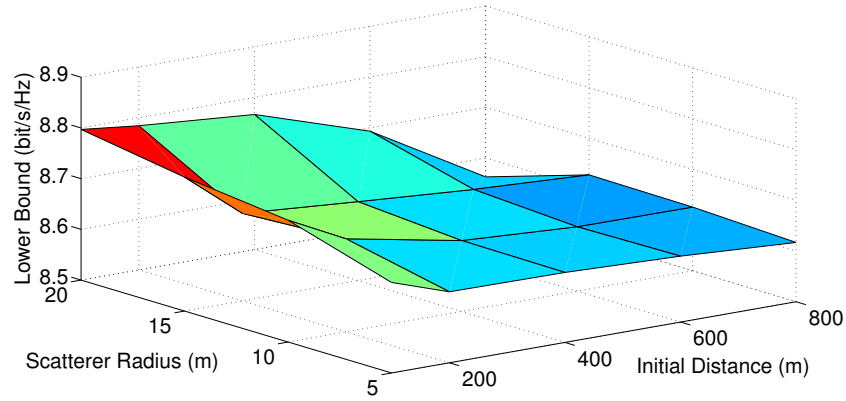


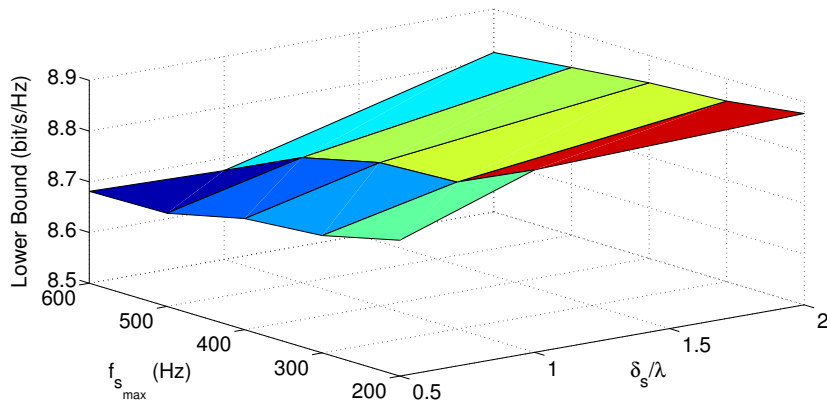
Figure 3.18: Spreading function of the source to relay channel impulse response. τ is excess delay; v is Doppler shift.

In Figure 3.18, the spreading function of the channel is shown, where v is the Doppler shift and τ is the excess delay. When the Doppler shift is small, the channel impulse response has highest power. However, the channel power decreases by increasing the Doppler shift.

Geometrical channel model is defined by immediate channel elements depending on the geometrical parameters. In Figure 3.19(a), the changes on lower bound is shown based on initial distances ($D_{sr} = D_{rd} = D_{sd}$) and scatterer radii ($R_r = R_s = R_d$). Since the longer distance causes higher interference on the channel, the lower bound decreases by increasing initial dis-



(a)



(b)

Figure 3.19: Impact of parameters to the lower bound on the capacity. (a) Lower bound depending on scatterer radii and initial distances. By increasing initial distance, the lower bound decreases. Conversely, lower bound increases by increasing scatterer radius. (b) Lower bound depending on antenna spacing (δ_s/λ) and maximum Doppler frequency ($f_{s_{max}}$). Lower bound increases by increasing antenna spacing since the effect of interference reduces. By increasing Doppler frequency, lower bound decreases since the scattering effect is increasing.

tance. Moreover, increased scatterer radius transform the channel behavior from interfered channel to multi-path channel. Therefore, lower bound increases by increased scatterer radius. In Figure 3.19(b), the effects of Doppler frequency($f_{s_{max}}$) and antenna spacing (δ_s) is shown. Since Doppler effect causes the distortion on channel, lower bound decreases by increasing maximum

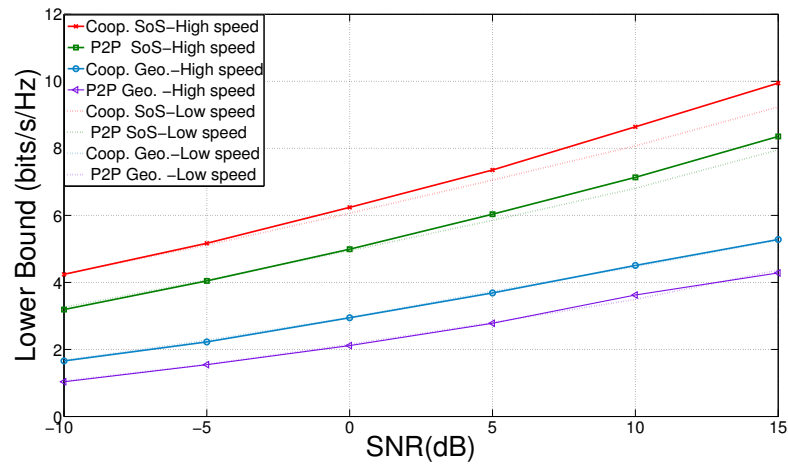


Figure 3.20: Comparison of lower bound on the network capacity given by two different models for both high and low speeds. SoS model has better rate performance since the excess delay (τ) is taken into account.

Doppler frequency value. Conversely, lower bound increases when the antennas move away each other since the mitigation of interference effect.

In Figure 3.20, the lower bound on the capacity of applied SoS model with LOS component and geometrical model [34] are compared for both high and low speed vehicles. By using the same amount of resources, the chosen model provides higher network capacity. The reason for this result is that the SoS model takes into account the excess delay of the time varying multipath channels while geometrical model assumes there is no excess delay. Adding to that, the SoS model does not need any rapid measurements, such as the distances and angles between cars. Since the geometrical model needs those measurements, the SoS model is more handy relative to the geometrical model for vehicle-to-vehicle (V2V) networks. The analysis of low speed vehicles, which is shown as dashed lines, indicate that the SoS model is more sensitive to speed changes, especially for high SNRs. In the same figure, the capacity of the P2P transmission is also shown for both models. The results expose the benefit of cooperative communication on CVNs.

In Figure 3.21, the autocorrelation function of both the applied SoS model and the existing geometrical model are compared with the theoretical model [37]. While the same resources are used in all model setup, statistics of SoS model matches with the reference model.

In Figure 3.22, the normalized spreading functions of both models are compared. The spread-

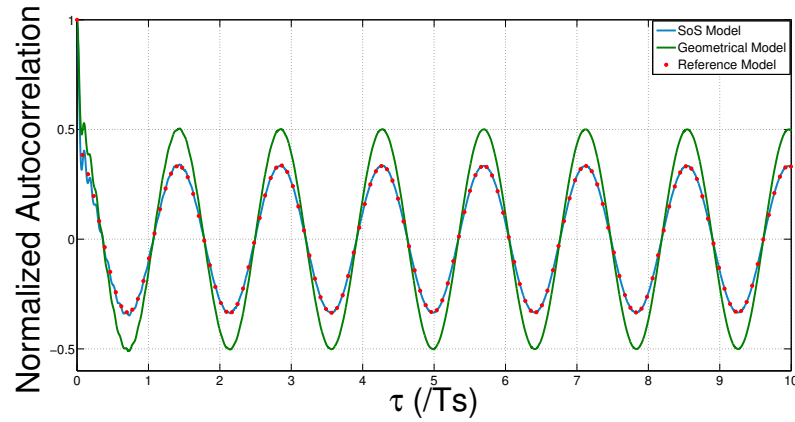


Figure 3.21: Comparison of normalized autocorrelation given by geometrical and SoS models. Although proposed SoS model and geometrical model use the same amount of resources, autocorrelation function of the SoS model matches with theoretical reference model.

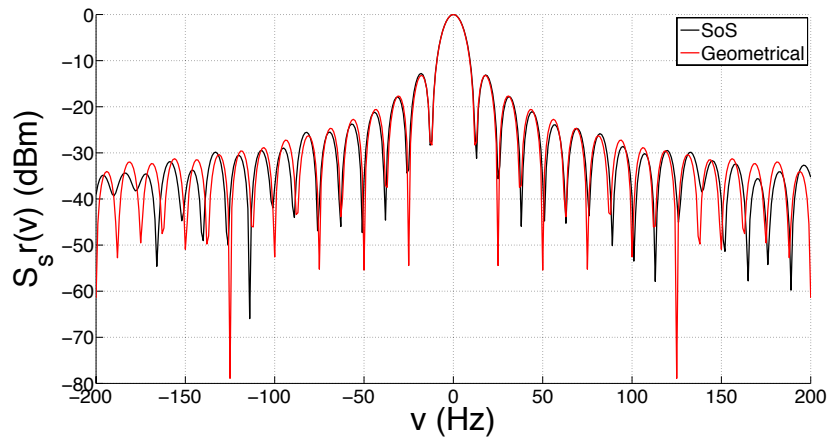


Figure 3.22: Normalized Spreading functions for both SoS and geometrical model. The amplitude of geometrical model decreases slightly faster than the amplitude of SoS model by increasing Doppler shift.

ing function of proposed SoS model is 3-D, as shown in Figure 3.18, since it is random process. However, geometrical model is random variable, so that, the comparison is done in 2-D platform by one of the excess delay value is chosen for SoS model. The Doppler effect is almost the same for both models but the geometrical model decreases a little sharper than the SoS model by increasing the Doppler shift.

After analyzing the performance using the SISO models, the lower bound on the capacity is

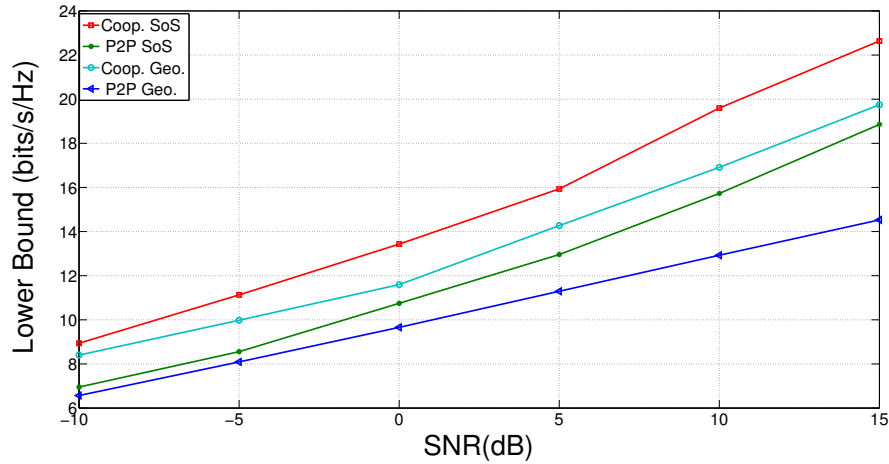


Figure 3.23: Lower bound on the capacity of MIMO SoS model with LOS component and geometrical model for both cooperative and direct transmissions. For the same input parameters SoS model has higher achievable rate than geometrical model. Both models provide better performance by using relay-based approach rather than P2P transmission.

analyzed for the MIMO relay-based CVNs. Since the other channel characteristics are the same with the SISO model, they are not denoted here. In Figure 3.23, the lower bound results are shown for both geometrical and SoS models. It can be observed that the cooperative transmission possess a higher capacity relative to the P2P transmission for both models due to the benefit of spatial diversity. In addition, as shown in Figure 3.23, the MIMO SoS model with an LOS component has a higher lower bound relative to the MIMO geometrical model for the same resources.

In Figure 3.24, the messages which are created in the transmission range around the relay vehicle are shown. The colors of messages are referred to the priorities of messages, and the messages with grey stars are selected to be rebroadcast. As shown in the figure, all AC_3 messages are rebroadcast without selection. Several other messages are selected based on the combination of their types, time stamps, and locations.

In Figure 3.25, the number of rebroadcast messages (rebroadcasting rate) is shown with respect to the number of connected vehicles. The number of rebroadcast messages linearly increases without any selection mechanism by the increasing number of vehicles in the experiment region. The data preference mechanism, known as packet-valuecast (PVcast), was proposed by Xiang *et al.* [71] and is used as a comparative approach. Compared with rebroadcasting without any selection,

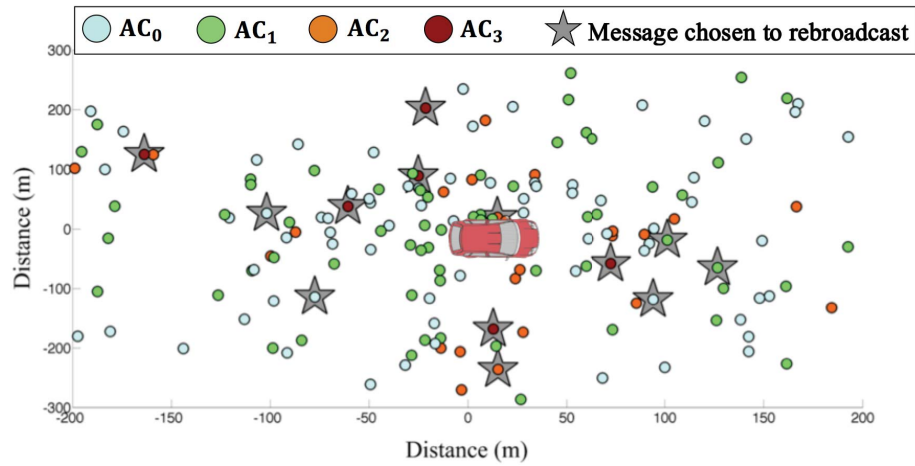


Figure 3.24: Message map. The points show the locations where the messages are created. The colors of messages are referred to the priorities of messages, and the messages with grey stars are selected to be rebroadcasted.

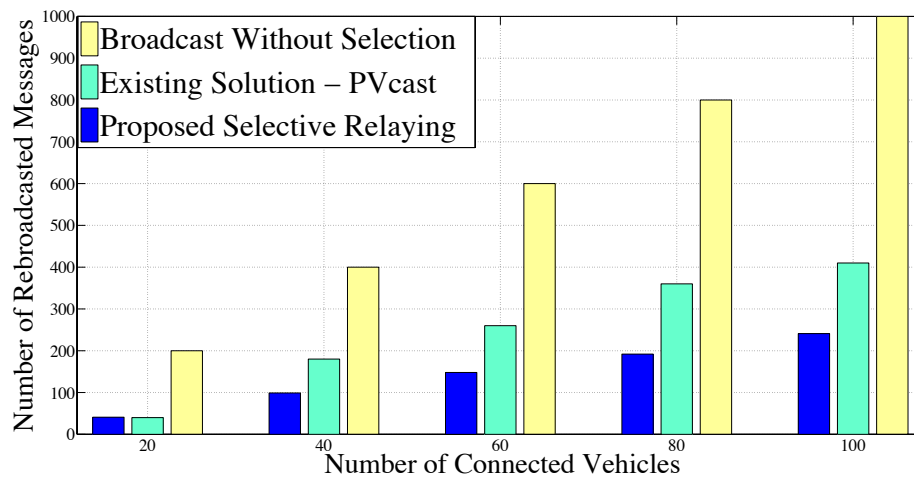


Figure 3.25: The number of rebroadcasted messages (rebroadcasting rate) with respect to the number of connected vehicles.

the proposed algorithm decreases the number of rebroadcast messages by around 75% without sacrificing the environmental awareness. Additionally, it also rebroadcast fewer messages than PVcast without sacrificing the environmental awareness since PVcast decides which packet will be rebroadcast based on their priority assigned by the proposed algorithm. Therefore, some of the redundant messages are rebroadcast more than one time if their assigned priority values are large. Since proposed selective message relaying algorithm considers both the priority of messages

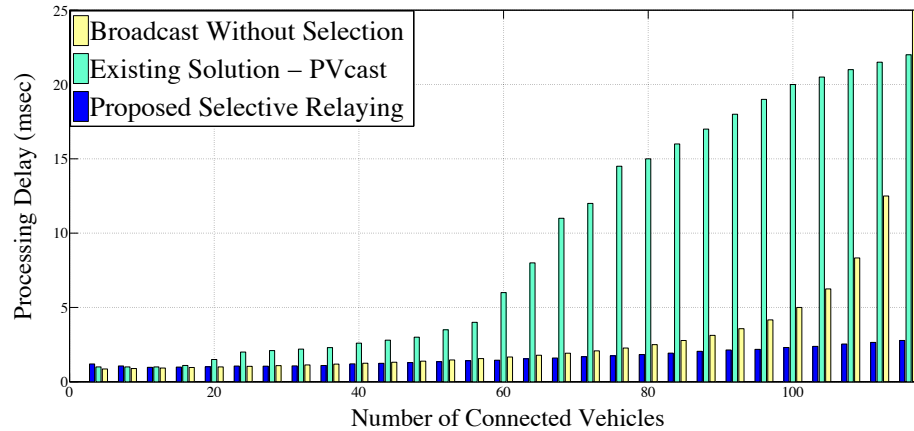


Figure 3.26: Processing delay with respect to the number of connected vehicles.

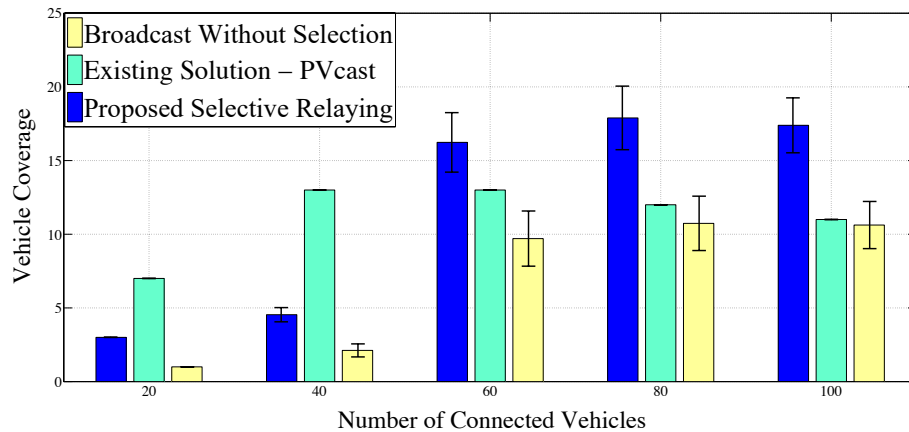


Figure 3.27: Vehicle coverage with respect to the number of connected vehicles.

and their uniqueness, it rebroadcasts less number of messages to provide the same environmental awareness.

In Figure 3.26, the processing delay is shown with respect to the number of connected vehicles³. In the cases of fewer vehicles, the proposed algorithm has the same or slightly higher processing delay than the two comparative approaches. This is due to the computation time of the proposed algorithm. However, in the cases of more vehicles, the proposed algorithm has significant processing delay reduction, compared with the two other approaches. This shows that the proposed

³Experiment is run with Intel Core *i7* and 2.2 GHz processor, and the selective message relaying algorithm takes less than 2 msec.

algorithm is less sensitive to the number of connected vehicles, and it provides better scalability for various network environments.

In Figure 3.27, vehicle coverage is shown with respect to the number of connected vehicles. In the cases of fewer vehicles, queuing delay is not a concern, and thus PVcast has high performance. However, as the number of connected vehicles increases, the proposed algorithm outperforms PVcast. This is because the proposed algorithm can reduce queuing delay and thus prevent message loss or expiration, demonstrating again that it has better scalability.

3.6 Chapter Summary

In this chapter, we explored large and small scale fading characteristics of CVNs. We analyzed large scale fading for different link types. The proposed large scale channel models are compared with the real-world measurements and observed that the results match. We derive two small scale channel models for Decode-and-Forward (DF) relaying. We analyzed the lower bound on the channel capacity for multi-hopping CVNs to compare the performance of various network settings. We explored the benefits of multi-hopping CVNs over P2P communication. Lastly, we proposed a selective message relaying algorithm to increase the performance of multi-hopping CVNs by solving message overhead on rebroadcasting operation at the relay vehicle. The proposed algorithm reduces 75% message rebroadcasting without sacrificing environmental awareness and has very good scalability which is especially important for future highly-loaded vehicular networks. In this chapter, we understand the system behavior by exploring the channel characteristics. In the following chapters, the distributed adaptation techniques are proposed by considering these channel characteristics. In addition to optimization of the relaying operation for multi-hop CVNs in this chapter, we propose a distributed congestion control algorithm for cooperation with the one-hop neighbors to make the CVNs more efficient in the next chapter to make the CVNs communication more reliable.

Chapter 4

Environment Aware Cooperative Distributed Congestion Control on Vehicular Network

Safety and efficiency applications in vehicular networks rely on the exchange of periodic messages between vehicles. The drawback of exchanging periodic cooperative messages is that they generate significant channel load. Decentralized Congestion Control (DCC) algorithms have been proposed to minimize the channel load. However, while the rationale for periodic message exchange is to improve awareness, existing DCC algorithms do not use awareness as a metric for deciding when, at what power, and at what rate the periodic messages need to be sent in order to make sure all vehicles are informed. In this chapter, we propose a transmit power control approach designed to achieve cooperative neighborhood awareness for vehicles, while the rate control is subsequently employed to utilize the available resources. Specifically, we propose an algorithm called ECPR (Environment- and Context-aware Combined Power and Rate Distributed Congestion Control for Vehicular Communication), which is a combined power and rate control DCC algorithm that aims to improve the cooperative awareness for challenging environments, while at the same time increasing the message rate when the environment and application re-

The work presented in this chapter has been published in parts at [P1] and [J7].

quirements¹ permits. To comply with target channel load/capacity requirements, ECPR employs an adaptive rate control algorithm. In this work, we use LIMERIC [78], a state-of-the-art adaptive rate control algorithm, although other adaptive rate control algorithms could serve the same purpose. We performed simulations with ECPR in an experimentally validated simulation tool [43] and showed that it can provide gains in terms of awareness or throughput in realistic propagation environments. The proposed mechanism is briefly presented in ETSI 101 613 [194].

Compared to current state-of-the-art, the main contributions of our work are:

- A practical algorithm to incorporate awareness – a key building block for CVN applications – as a core metric for congestion control in CVNs. ECPR proactively considers the effect of power adaptation on rate adaptation and *vice versa*, so that it can adapt the mechanisms more efficiently at the next algorithm step.
- By adjusting the transmit power based on the awareness criterion, we enable: i) congestion control adaptation to the dynamic propagation environment surrounding vehicles; and ii) effective adaptation of cooperative awareness range based on the application context, including requirements of different safety and non-safety applications, speed of vehicles, and different traffic conditions per direction.
- By combining rate and awareness control, the proposed algorithm can achieve one of the following goals: i) improved channel utilization (in terms of the overall number of messages exchanged) for a given awareness rate; or ii) improved cooperative awareness for a given channel utilization;

We perform extensive simulations including both realistic propagation and environment modeling (*e.g.* large- and small-scale fading parameters, dynamic transitions between LOS and NLOS links based on real building and vehicle locations) as well as realistic vehicle contexts (varying demand on both awareness by range and rate). We show that ECPR increases awareness by up to 20% while keeping the channel load within reasonable bounds and interference at almost the same level. When the target awareness distance permits it, our proposed algorithm improves the average message rate by approximately 18%, while keeping the target awareness.

¹We use the term “application requirements” to encompass the effects that determine the rate and awareness requirements for a vehicle (*e.g.*, speed, traffic conditions, and currently active application).

4.1 Environment- and Application Context-aware Congestion Control

The work presented in this chapter aims at designing a novel DCC solution for V2V communication that can satisfy the target awareness levels for different application contexts in different realistic propagation environments. As noted earlier, cooperative awareness is vital for CVNs since many applications need to be aware of neighboring vehicles to trigger the correct type of action for avoidance of hazardous situations (*e.g.*, accident prevention). To that end, in this section we discuss the main design goals for DCC algorithm and introduce metrics we use for evaluation of the algorithms.

4.1.1 Design goals

To obtain acceptable performance in terms of cooperative awareness, DCC algorithms need to take into account the following aspects:

- *Application context*, determined by vehicular traffic conditions and application constraints, yields the requirements in terms of rate (amount of data) and communication and awareness range. Based on the application context, the DCC algorithm needs to distribute the available channel resources in a fair way (fair both in terms of achieved awareness and rate).
- Due to varying vehicular traffic density and mobility, *the network topology* is highly dynamic and depends on the time of day, type of road and other features [33,195]. The DCC algorithm needs to be adaptive with respect to network dynamics at a rate higher than the rate of change of network.
- *The propagation environment* where vehicular communication occurs can be highly varying, even within a relatively small area. Environment characteristics of urban, suburban and rural areas create different challenges for congestion control and awareness [46]. The environment creates effects similar on network topology to that of varying traffic density and mobility, albeit with geographically constrained dynamics.
- In addition to the effect of static objects near the road, *surrounding vehicles* also introduce

significant variation in the reception probability and network topology. Depending on vehicle size, a vehicle can completely block the communication between two other vehicles [196]. Hence, a vehicle on a highway with dense traffic (*e.g.*, morning rush hour) will have larger number of neighbors and a limited communication range due to the obstruction by surrounding vehicles; on the same highway during late of night, a vehicle will have fewer neighbors and an increased range. The DCC algorithm should be able to adapt to such variations.

- Electromagnetic emission regulations, limited channel resources, and potentially high number of communicating entities (including vehicles and roadside units) create practical limits on the ability to control the power and rate parameters.

Figure 4.1 shows how the physical environment affects the awareness range [197], whereas Figure 4.2 shows how the application context requirements affect the target awareness range [198]. In reality, there will exist numerous scenarios where the effects of the environment and application context will be combined, with the applications setting the awareness and rate requirements and the environment shaping the awareness range. Our goal in this study is to design a DCC solution that can efficiently support the functioning of safety and non-safety applications in diverse and dynamic CVN scenarios.

4.1.2 Metrics

One of the main goals of cooperative awareness is to enable drivers/vehicles to enhance their knowledge of the environment in order to augment the information that they can obtain visually. To that end, cooperative message exchange mechanisms need to ensure that vehicles are aware of other relevant vehicles within the same geographical proximity, including those that are in NLOS conditions. However, achieving this goal efficiently is a challenge since environments where vehicular communication occurs are quite diverse. For example, the transmit power required to send a message to a vehicle in an open environment (*e.g.*, highway scenario) at a certain distance will likely be much lower than the power required to send a message to a vehicle at the same distance in a NLOS environment (*e.g.*, urban scenario) as shown in Figure 4.3 [46].

To evaluate cooperative awareness in vehicular environments, we use two metrics introduced

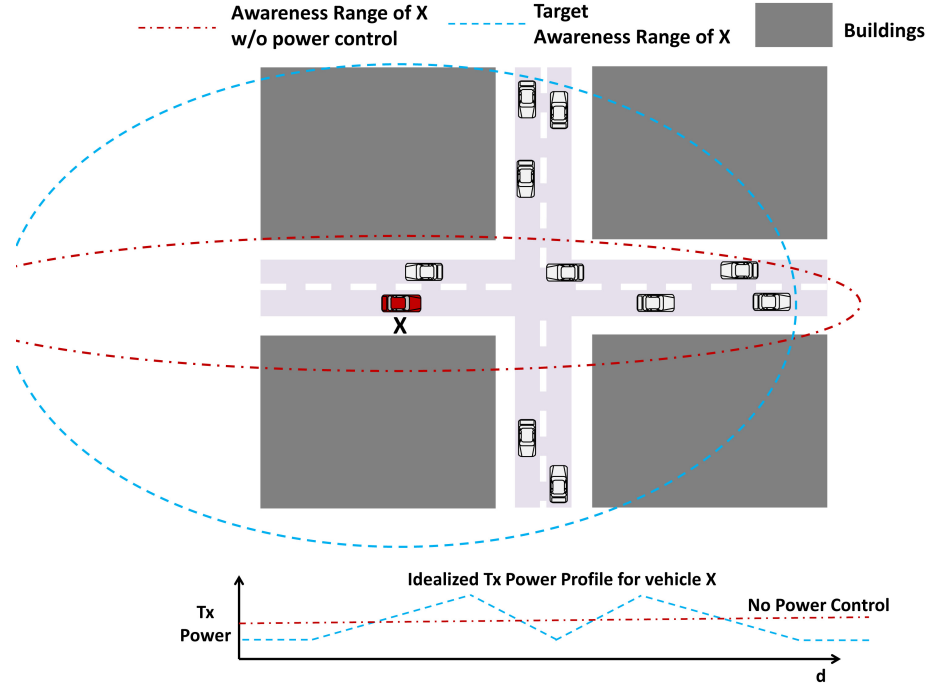


Figure 4.1: An example of how environment shapes the awareness range. Due to the particular environment layout, with buildings surrounding the intersection, if it is using fixed transmit power, vehicle X is likely to inform the vehicles on the same road of its existence, with a limited awareness of vehicles on the perpendicular road, up until X is in the intersection, at which point vehicles on both roads are likely to be aware of it. However, for active safety applications, awareness of vehicles on perpendicular road is more valuable than that on the same road, since the drivers of those vehicles cannot see vehicle X. Thus, for most CVN applications, it is assumed that the target awareness/communication range is a circular shape (or as circular as possible) of certain radius. Achieving such range in different environments requires power control. Lower part of the figure shows an idealized transmit power profile to adapt to the intersection environment for vehicle X as it travels through the intersection.

in previous work [46]: Neighborhood Awareness Ratio (NAR) and Ratio of Neighbors Above Range (RNAR). For completeness, we define these metrics as follows:

- **NAR**: The proportion of vehicles in a specific range from which a message was received in a defined time interval. Formally, for vehicle i , range r , and time interval t , $NAR_{i,r,t} = \frac{ND_{i,r,t}}{NT_{i,r,t}}$, where $ND_{i,r,t}$ is the number of vehicles within r around i from which i received a message in t and $NT_{i,r,t}$ is the total number of vehicles within r around i in t (we use $t=1$ second). This metric measures the ability of cooperative message exchange to fulfill its purpose: enable cooperative awareness.

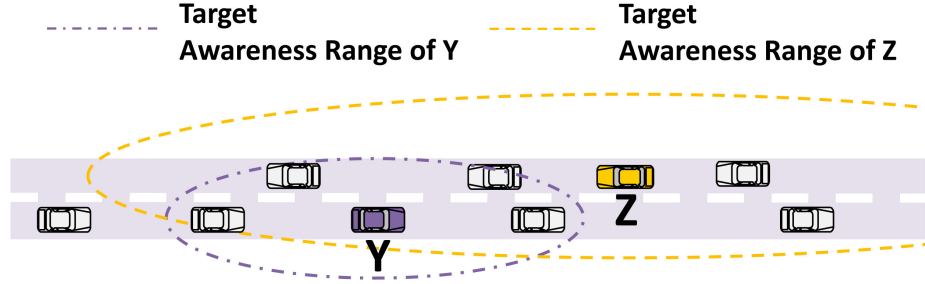


Figure 4.2: Depending on the application context, which includes the speed of the vehicle, traffic context and the type of currently active application, vehicles can have different target awareness ranges. For example, vehicle Y can be going at a lower speed than vehicle Z, in which case it might require smaller awareness range. Similarly, vehicle Z might be executing a safety-critical application (*e.g.*, emergency vehicle notification), in which case it requires larger awareness range

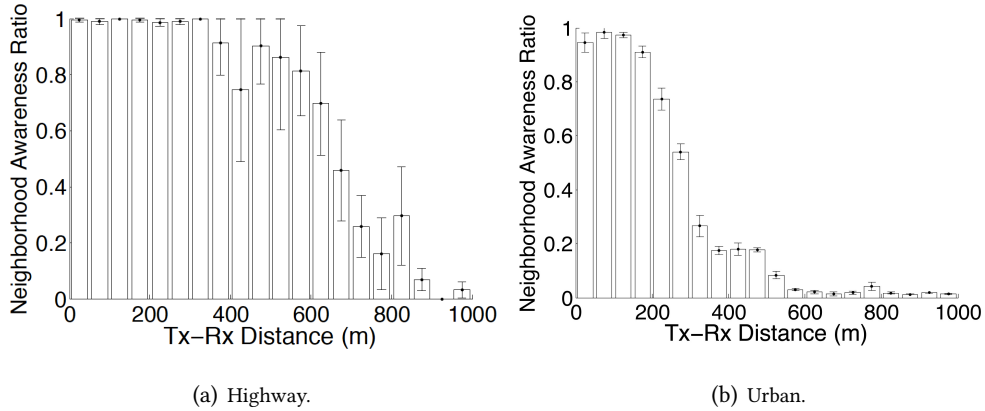


Figure 4.3: Measurements of NAR in Tampere, Finland. Measurements in both environments were collected using in the same measurement run based on the same vehicles, fixed transmit power, and 10 cooperative messages sent per second.

- RNAR:** For a vehicle i , range r , and time interval t , the ratio of neighbors that are above a certain distance from the observed vehicle $RNAR_{i,r,t} = \frac{NA_{i,r,t}}{N_{i,t}}$, where $NA_{i,r,t}$ is the number of vehicles above r from which i received a message in t (again, we use $t=1$ second) and $N_{i,t}$ is the total number of vehicles from which i received a message in t (irrespective of r). This metric gives an indication of potentially unnecessary traffic overheard from distant neighbors (*i.e.*, those that are not relevant for current application context). Once the technology is deployed at a large scale (*i.e.*, with communication equipment installed in most vehicles), such traffic will translate to unwanted interference.

In addition to NAR and RNAR, we also analyze the the performance of DCC in terms of the following metrics.

- ***Average Message Rate*** shows the number of messages that a vehicle can transmit per second, averaged over all vehicles for a given second.
- ***Average Transmit Power*** shows the average transmit power messages that a vehicle transmits, averaged over all vehicles for a given second.
- ***Channel Busy Ratio (CBR)*** is defined as the proportion of channel time where the energy measured on the channel is above the Clear Channel Assessment (CCA) threshold.

4.2 Proposed ECPR Algorithm

In this section, we describe the proposed ECPR (Environment- and Context-aware Combined Power and Rate Distributed Congestion Control) algorithm. The goal of ECPR is to satisfy the requirements of target awareness levels for different application contexts in different realistic propagation environments, along with utilizing the available channel resources. Due to possibly different application contexts and environments, the vehicles will have different target awareness ranges and different target rates. To that end, ECPR uses power to control awareness range (distance) for the vehicles, whereas it uses rate to utilize the channel resources as allowed by the awareness requirements. In other words, ECPR attempts to satisfy the awareness requirements, at the same time maximizing the rate of messages through rate control. If the vehicles require low rates in order to not overload the channel, ECPR will set the transmit power of the vehicles to a maximum value. However, when the channel load increases (either due to higher rate requirements or due to an increased number of vehicles), ECPR is able to reduce the power in order to support such scenarios by considering the awareness requirement. Below we explain how power and rate control components are implemented, along with the way they are combined to reach the abovementioned goals.

4.2.1 Power Adaptation for Awareness Control

The power adaptation component of ECPR adapts the transmit power based on the current target awareness range set by the application context. ECPR is capable of adapting to dynamic scenarios with varying application contexts and in different environments without requiring *explicit knowledge about the surroundings*, such as map information. To do so, it needs to estimate the channel path loss for all vehicles from which a message has been received the past time segment t . Consequently, each vehicle requires knowledge of the transmit power level of the messages sent from each of its neighbors. The value of neighbor's transmit power information can be transmitted in the form of an integer value (e.g., between 0 and 33 dBm), which can be piggybacked in the transmitted messages (e.g., in cooperative awareness messages or in data packets).

To adjust the transmit power in order to meet the awareness requirement, ECPR use Path Loss Exponent (PLE) estimation. The transmit power adaptation algorithm is described as follows:

- **Define:** *Ego vehicle:* The vehicle that is currently estimating its DCC parameters;
Neighbor: Vehicle from which ego vehicle received a message within time segment $[t - 1, t]$ sec
- **Given:** Ego vehicles' transmit power at time t : $P_e^{Tx}(t)$;
 i^{th} neighbor's transmit power at time t : $P_i^{Tx}(t)$, where $i = 1, \dots, N$ (N : Known number of neighbors within range);
 Target awareness range of ego vehicle $r_e(t)$;
 Target awareness percentage of ego vehicle within $r_e(t)$ (Target NAR described in Section 4.1.2) : $TA_e(t)$
- For each received message, calculate $d_{ij}(t)$, distance between ego vehicle and i^{th} neighbor at time t when message j was received
- Select neighbors that are within target awareness range $r_e(t)$; select messages which are received from neighbors within $r_e(t)$
- Compute $PLE_{ij}(t)$ (PLE for message j from neighbor i) by using log-distance path loss as

per [171]:

$$PLE_{ij}(t) = \frac{PL_{ij}(t)}{10 \log_{10} \left(\frac{4\pi}{\lambda} d_{ij}(t) \right)}, \quad (4.1)$$

where λ the signal wavelength and $PL_{ij}(t)$ is the path loss for message j of neighbor i :

$$PL_{ij}(t) = P_i^{Tx}(t) - P_{ij}^{Rx}(t), \quad (4.2)$$

where $P_i^{Tx}(t)$ and $P_{ij}^{Rx}(t)$ are the transmit (Tx) of neighbor i and receive (Rx) power of j^{th} message from neighbor i , respectively.

- Calculate ego's nodes transmit power required to reach i^{th} neighbor for next time step, $P_{e \rightarrow i}^{Tx}(t+1)$, using $PLE_{ij}(t)$ and calculating the mean transmit power required for messages received from i^{th} neighbor (with the mean over messages taken so as to counter the effects of fading):

$$P_{e \rightarrow i}^{Tx}(t+1) = \frac{1}{m} \sum_{j=1}^m P_{ij}^{Rx}(t) + 10 PLE_{ij}(t) \log_{10} \left(\frac{4\pi}{\lambda} r_e(t) \right). \quad (4.3)$$

- Set ego node's transmit power for next time step ($t+1$) by considering the target awareness distance $r_e(t)$ and target awareness percentage $TA_e(t)$, provided as input of the application context. Sort the required transmit power to each neighbor and select $TA_e(t)$ -th percentile transmit power:

$$P_{_sorted}_e^{Tx} = \text{sort}_{i=1}^N (P_{e \rightarrow i}^{Tx}(t+1)), \quad (4.4)$$

$$P_e^{Tx}(t+1) = P_{_sorted}_e^{Tx}[\text{round}(TA_e(t) * N)]. \quad (4.5)$$

Implicitly, by estimating the PLE from the received messages to adjust the transmit power, ECPR estimates what are the “worst” channels with *all* vehicles within the awareness range r_e (*i.e.*, not only those from which a vehicle received messages correctly). By receiving messages from enough neighbors, ECPR gets an idea at what transmit power messages need to be sent at in order to reach the vehicles in r_e . In other words, by using PLE estimation, ECPR attempts to reach even those vehicles from which the ego vehicle has not yet received a message. As long as the received power is higher than carrier sensing threshold, the transmit power at the next time step to the corresponding neighbor can be estimated. For the extreme cases such as very large path loss

with a short distance, probably more than one neighbor will suffer from large path loss issue in the current environment. In that case, ECPR calculates Equation 4-5 and keep the transmit power high to reach the target awareness. The frame error level (less than $< 5\%$) is neglected since there is not a significant impact on performance. It will be shown in Section ?? that ECPR is a robust adaptation mechanism even in situations with significant MAC layer collisions.

4.2.2 Rate Adaptation

In this work, we employ the LInear MESSage Rate Integrated Control (LIMERIC) algorithm [78] to perform the rate adaptation aspect of ECPR due to its ability to converge to a fair and efficient channel utilization.² LIMERIC takes the current channel busy ratio (CBR) and the current beacon rate as an input to the rate adaptation algorithm. The next beacon rate is adjusted to keep the current CBR under the threshold CBR, which is set to 0.6 in this work [73]. The next message rate ($R_j(t)$) adaptation is done by Monte Carlo iteration at each ego node as defined below:

$$R_j(t) = (1 - \alpha)R(t - 1) + \text{sign}(R_g - R_c(t - 1))\min[X, \beta * |R_g - R_c(t - 1)|], \quad (4.6)$$

where R_c is the message rate, α and β are the convergence parameters, and R_g is target rate which satisfies the threshold CBR. For a detailed description of LIMERIC, we refer the reader to Bansal *et al.* [78].

Recent measurement-based studies showed that message exchanges in vehicular environments are dominated by shadowing scenarios (*i.e.*, obstruction by buildings, vehicles), where messages are both received and lost in bursts depending on the channel quality [46, 199]. This implies that sending fewer high-power messages in NLOS scenarios have a better chance of creating awareness between vehicles than sending multiple successive messages at a lower transmit power. However, the current state-of-the-art with respect to DCC algorithms do not provision for making sure that the hard-to-reach vehicles are informed via cooperative awareness message exchange. Furthermore, depending on the speed of the vehicle, the type of traffic context (*e.g.*, congested highway, busy or empty intersection) and the type of active application [198], target regions of interest (which directly translates into awareness range) can vary for different vehicles. Rate-control-only

²We note that ECPR is capable of performing combined adaptation for congestion control with other adaptive rate control algorithms.

Table 4.1: Parameters used in the proposed algorithm

Parameter	Definition
t	Time (sec)
$r_e(t)$	Target awareness range at time t (m)
P_i^{Tx}	Transmit Power of j 'th message from neighbor i within $r_e(t)$ (dBm)
P_{ij}^{Rx}	Rx Power of j 'th message from neighbor i within $r_e(t)$ (dBm)
$d_{ij}(t)$	i^{th} neighbor's distance within $r_e(t)$ at time t when receiving message j (m)
$DefaultTxPwr$	Default transmit power (dBm)
$TA_e(t)$	Target awareness of ego node at time t (no unit)
$CBR(t)$	Channel Busy Rate at time t (no unit)
lm_j	Length of the j 'th message received by ego vehicle (byte/sec)
C	Capacity of channel in terms of time (byte/sec)
$a = 0.1, b = 1/150$	LIMERIC parameters (see eq. 4.6) (no unit)
CBR_{Th}	Threshold CBR (no unit)
δ_A	Difference between target and actual awareness (no unit)
$eNAR(t)$	Estimated Neighbor Awareness Ratio at time t (no unit)
δ_R	The ratio of the difference between target and actual rate to target rate (no unit)
$TR(t)$	Target message rate at time t (Hz)
$BR(t)$	Message rate at time t (Hz)
γ	Awareness/rate preference coefficient (no unit)

algorithms, which are proposed for the initial iteration of V2X systems [73], cannot accommodate for different awareness ranges.

4.2.3 Combining power and rate control

Algorithm 2 describes the steps of the ECPR algorithm, whereas Table 4.1 summarizes the parameters used by ECPR. The proposed combined control algorithm adapts the next transmission power based on the current path loss ($PL_{ij}(t)$) and path loss exponent ($PLE_{ij}(t)$) for each message (j) received from the neighbors (See Algorithm 2: Line 1-2). If the neighbor i was already ego node's neighbor in the previous time step, the algorithm assigns the required transmit power to

Algorithm 2 Environment-Aware Combined Power and Rate Control for Vehicular Communication (ECPR) algorithm

```

1:  $PL_{ij}(t) = P_i^{Tx}(t) - P_{ij}^{Rx}(t)$ 
2:  $PLE_{ij}(t) = \frac{PL_{ij}(t)}{10 \log_{10}(\frac{4\pi}{\lambda} d_{ij}(t))}$ 
3: if  $Neighbor_{e \rightarrow i}(t) \in Neighborhood_e(t-1)$  then
4:    $P_{e \rightarrow i}^{Tx}(t) = \frac{1}{m} \sum_{j=1}^m P_{ij}^{Rx}(t) + 10 PLE_{ij}(t) \log_{10}(\frac{4\pi}{\lambda} r_e(t))$ 
5: else
6:    $P_{e \rightarrow i}^{Tx}(t) \leftarrow DefaultTxPwr$ 
7: end if
8:  $P_{sorted_e}^{Tx} = sort_{\forall i, j \in N}(P_{e \rightarrow i}^{Tx}(t+1))$ 
9:  $P_e^{Tx}(t+1) = P_{sorted_e}^{Tx}[round(TA_e(t) * N)]$ 
10:  $CBR(t) = \sum_{j=1}^n lm_j / C$ 
11:  $BR(t+1) = (1-a)BR(t) + sign(CBR_{Th} - CBR(t)) * min[X, b(CBR_{Th} - CBR(t))]$ 
12:  $\delta_A = TA_e(t) - eNAR(t)$ 
13:  $\delta_R = \frac{TR(t) - BR(t)}{TR(t)}$ 
14: if  $CBR(t) < CBR_{Th}$  then
15:   Apply  $P_e^{Tx}(t+1)$ 
16: else
17:   if  $P_e^{Tx}(t+1) \leq P_e^{Tx}(t)$  then
18:     Apply  $P_e^{Tx}(t+1)$ 
19:   else if  $\delta_A \geq \gamma \delta_R$  then
20:     Apply  $P_e^{Tx}(t+1)$ 
21:   else
22:      $P_e^{Tx}(t+1) \leftarrow P_e^{Tx}(t)$ 
23:   end if
24: end if

```

this neighbor based on the current $PL_{ij}(t)$, $PLE_{ij}(t)$, and target awareness range. Conversely, if this vehicle was not a neighbor to the ego node in the previous time step, a default value (e.g., 10 dBm or 23 dBm in our simulations) is used as needed in order for the transmission power to

reach this neighbor. By using the default transmit power value, the ego node increases the probability of being heard by those nodes for which it does not know what kind of power is needed to reach them (See Algorithm 2: Line 3-6). Once the ego node has the transmission power information it needs to reach each of the neighbors, it sorts these values from the least to the most. The next transmission power level of the ego node is chosen by considering the target awareness percentage. In other words, the smallest value that covers $TA\%$ for all neighbors is chosen as the next transmit power (See Algorithm 2: Line 8-9). In terms of rate adaptation, ECPR adapts the rate by using the current message rate and channel load (*i.e.* CBR). The ratio of the messages received divided by the channel capacity is defined as the CBR (See Algorithm 2: Line 10-11) - this is in line with the standardized CBR calculation approaches [73].

Furthermore, as Algorithm 2 shows, the transmit power control takes into account the channel load (CBR), such that the transmit power is not increased if the CBR threshold is reached. The power control algorithm interacts with the rate control, such that the power and rate control “share the load” in case of high CBR: the relationship between the target and current beacon rate BR and the current and target awareness determines whether or not the transmit power will be changed (either increased or reduced). The value of coefficient γ determines whether awareness or rate control is prioritized (In this study, we use the same weight for the awareness and rate: $\gamma=1$). Furthermore, in the case of high CBR, ECPR prevents a significant increase of the channel load that could be caused by the application context suddenly increasing the target awareness range r_e . However, we note that safety-critical messages generated due to hazardous events are going to be sent at a high power and rate that are not governed by the DCC algorithm. Therefore, controlling the power and rate of cooperative messages will not affect safety-critical messages (See Algorithm 2: Line 10-11). For clarity, Table 4.2 shows the transmit power control actions undertaken by ECPR depending on the channel load (CBR), awareness, and rate.

The awareness metric measures the awareness of *neighboring vehicles* about the ego vehicle, thus it can be estimated at ego vehicle *locally* by using the channel loss to each neighbor and the transmit power that will be used at the ego vehicle at $t + 1$. Since obtaining the NAR metric from a receiver’s perspective as defined in Section 4.1.2 would require a vehicle to know about all vehicles within r (in which case, by design, its NAR for r would be 1), we define the estimated NAR (eNAR)

Table 4.2: States that affect transmit power adaptation

State	CBR vs. Target	Awareness vs. Target	Rate vs. Target	Transmit Power at $t+1$
1	<	<	=	Apply $P_e^{Tx}(t+1)$
2	<	\geq	=	Apply $P_e^{Tx}(t+1)$
3	<	<	<	Apply $P_e^{Tx}(t+1)$
4	<	\geq	<	Apply $P_e^{Tx}(t+1)$ if $\leq P_e^{Tx}(t)$
5	>	<	=	Apply $P_e^{Tx}(t+1)$ if $\leq P_e^{Tx}(t)$ OR $\delta_A \geq \gamma\delta_R$
6	>	\geq	=	Apply $P_e^{Tx}(t+1)$ if $\leq P_e^{Tx}(t)$
7	>	<	<	Apply $P_e^{Tx}(t+1)$ if $\leq P_e^{Tx}(t)$ OR $\delta_A \geq \gamma\delta_R$
8	>	\geq	<	Apply $P_e^{Tx}(t+1)$ if $\leq P_e^{Tx}(t)$

from transmitter's perspective as follows:

$$eNAR_r(t) = \frac{ND'_r(t)}{N_r(t)}, \quad (4.7)$$

where $N_r(t)$ is the number of vehicles within r at time t which ego vehicle *detected* (i.e., received a cooperative message from), and $ND'_r(t)$ is the estimated number vehicles in $N_r(t)$ that detected the ego vehicle, calculated as:

$$ND'_r(t) = \epsilon \cdot \sum_{i=1}^N I(P_e^{Tx}(t-1) + PL_{e \rightarrow i}^{Tx}(t-1) > P_{Th}^{Rx}), \quad (4.8)$$

where I is the indicator function, $PL_{e \rightarrow i}^{Tx}(t-1)$ is the channel loss from ego vehicle to neighbor i , and P_{Th}^{Rx} is the receiver sensitivity threshold. Effectively, the ego vehicle uses the channel reciprocity theorem ($PL_{e \leftarrow i}^{Tx} = PL_{e \rightarrow i}^{Tx}$) [171] to estimate the proportion of its neighbors that were able to receive cooperative messages from it in the previous time step. The estimation error for number of neighbors is defined as ϵ and is set to $[-10, 10]\%$. It is possible that a comparatively high power signal is lost due to strong interference (although not too frequently, since CSMA/CA mechanism and congestion control mechanism are in place). Hence, Equation (4.8) can introduce false positive cases which lead to an inaccurate number of neighbors.



Figure 4.4: Regions used for highway and urban simulations (circled) on the topology of Newcastle, UK. Both regions have an area of approximately 1km^2 . White outlines represent buildings that were incorporated in simulations for realistic propagation modeling.

At low densities, when vehicles have a small number of neighbors, the eNAR estimate can be incorrect because of a small number of data points it needs to work with. However, in low density cases, vehicles will almost always be able to achieve the maximum rate and awareness, since the channel load at low densities will be low. Therefore, knowing the correct eNAR is not necessary. As the network density increases and vehicles start having more neighbors and they have a larger number of data points to work with (*e.g.*, 100 instead of 10 neighbors), which makes the eNAR estimate more accurate.

4.3 Numerical Results

To evaluate the performance of ECPR, we implemented it in the GEMV² V2V propagation simulator [43]. In terms of parameters, the time step used for the ECPR time step duration was set to 200 *ms*. For a given target range r , we use a target awareness $TA = 85\%$. We use omnidirectional antennas on the vehicle roof and evaluate the DCC performance on a single channel. We set the maximum transmit power to 23 *dBm* and the maximum beacon rate to 10 *Hz*. We used the performance metrics described in Section 4.1.2.

To give a physical perspective to the parameters relevant for ECPR, the typical values for

Table 4.3: System Parameters Setup for the Simulations.

Parameter	Value
Carrier sense threshold [dBm]	-90
Data rate [Mbps]	6
Measurement period [ms]	200
Min. and Max.packet transmission frequency [Hz]	1 and 10
Min. and Max. transmission power [dBm]	0 and 23
Min. and Max. awareness range [m]	20 and 500
Target neighbor awareness ratio	85%
Threshold Channel Busy Ratio	60%

awareness range r are from 20 to 500 m , depending on application context; similarly, target awareness within r , TA , will be dependent on the application context and can range from *e.g.*, 50% to 100%; P_e^{Tx} is usually limited from 0 to 23 dBm in radios used for V2V communication, whereas the message rate BR is usually set between 1 and 10 Hz for cooperative messages [73]. Communication parameters considered in this chapter are summarized in Table 4.3.

Since the goal of this study is to show the feasibility of environment- and context-aware DCC control by leveraging the benefits of both power and rate adaptation, we choose to compare the proposed ECPR algorithm with LIMERIC (rate-only DCC algorithm), the power-control only component of ECPR, and a scenario without DCC (*i.e.*, messages are set with fixed rate and power irrespective of the channel conditions).

Simulated Environments: One of the most challenging scenarios for DCC algorithms is to ensure they properly function in any kind of environment. To that end, we perform simulations using the city of *Newcastle upon Tyne, England* as shown in Figure 4.4. The region around *A167* is chosen for the highway scenario. A part of the city grid around *Princess Square* is used to simulate an urban area. We used 1 km^2 area and 500 vehicles for both the highway and urban simulations. Vehicular mobility is generated using SUMO [200], whereas OpenStreetMap [201] is used to obtain the outlines of buildings and foliage for accurate propagation modeling.

Application Context: Varying Target Rate and Target Awareness Distance: As shown in Figure 4.2, depending on the application context, different vehicles can have different awareness range and rate requirements at the same time. To test ECPR with varying awareness range

Table 4.4: Tests defined with different target awareness range and message rate combinations to stress-test ECPR.

	Target Awareness Range	Target Message Rate
Test 1	Same for all vehicles (90 m)	Same for all nodes (10 Hz)
Test 2	Same for all vehicles (90 m)	Uniformly distributed between 5 and 10 Hz
Test 3	Chosen randomly from set $S = [30, 60, 90, 120, 150, 180 \text{ m}]$	Same for all nodes (10 Hz)
Test 4	Chosen randomly from set $S = [30, 60, 90, 120, 150, 180 \text{ m}]$	Uniformly distributed between 5 and 10 Hz

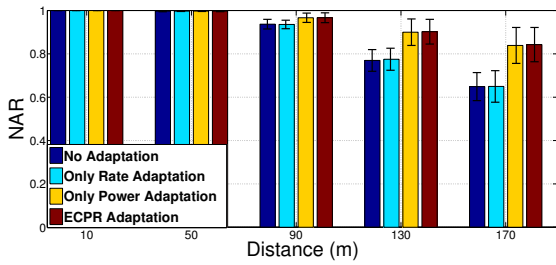
and rates, we perform four types of tests described in Table 4.4. In Test 1, each vehicle’s target awareness range is set to 90 m and target beacon rate is 10 Hz. In Test 2, the target awareness distance is 90 m and target beacon rate is different for all ego nodes. The target rate is chosen uniformly across an interval of $[5, 10]$ Hz. In Test 3 and 4, the target awareness distances are selected uniformly at random.

4.3.1 Simulation Results

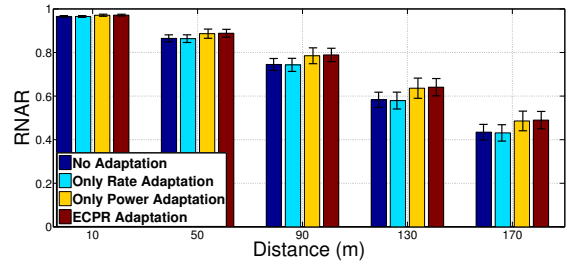
In this section, we compare several results compare the existing solutions with ECPR by providing mean and standard deviation values. Furthermore, performance results for the individual vehicles are provided in order to prove that individual vehicle behavior matches with the average values. Then, ECPR performance is shown with different target awareness range and target message rate for both highway and urban scenarios. Finally, effects of medium access layer collisions are discussed.

4.3.1.1 Comparison of ECPR with LIMERIC, power-only algorithm, and no DCC

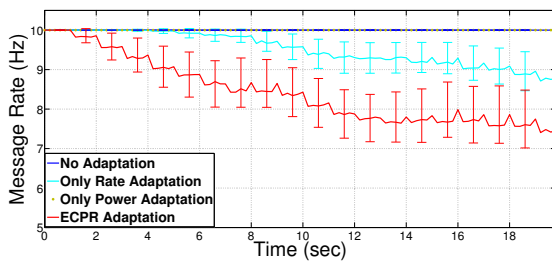
In this subsection, we compare the performance of ECPR relative to LIMERIC (rate-only algorithm), the power-control only component of ECPR (described in Section 4.2.1), and a scenario without DCC. To obtain a fair comparison, we use only Test 1 from Table 4.4 (*i.e.*, same awareness range and rate requirements for all vehicles). We perform simulations with different default transmit power settings: these affect the initial power levels for radios employed in the ECPR and



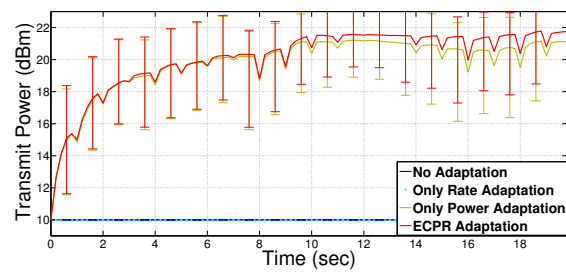
(a) Neighbor awareness vs. transmission distance



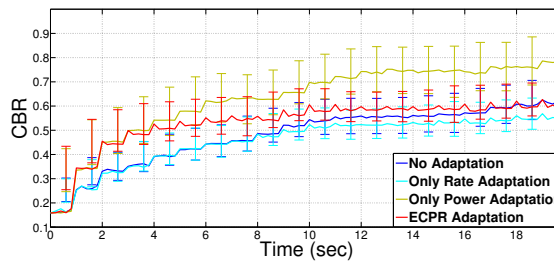
(b) Neighbors above range causes unwanted interference vs. transmission distance



(c) Message rate



(d) Transmit power



(e) Channel busy ratio (CBR)

Figure 4.5: Target Awareness 85%, Target Awareness Distance = 150m, default Tx Power = 10 dBm. Urban Scenario. Power-only algorithm achieves awareness (NAR) comparable to ECPR; however, due to it not taking channel load (CBR) into account, it exceeds the target CBR.

power-only adaptation scenarios, whereas for no DCC and rate-only DCC scenarios the default power is used throughout the simulation.

Figure 4.5 shows the results for the urban environment with a target awareness range of 150 m, a default transmit power of 10 dBm. Compared to rate-only (LIMERIC), ECPR can achieve a 20% increase in points better awareness at the target distance by reducing the average rate from

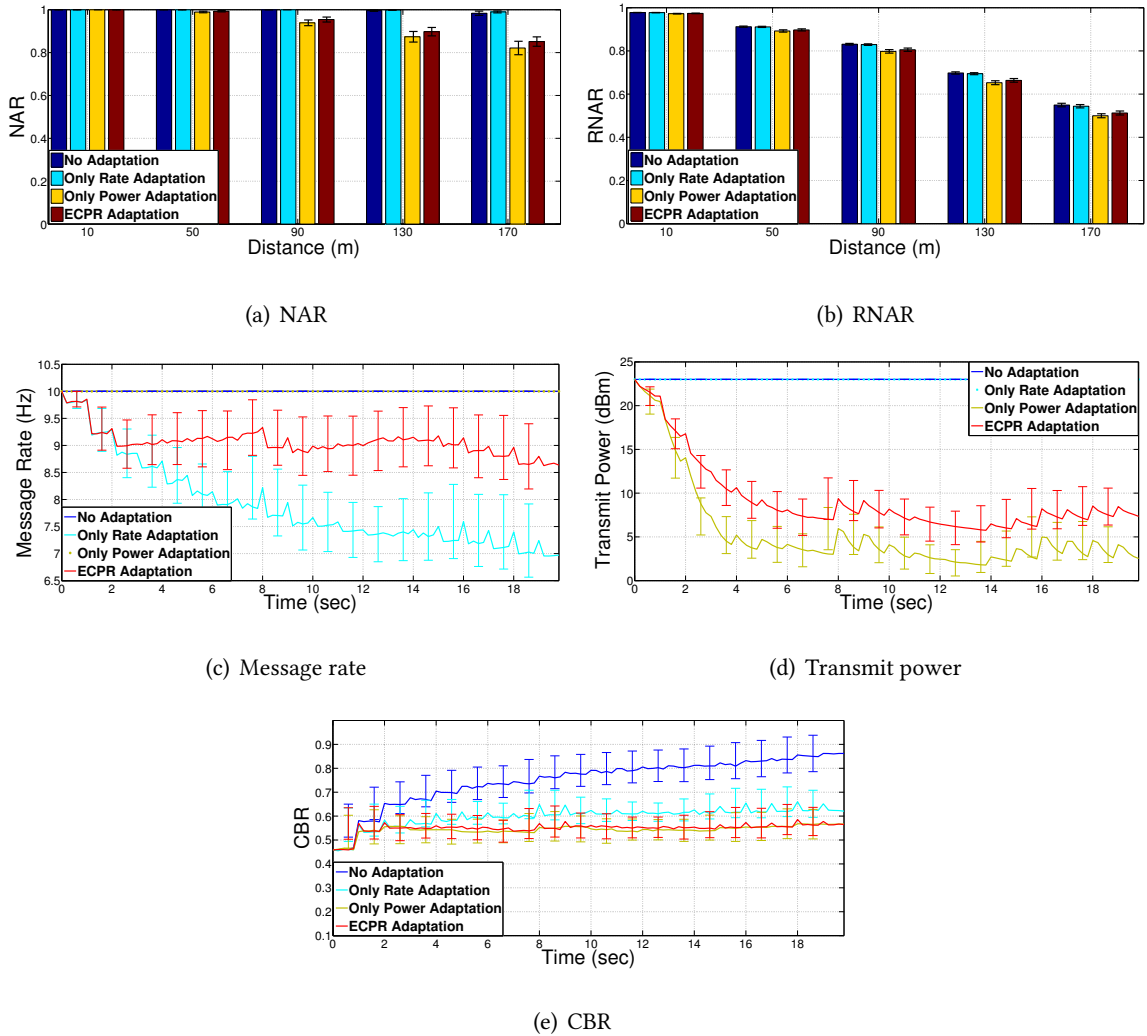


Figure 4.6: Target Awareness 85%, Target Awareness Distance = 50m, default Tx Power = 23 dBm. Urban Scenario. In this application context, ECPR can reduce the average power while not jeopardizing awareness. This allows for increase of overall throughput in the system as visible through increased average rate, while at the same time keeping the average CBR lower than that of rate-only algorithm.

approximately 9 Hz to 8 Hz. This scenario can be regarded as awareness-focused, where an application (e.g., intersection collision detection) requires vehicles to be aware of other vehicles within 150 m range. In this case, it is reasonable to trade some of the rate to increase the transmit power (Figure 4.5(d)) and obtain an overall better awareness, since the messages that are traded for increased awareness are likely cooperative awareness messages at lower power, which would not

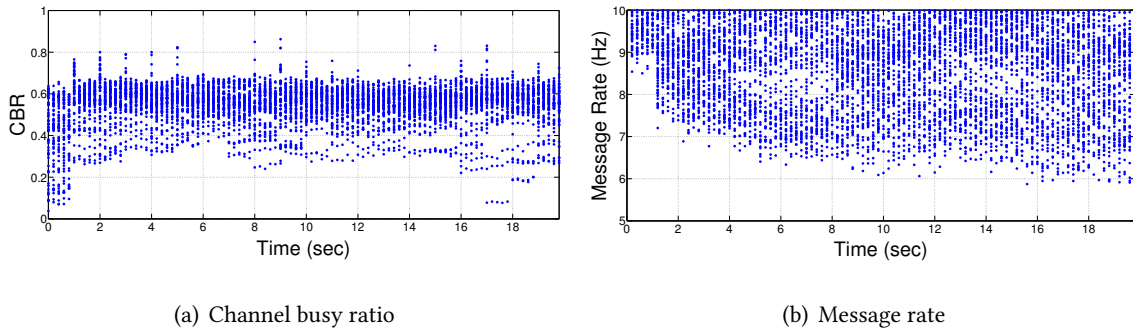
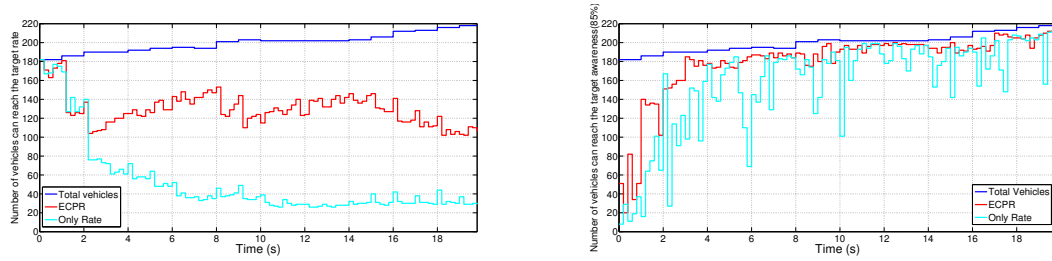


Figure 4.7: Randomly selected 100 vehicles for Target Awareness Distance = 50 m, default Tx Power = 23 dBm.

be able to reach all vehicles at desired range, which defeats the purpose of sending those messages in the first place. Power-only algorithm achieves awareness (NAR) comparable to ECPR; however, due to not taking channel load (CBR) into account, it would exceed the target CBR.

Figure 4.6 shows results for an urban environment with target awareness range of 50 m, default transmit power of 23 dBm and showing how ECPR can achieve up to 25% better average message rate, for the same satisfying requirement of the awareness rate at target awareness range. In this scenario, because the application context allows it, ECPR can reduce the average power (Figure 4.6(d)) while not jeopardizing awareness. This allows for an increase of overall throughput in the system (see Figure 4.6(c)), while at the same time keeping the average CBR lower than that of rate-only algorithm (see Figure 4.6(e)). In this scenario, no DCC adaptation performs as well as rate-only in terms of awareness; however, the CBR target is not satisfied. This emphasizes the need for DCC algorithms, since without adaptation there is a risk of channel overload and communication breakdown in case of high vehicular density. Note that ECPR can only adapt to awareness and rate requirements to the extent allowed by the physical surroundings (*e.g.*, it is not possible to reach 500 m awareness range with 95% awareness rate without very high transmit power) and transmit power parameters (which we limit to 0 – 23 dBm range so as to comply with the capabilities of existing IEEE 802.11p radios).

In Figure 4.7 the per-vehicle behavior of the CBR and rate for 100 randomly chosen vehicles is shown. Although CBR overshoots the threshold CBR at each time step for both scenarios, it happens for one time step only, specifically when new vehicles enter the simulation. In the next step,

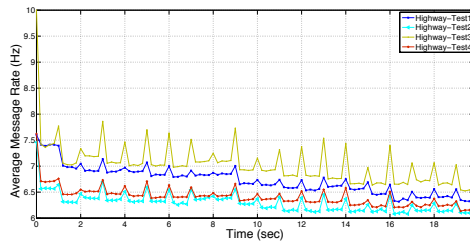


(a) The number of vehicles that can achieve the target message rate for Target Awareness Distance = 50 m, default Tx Power = 23 dBm. (b) The number of vehicles that can achieve the target awareness. Target Awareness Distance = 150 m; default Tx Power = 10 dBm.

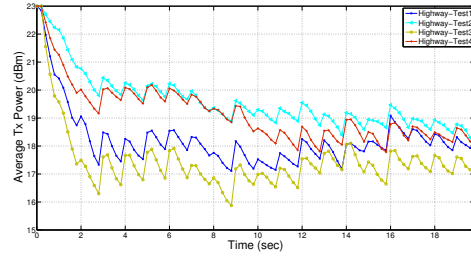
Figure 4.8: The number of vehicles that can achieve the target awareness. The number of vehicles that can reach awareness target, 85%, and rate target, 10 Hz, for rate-only algorithm and ECPR. As a result of adaptation on transmission power on ECPR, frequency reuse is able to be used more actively, more vehicles reach the target message rate, and reaches target awareness more stably than rate-only adaptation.

the ECPR adapts the beacon rates to keep the CBR under the threshold. Regarding per-vehicle statistics, the results show that ECPR can control the load and can meet the target rate for all vehicles whose awareness requirements and environment allow it. It is important to note that ECPR aims to reach both the target awareness range and message rate based on the application requirements and given the constraints of specific physical environment. This results in a relatively large message rate spread, since the environment dictates that some vehicles need to transmit at higher power to reach the neighbors to which it has a bad channel (e.g., those behind a corner), which in turn increases the load for those neighbors to which it has a good (LOS) channel. In other words, combined awareness and rate control will not result in the same message rate at all vehicles unless their propagation environment is the same.

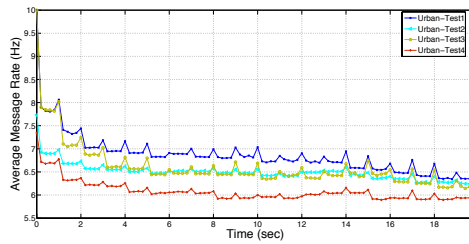
In Figure 4.8(a) the number of vehicles that can achieve the target message rate, 10 Hz for this experiment, is shown for rate-only and ECPR adaptations. Since ECPR adapts the transmission power to various context, transmission power is reduced if needed. As a result of adaptation on transmission power, frequency reuse is able to be used more actively and more vehicles reach the target message rate than rate-only adaptation. In addition to target rate, the number of vehicles that can achieve the awareness target, 85%, is compared in Figure 4.8(b). Rate-only adaptation uses default transmission power therefore has limited capability to achieve target awareness for



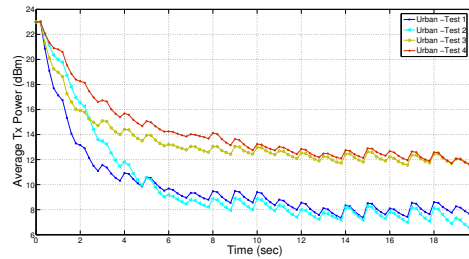
(a) Highway scenario average message rate



(b) Highway scenario average transmit power



(c) Urban scenario average message rate



(d) Urban scenario average transmit power

Figure 4.9: Average transmit Power and beacon rate for highway and urban environments. The relationship between average message rate and average transmit power is reversely proportional on each environment.

any kind of application while ECPR can adapt the transmission power to changing application and environment. Consequently, ECPR reaches target awareness more stably than rate-only adaptation.

ECPR is tested for different default transmission power values to see its adaptation ability to any environment and context cases. However, we use 10 dBm power and 150 m target range (low default power, high range requirement) and 23 dBm power and 50 m target range (high default power, low range requirement) to show how ECPR performs in comparatively extreme cases.

4.3.1.2 Different Target Rate and Awareness Distance Sets for Combined Algorithm: Urban vs Highway Environment

Figure 4.9 shows average message rates and transmit powers for different tests. Target awareness range and message rate are denoted in Table 4.4. The relationship between average message

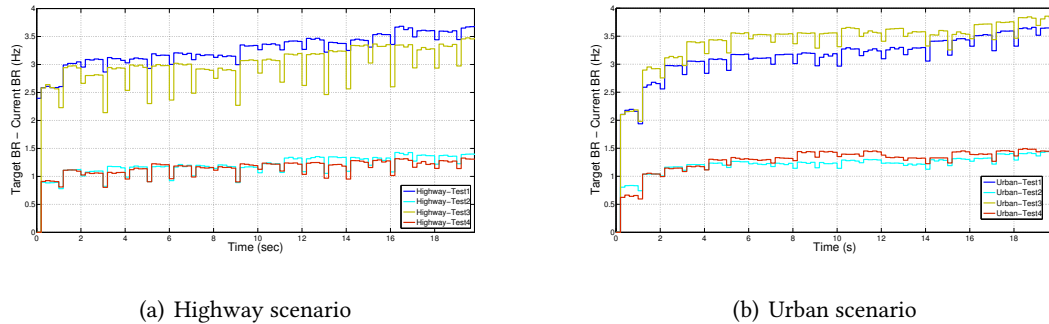


Figure 4.10: Average difference between target and achieved message rate for highway and urban environments. Test 1 and 3 target the maximum message rate, the difference between target and current rate is higher than in Test 2 and Test 4. The target rate is on average less than maximum rate, thus the difference of achieved to target rate is less.

rate and average transmit power is reversely proportional on each environment: the lower the average power, the smaller the message coverage, resulting in better channel reuse and higher rate. The average rate is similar in the two environments because the high density of vehicles means that the channel is loaded most of the time. Interesting to note is that in urban scenarios, the average power converges to a value lower than in highway scenarios; this can be attributed to the increased number of neighbors for the same range in urban environment. Thus, the channel becomes more congested from neighbors at shorter distance and requiring lower power to reach them. In turn, this offsets the range limitations due to obstructing buildings requiring larger power for the same range at highways.

Figure 4.10 shows the difference between the target message rates and the achieved rate for both urban and highway scenarios. Since Test 1 and 3 target the maximum message rate, the difference between target and current rate is higher than in Test 2 and Test 4. In other words, in Tests 2 and 4, the target rate is on average less than maximum rate, thus the difference of achieved to target rate is less.

Figure 4.11 shows the average CBR levels and their standard deviations for each time step for all tests. As expected, the test which has higher average message rate also has higher CBR values. However, average CBR values never overflow the CBR threshold, which is 0.6 with ± 0.05 tolerance. Although new vehicles entering the simulation and starting at maximum transmit power

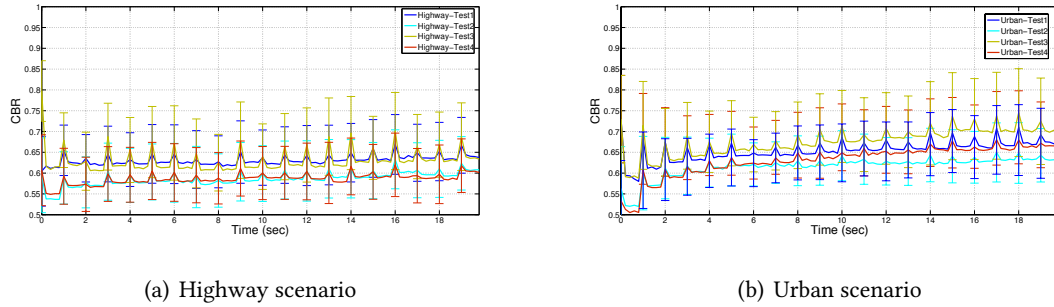


Figure 4.11: Standard deviation and mean of CBRs in highway and urban environments. The threshold CBR value is set as 0.6 with ± 0.05 tolerance. In urban scenario, average CBR is higher than in the highway scenario. The reason is that each ego node needs to communicate with a larger number of neighboring vehicles in urban environment than highway due to the vehicles being concentrated around intersections; combined with higher power to achieve the same awareness, this results in higher overall CBR.

join the communication at each second, ECPR adapts the power and message rate at the next time step and decreases the CBR to threshold value. In urban scenario, average CBR is higher than in the highway scenario. The reason is that each ego node needs to communicate with a larger number of neighboring vehicles in urban environment than highway due to the vehicles being concentrated around intersections [202]; combined with higher power to achieve the same awareness, this results in higher overall CBR.

The results show that ECPR can effectively adapt the power and rate to achieve the target requirements on awareness and rate given by the application context, irrespective of the propagation environment. Since it has the ability to obtain higher average rate when the awareness requirements allow it, at the same time maintaining or reducing the CBR as compared to rate-only solution, it can be used to improve the overall system throughput. Conversely, if the awareness requirements are more stringent or the propagation environment more harsh, ECPR efficiently trades rate to improve the awareness.

4.3.1.3 Effect of Medium Access Layer Collisions

To investigate the effect of Medium Access Layer (MAC) collisions on the performance of ECPR, we perform simulations with the same network conditions as for the scenario shown in Fig-

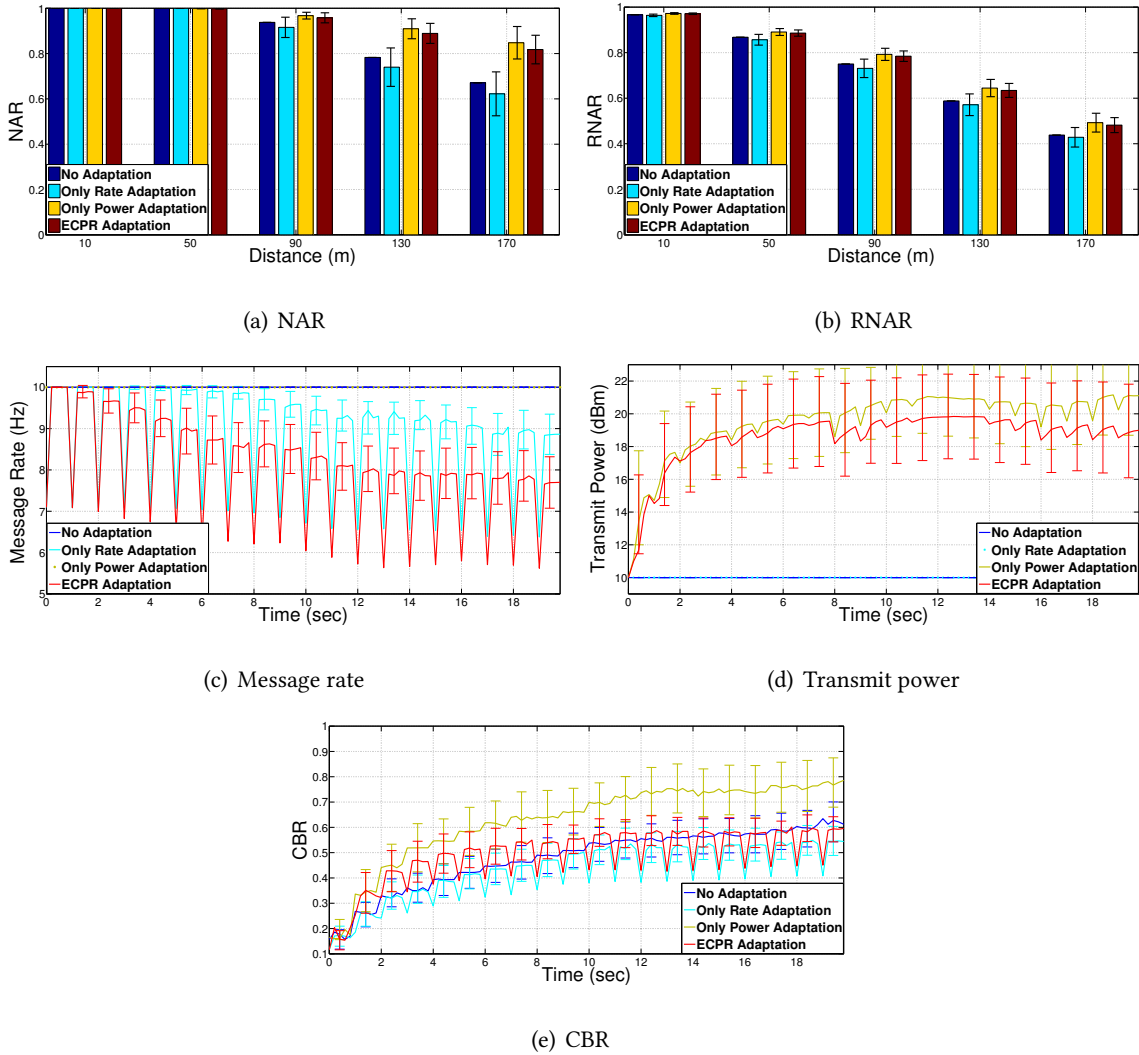


Figure 4.12: Target Awareness 85%, Target Awareness Distance = 50m, default Tx Power = 23 dBm. Urban Scenario with MAC collisions.

ure 4.5 (Target Awareness 85%, Target Awareness Distance = 150m, default Tx Power = 10 dBm), with increased loss due to MAC collisions (note that results in Figure 4.5 consider no loss due to MAC collision). The collision statistics are defined as follows: when CBR is below 20%, 20 – 30%, 30 – 40%, 40 – 50%, 50 – 60%, and above 60%, MAC layer collision causes 0%, 1%, 3%, 7%, 10%, 30% packets drops, respectively. These parameters are selected to represent harsh conditions caused by progressively increasing collisions with the increase in channel load [203]. Compared with Figure 4.5, Figure 4.12(a)– 4.12(b), shows that the effect of MAC collisions is quite limited in

Table 4.5: Average percentage of potentially hidden nodes for ECPR and rate-only (LIMERIC) algorithm.

	Transmit Power = 23 dBm Awareness Range = 50 m		Transmit Power = 10 dBm Awareness Range = 150 m	
	50 Vehicles	100 Vehicles	50 Vehicles	100 Vehicles
ECPR	12.9%	22.4%	8.5%	17.4%
LIMERIC	11.9%	23.2%	8.7%	16.5%

terms of the key performance metrics of ECPR (NAR, RNAR); similarly limited difference can be observed in Figures 4.12(c)– 4.12(e) in terms of the resulting network parameters (message rate, transmit power, and CBR). Therefore, we conclude that ECPR utilizes channel as effective as possible while keeping CBR under the threshold even in the face of MAC collisions. In Figure 4.12(c), the dip points are how network parameters react to changes without any adaptation yet. The ECPR adapts the parameters to the optimum values every 200 *msec* by considering the resource limitations.

Hidden node problem is another access layer consideration that can be caused by the propagation environment layout as well the transmit power variations. To illustrate the issue, consider the scenario in Figure 4.1, where two vehicles on perpendicular roads are trying to transmit to vehicle in the center of intersection; if those two vehicles cannot “hear” each other, they create the hidden node problem on the vehicle in the intersection. For each of A’s neighbors, we check if that neighbor can “hear” from A’s other neighbors. Each pair of A’s neighbors that cannot hear each other is counted as potentially causing a hidden node problem at A. Thus, the percentage of hidden nodes is computed as the proportion of potentially hidden node pairs to total number of communication pairs. The results in Table 4.5 show that ECPR results in comparative percentage of hidden node pairs as LIMERIC (i.e., ECPR does not increase the probability of hidden nodes).

4.4 Chapter Summary

In this chapter, we proposed a combined rate and power DCC algorithm that efficiently achieves the target awareness and rate requirements given by the application context (e.g., target applica-

tions, vehicle speed, traffic density) in varying propagation environments. By using path loss exponent estimation, ECPR adapts the transmit power to reach the target awareness range. ECPR controls the channel load by adjusting the rate and power according to the current channel load, awareness range, and rate information. We show that ECPR has the ability to obtain higher rate when the awareness requirements allow it, improving the average rate by 15+%, while keeping the target awareness and channel load. If the awareness requirements are more stringent or the propagation environment more harsh, ECPR efficiently trades rate to improve the awareness by up to 20 percentage points. As defining a DCC algorithm for DSRC links in this chapter, we propose a practical DSA technique in the following chapter. While ECPR increases the environmental awareness and achieves the application requirements for high priority messages in DSRC band, the proposed DSA technique in the next chapter provides DTV channel access strategy for low priority messages. Nevertheless, the messaging overhead is avoided and the communications between vehicles become more reliable.

Chapter 5

Cooperative Spectrum Sensing and Bumblebee-Inspired Channel Switching Decision

The wireless spectrum scarcity issue, currently experienced by several sectors within modern society, is also beginning to impact the automotive industry although connected vehicles have significantly enabled research and development into intelligent transportation. It is predicted that the connected vehicle technology and the currently allocated 6 channels of DSRC spectrum band will be insufficient for meeting all connectivity needs of the emerging ITS architecture. Consequently, in many of the envisioned scenarios, the use of other wireless spectrum band such as TV white space (TVWS) is viewed as a potential solution of the spectrum challenges faced by connected vehicles. In this chapter, we propose a novel distributed dynamic spectrum access techniques for CVNs. We first propose a voting based adaptive cooperative sensing algorithm for connected vehicles. Once vehicles access the Digital television (DTV) band as secondary users (SUs), they need to decide to whether keep staying in the current channel or switch to another channel with a better quality although its switching cost. To enable vehicles effectively meet this challenge, we devised a bumblebee-inspired decision-making algorithm in which channel energy information stored and updated in memory to estimate qualities of channel options and then weighed against switch costs

The work presented in this chapter has been published in parts at [J5], [J4], [J3], [J2], and [J1].

to determine optimal (benefit/cost) channel selection.

5.1 A Voting Based Distributed Cooperative Spectrum Sensing Strategy

Cooperative spectrum sensing is a promising approach for enabling greater robustness and reliability in vehicular dynamic spectrum access (VDSA) networks. The unique characteristics of CVNs challenges channel access designs [3]. Firstly, highly dynamic vehicular environments requiring a fast sensing algorithm that makes channel sensing optimization more challenging. The features specific to vehicular communications such as Doppler effect, multipath fading channels, transmission errors affecting the control messaging should be considered in the proposed solutions. Furthermore, implementation of information sharing in cooperative sensing frameworks needs to be evaluated. Limited capability to handle computational complexity hardware components and processing latency.

To deal with these challenges on VDSA, we propose a novel cooperative distributed spectrum sensing mechanism that uses an adaptive detection threshold for sensing and a robust voting mechanism for cooperative decision-making. The proposed mechanism selects an available channel for a SU vehicle across a shorter time period relative to the channel coherence time. The adaptive detection threshold is optimized by using a numerical method based on minimizing the probability of incorrect detection, as well as used for the individual detection of available channels. Due to the cooperative nature of connected vehicles, the decision of individual channel sensing is broadcast to nearby one-hop neighbors. When the vehicle receives a list of available channels, it evaluates this information based on the weighting functions of its neighbors as well as its own. Employing an interdisciplinary method, called entropy-based weighting, the credibility of the information provided by the neighbors is determined. By taking into account the computational load and processing latency, the switching mechanism either selects the proposed voting mechanism for low traffic scenarios or an equally-weighted voting mechanism based on the literature for dense traffic conditions. The numerical results show that the detection error of the spectrum sensing process converges to zero when employing the proposed distributed cooperative mechanism. To the best of our knowledge, a concrete mechanism on how to use the shared information is a novel research

idea despite the fact that cooperative sensing techniques have been extensively studied. Additionally, there does not exist a fast adaptive spectrum awareness mechanism for a highly dynamic vehicular environment in the current state-of-the-art. When compared to current techniques presented in the open literature, our proposed solution has the following contributions:

- A fast optimization algorithm based on an energy decision threshold that provides an adaptive decision scheme to handle highly varying vehicular environments.
- An energy detector that considers Doppler effects, multipath channel characteristics, and fading effect.
- A procedure that enables the sharing of available channel information between vehicles without affecting the periodic control messaging.
- A novel and practical voting scheme that is derived from entropy-based credibility functions of neighbors and the vehicle's own information.
- A switching mechanism that considers the tradeoff between the computational cost/latency and robust spectrum sensing.

5.1.1 Connected Vehicle Environment Setup

Figure 5.1 illustrates a typical connected vehicle topology. The red vehicle is referred as an *ego vehicle*, while the white vehicles are referred to as *neighbor vehicles*. The communication links can be either LOS or NLOS, and both can be dynamically changing over time. In our proposed distributed sensing mechanism, each vehicle individually performs spectrum sensing. Hence, every vehicle will possess its own decision on which channels are available to use for the SU vehicles. The proposed cooperative spectrum access uses the DSRC channels for sharing spectrum awareness. For the data traffic, DTV is used as SUs when the registered PUs do not use it. Once the DTV channel is accessed based on cooperative sensing as the SU, the data traffic is provided on DTV channel.

The distributed spectrum sensing operation is performed based on detecting the energy levels of the channels. Thus, the accuracy of the proposed algorithm depends on the employed channel propagation model. In this work, we use a sum-of-sinusoids model defined in Chapter 3, in order

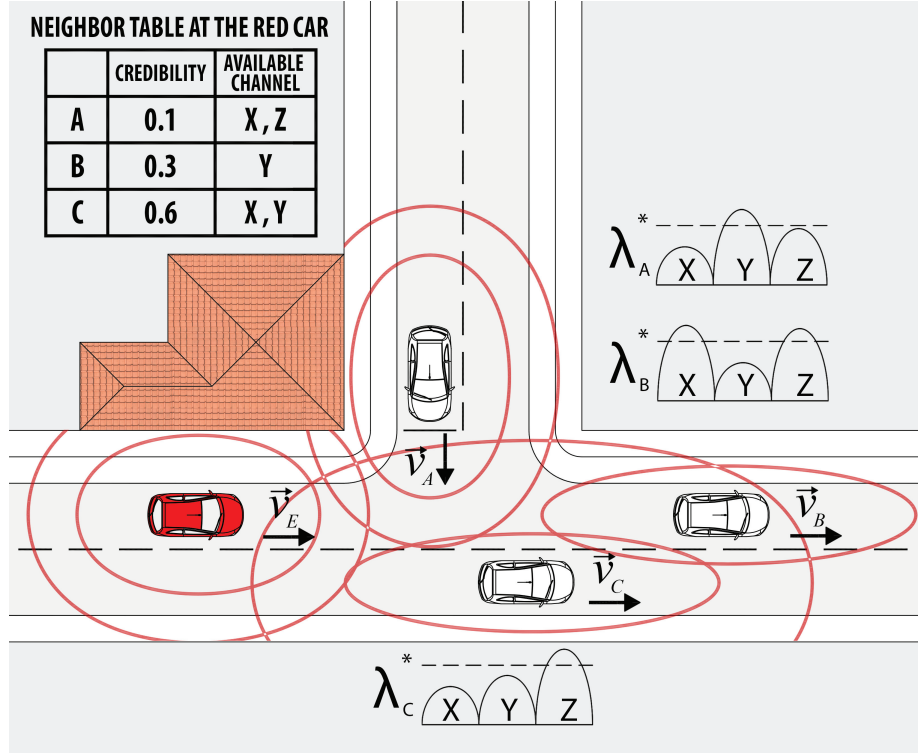


Figure 5.1: Proposed concept diagram of connected vehicle environment: Each vehicle detects the available channels individually and shares the channel information with the one-hop neighbors in the next control message. Each vehicle decides the available channel list by using the information received from neighbors, if available.

to obtain an accurate channel envelope, $h_k(t)$. Using the channel impulse response, we can formulate a M -ary hypothesis test [204] such that the spectrum sensing operation performs a binary hypothesis test as follows:

$$\begin{aligned}
 H_0 : r(t) &= \sum_{t=0}^{\infty} n_r(t) \\
 H_1 : r(t) &= \sum_{t=0}^{\infty} h(\tau, t)x(t - \tau) + n_r(t),
 \end{aligned} \tag{5.1}$$

where $r(t)$ is the received signal, $x(t - \tau)$ is the transmitted signal, $n_r(t)$ is the noise effect. The hypothesis of the absence and presence of the PU are H_0 and H_1 , respectively. The comparison of the energy detection threshold and the energy level of the received signal, E_r , yields the decision

of channel's availability to be used by SU vehicle, namely:

$$\begin{aligned} H_0 : E_r &= \frac{1}{T} \sum_{t=1}^T |r(t)|^2 < \lambda_j \\ H_1 : E_r &= \frac{1}{T} \sum_{t=1}^T |r(t)|^2 > \lambda_j, \end{aligned} \quad (5.2)$$

where λ_j is the energy detection threshold and T is the number of samples. Due to the dynamic vehicular environment, the energy detection threshold, λ_j^1 , will be individually adapted at each vehicle based on minimizing detection error. This TVWS information as a result of spectrum sensing is periodically broadcast in the control messages. Without loss of generality, the broadcast period is defined to be 100 msec such that 10 broadcasts occur per second [205].

Each vehicle receives control messages from its one-hop neighbors whose received power is higher than the message received threshold. The available channel list to be used by the SU vehicle is based on the neighbor's individual decision that is collected from all the control messages. The ego vehicle detects the credibility of the neighbors based on their signal-to-noise-ratio (SNR). The credibility of the neighbors are used for defining the weights of the neighbors such that weighted voting can be performed, as shown at the Neighbor Table in concept diagram. For example, in Figure 5.1 we observed that the ego vehicle defines Neighbor A's credibility as 0.1, Neighbor B's credibility as 0.3, and Neighbor C's credibility as 0.6. Consequently, Channel Y would be chosen with the highest vote as 0.9.

If the individual sensing is ready at the onset of the control messaging period, it is not sent during the current phase of messaging and instead sent in the next messaging phase. This procedure helps preventing the sensing algorithm from causing delays with respect to messaging. When a vehicle receives a list of the available channels, it evaluates this information with the neighbors' credibility. In case a vehicle does not receive any information regarding available channels, it will only utilize its own individual decision.

¹Since the sensing mechanism is performed distributed, all vehicles have individual energy detection calculation. The subscript j for individual vehicle is used to highlight this distributed sensing mechanism.

5.1.2 Proposed Optimal Energy Detection

Energy detection uses the energy spectra of the received signal in order to detect the busy channels across a frequency band. Hypothesis testing is performed by comparing the channel energy with an energy threshold, λ_j . When the channel energy is observed to be less than the energy threshold, the channel is defined as available. Otherwise, the channel is defined as busy. Since vehicular environments potentially vary rapidly over time, the signal-to-noise ratio (SNR) will also fluctuate thus yielding detection errors. Therefore, fixed energy detection threshold may not work efficiently in vehicular communication environments.

We define an optimization problem based on minimizing the probability of incorrect detection (P_j^{inc}) in order to adapt the energy detection threshold. Most approaches find the optimum threshold by either minimizing the probability of false alarm or maximizing the probability of successful detection [206]. However, the detection performance is actually affected by both phenomena. Therefore, we use the probability of incorrect detection P_j^{inc} for Vehicle j based on Bayesian statistics in order to obtain the optimum detection threshold as follows:

$$P_j^{inc} = P(H_0)P(E_j > \lambda_j|H_0) + P(H_1)P(E_j \leq \lambda_j|H_1), \quad (5.3)$$

where $P(H_0)$ refers to the probability that the channel is available, which has an exponential distribution based on its field measurements [207]. $P(H_1)$ is probability that the channel is busy, which is equal to $1 - P(H_0)$, $P(E_j > \lambda|H_0)$ refers to the probability of false alarm, P_j^f , where the energy detector decides that a PU issuing the channel when in fact it is not, and $P(E_j \leq \lambda|H_1)$ is the probability of missed detection, P_j^m , where the energy detector decides that no PU is present in the channel when in fact it is. The optimum energy threshold minimizes the probability of incorrect detection, λ_j^* :

$$\lambda_j^* = \underset{\lambda_j > 0}{\operatorname{argmin}} P_j^{inc}. \quad (5.4)$$

Closed form derivations of $P(E_j > \lambda|H_0)$ (P_j^f) and $P(E_j \leq \lambda|H_1)$ (P_j^m) are needed to solve the optimization problem. Digham *et al.* derived the closed form expression of the probability of

successful detection of Rayleigh fading for Vehicle j as follows [141, 208]:

$$P_j^d = e^{-\frac{\lambda_j}{2}} \sum_{s=0}^{N/2-2} \frac{\left(\frac{\lambda_j}{2}\right)^s}{s!} + \left(\frac{1 + \overline{SNR}_j}{\overline{SNR}_j}\right)^{N/2-1} \left[e^{-\frac{\lambda_j}{2(1+\overline{SNR}_j)}} - e^{-\frac{\lambda_j}{2}} \sum_{s=0}^{N/2-2} \frac{\left(\frac{\lambda_j \overline{SNR}_j}{2(1+\overline{SNR}_j)}\right)^s}{s!} \right], \quad (5.5)$$

where N is the number of samples, \overline{SNR}_j is the average SNR for N samples where $\overline{SNR}_j(dB) = E_r - E_{noise}$ giving E_r is defined in Equation (5.2) and E_{noise} is the noise floor. The SNR value varies based on changes of the signal energy and channel envelope. This dynamically changing environment motivates the need for an adaptive solution. Thus, the probability of missed detection, which is equal to $P_j^m = 1 - P_j^d$, is used to find the adaptive energy threshold as shown in Equation (5.4). The probability of false alarm of the Rayleigh fading for Vehicle j is the same as the AWGN scenario [141, 208]:

$$P_j^f = \frac{\Gamma(N/2, \overline{SNR}_j/2)}{\Gamma(N/2)}. \quad (5.6)$$

The optimum energy detection threshold can be solved by applying numerical methods to the optimization problem defined in Equation (5.4). One optimization method that is often used is the Gradient method. This technique finds the optimal points of the fitness function by discovering those points where the slope is equal to zero, *i.e.*:

$$\frac{\partial}{\partial \lambda} P_j^{inc}(\lambda_j^*) = 0 \quad (5.7)$$

Another optimization technique to find the optimal points of the fitness function is the Newton's method. The method finds the distance between two values of λ_j in the fitness function space, *i.e.*, $P_j^{inc}(\lambda_j)$. The iteration is carried on until the distance is smaller than error tolerance. The mathematical representation of the method is defined as [209]:

$$\lambda_{n+1} = \lambda_n - \frac{P_j^{inc}(\lambda_n)}{\frac{\partial}{\partial \lambda} P_j^{inc}(\lambda_n)} \quad (5.8)$$

The proposed algorithm should operate in less time than the coherence time of the vehicular communication channel. Although the Gradient and Newton's methods are the most common optimization methods, they include a derivative that may incur a penalty in terms of computational cost and time. An alternative to these approaches is the Secant Method, where instead of

a derivative, the difference of the error functions between two iterations is performed assuming linearity [209]. Since this assumption would be valid with respect to discrete time vehicular communications, we can obtain an accurate optimum value with a rapid convergence with respect to this method as follows:

$$\lambda_j[n+1] = \lambda_j[n] - P_j^{inc}[n] \frac{\lambda_j[n] - \lambda_j[n-1]}{P_j^{inc}[n] - P_j^{inc}[n-1]}, \quad (5.9)$$

where n is the iteration index. The optimum energy threshold value, λ_j^* , is equal to $\lambda_j[n+1]$ when $\lambda_j[n+1] - \lambda_j[n] \leq 10^{-4}$ assuming as error tolerance of 10^{-4} . Note that the error tolerance can be selected depending on the required sensitivity of the application.

Once the optimum energy detection threshold is obtained, the energy level of channel is then compared with this threshold. In the event that the channel's energy level is less than the energy threshold, this implies that only noise floor is present across the channel and this channel is available for usage by SUs.

5.1.3 Proposed Entropy-Based Weighted Cooperative Spectrum Sensing

The proposed cooperative spectrum sensing approach builds upon our distributed individual sensing mechanism, where each vehicle detects channel availability individually, and transmits this information to their one-hop neighbors along with the control messages. When the channel availability cannot be detected between the transmission of control messages, the process will not pause for the detection information. Instead, the available channel information will not be transmitted in the control message, but will be transmitted in the subsequent message.

At the receiver side, the vehicle obtains the available channel information from each control message transmitted from the one-hop neighbors. By using the existing periodical beacon messages to share channel information, it is not necessary to transmit any additional messages. Thus, the proposed approach avoids causing extra messaging overhead. In the case that none of the neighbors have transmitted any available channel information, the receiver vehicle will use its own detection information. Otherwise, the vehicle will gather the available channel lists and evaluate the detection results. Each neighbor has a different credibility level since the control messages may be exposed to transmission errors. Therefore, the evaluation at the vehicle is based on the credibility function of each neighbor as well as its own.

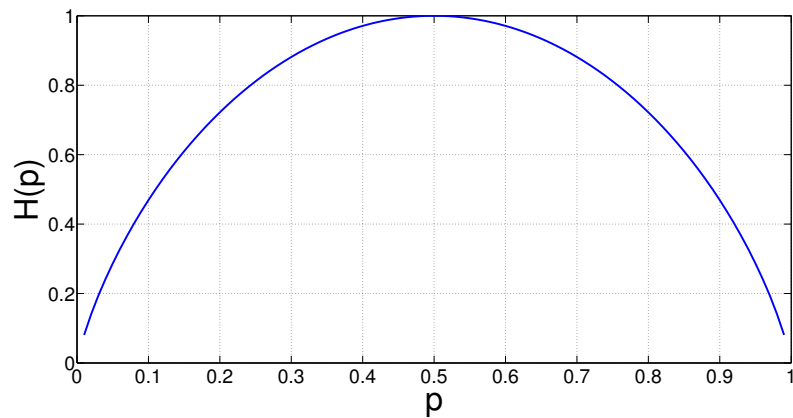


Figure 5.2: The behavior of entropy function. Note how the Uncertainty converges to zero if the probability of random event occurring gets closer to the edges and at the peak value for $p = 0.5$.

In this work, we define the credibility function via an entropy paradigm. Entropy defines the uncertainty of random events [210]. The entropy behavior of a binary random event is illustrated in Figure 5.2, where the uncertainty converges to zero when the probability of a random event approaches the edges. For example, if the probability of an event occurring is 0.99, it means that it is much more likely to occur, thus the uncertainty is almost zero. Conversely, if the probability of an event occurring is 0.5, it is equally likely the event may occur or not. Hence, the entropy as a measure of uncertainty peaks at the value of 1. Besides physics and mathematics [211, 212], entropy-based weight functions are used in numerous disciplines such as economics and biology [213, 214]. Likewise, Yuming *et al.* used weighting functions based on entropy in order to find the priority of channel parameters during spectrum sensing operations, *e.g.* channel capacity, acceptable error rate, delay [215].

In this work, we define the entropy as a function of the probability of incorrect detection (see Equation (5.3)) and the probability of correct detection, which is the complement of the probability of incorrect detection, *i.e.* $P_{ij}^{cor}(\lambda_j^*) = 1 - P_{ij}^{inc}(\lambda_j^*)$. Each vehicle transmits its own value for the probability of incorrect detection in the control messages. This shared information does not cause any extra computation burden since the vehicle already computes the probability of incorrect detection in order to find the optimum energy detection threshold. Moreover, the control message characteristics, *i.e.*, message length and transmission power, does not change since the probability information to be shared in the control message is relatively small. Since the probability of incor-

rect detection is formed by using SNR as well as the channel model defined in Section 5.1.1, the effects of shadowing, multipath fading, and distance are all included in the credibility function.

The ego vehicle considers the neighbor decisions only if the probability of incorrect detection is less than 0.5, since a high value for the probability of incorrect detection means the neighbor decisions are very unreliable for some reason, *e.g.*, transmission error, too noisy channel, too low SNR. Please note that any value less than or equal to 0.5 can be chosen. In this work, we choose 0.5 for representation of the performance since it is the worst possible case. If the proposed mechanism can provide a error-free detection even in the case where the uncertainty is at its maximum, the proposed mechanism should be sufficiently reliable for more optimistic setups, *e.g.*, threshold is less than 0.5. As a result, the ego vehicle does not use unreliable neighbor decisions. By this way, we use only right half of the entropy function in Figure 5.2. The ego vehicle i computes its j^{th} neighbor's entropy using the following expression:

$$H_{ij} = -P_{ij}^{cor}(\lambda_j^*) \log_2 P_{ij}^{cor}(\lambda_j^*) - P_{ij}^{inc}(\lambda_j^*) \log_2 P_{ij}^{inc}(\lambda_j^*), \quad P_{ij}^{inc}(\lambda_j^*) \leq 0.5. \quad (5.10)$$

Entropy function considers all factors of vehicular environment that affects probability of correct and incorrect detection. As noted above, the entropy paradigm is the measure of uncertainty, where we define the neighbor's credibility using the complement of the entropy. The ego vehicle i defines the weighting of all the neighbors and itself based on the complementary of the entropy (uncertainty) as follows:

$$w_{ij} = \frac{1 - H_{ij}}{\sum_{k=0}^M (1 - H_{ik})}, \quad (5.11)$$

where M is the total number of neighbors. The summation used in the denominator is from $k = 0$ to M since $k = 0$ refers to ego node's own entropy. The credibility levels are used for voting on the available channels. Cooperative sensing provides a reliable sensing scheme since the proposed mechanism implements the decision by evaluating the information received from all neighbors [216]. In this case, several of the neighbors may send incorrect or corrupted data, and the voting scheme will provide a decision based on the combination of correct and incorrect data received from all neighbors. Therefore, the channels, which might be corrupted by malicious attackers and/or transmission errors, will be repaired by the cooperative sensing scheme. The channel that has the highest weight value in total is chosen for transmission. In the case where

Table 5.1: Vehicular Density for Traffic Classes.

Class	Vehicular Density
Sparse	50 <i>vehicle/km²</i>
Medium	100 <i>vehicle/km²</i>
Dense	250 <i>vehicle/km²</i>
Extreme	400 <i>vehicle/km²</i>

none of the channels are available to be used by SUs, the result of voting mechanism will be zero for all DTV channels. Hence, the ego vehicle will perform the traditional frequency re-use technique. If there are no available channels to access even with frequency re-use mechanism, the ego vehicle will wait for the next energy detection period to perform the proposed mechanism.

5.1.4 Proposed Switching Mechanism between Weighted and Equally Voting

The entropy-based weighting of neighbor channel availability decisions is a robust approach with respect to adapting to a dynamically changing environment. The equal voting mechanism presented by the current-state-of-the-art can cause decision error especially in the case of a low number of neighbors as well as numerous obstacles located within the environment. On the other hand, one drawback of entropy-based weighted voting is that it increases the computational complexity of the implementation as well as the process latency. We propose a switching mechanism to deal with this tradeoff. Based on our approach, the ego vehicle uses the entropy-based weighted voting in the case of sparse traffic conditions. Otherwise, it uses an equally-weighted voting approach that provides a cooperative decision possessing that is less complex in the event of a large number of vehicles. We define the variable switching threshold in order to differentiate the sparse and dense traffic conditions. In the literature, there are several studies that predict the current traffic density [217]. In this work, we define the density, D , based on the number of neighbors in the communication range as follows [218]:

$$D(\text{vehicles}/\text{km}^2) = \frac{\text{Number of Neighbors} + 1}{\text{Transmission Range}}. \quad (5.12)$$

The total number of vehicles that can communicate within the transmission range is computed

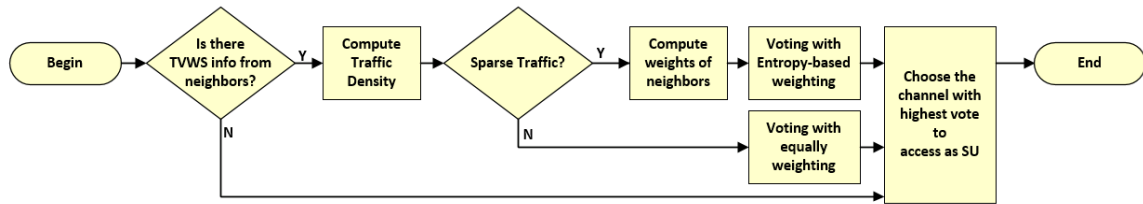


Figure 5.3: Flow chart of the cooperative voting algorithm at the receiver. If the vehicle receives an available channels list from nearby neighbor(s), it checks the number of neighbors. In case the number of vehicles is less than the threshold, it computes the weight functions of all the neighbors and itself when voting on the channel status. The channel that has the largest number of votes is chosen for the data transmission. In case the number of vehicles exceeds the threshold, an equally-weighted voting mechanism is employed. If the vehicle does not receive any available channel information from its neighbors, it trusts its own detection result.

as a function of the number of neighbors and the ego node. Standards on mobility models provide a definition of sparse, medium, dense, extreme dense traffic cases [73, Table 18]. In Table 5.1, the density for the traffic cases are listed based on ETSI TR 101 612 [73]. The ego vehicle computes the traffic density and compares the current density with the values in Table 5.1. In this case, the ego vehicle decides whether it is denser than the medium traffic class, *i.e.*, the density is higher than $100 \text{ vehicle}/\text{km}^2$, and the ego vehicle decides whether there are enough neighbors to perform accurate equally-weighted voting mechanism. Otherwise, it uses an entropy-based weighting mechanism to choose the DTV channel in order to access as SU.

The cooperating sensing mechanism including a switching operation is shown in Figure 5.3. The proposed mechanism performs individual distributed spectrum sensing using an optimal energy threshold. Once the decision of the neighbors are shared, the vehicle uses this information in order to vote on the availability of channels for use by an SU vehicle. If the number of neighbors is less than the neighbor threshold, the voting is performed by using an entropy-based weighted voting approach. Otherwise, the voting mechanism considers each vehicle with equal weighting. In the next section, the numerical results of proposed mechanism will be provided.

5.2 Bumblebee-Inspired Channel Switching Decision

Once the spectrum sensing is performed and the DTV channel is accessed by SU vehicle, the next research question is whether the SU should stay in the same channel or it should switch to

other DTV channel. If the current channel has a bad quality relative to other channels, it is required to switch to the other channel. However, each switching operation has a switching cost due to the computation, energy, and time consumption. It is not possible to use a fixed switching decision threshold since the vehicular environment is highly dynamic and the threshold which is valid for one environmental condition may give inaccurate decision in another conditions. To deal with this issue, we propose an adaptive switching decision based on an adaptive behavioral responses model of animals exposed to similar sensory conditions in their natural habitat. In particular, we focus on bumblebee foragers since they have evolved cognitive abilities that enable them to make adaptive behavioral decisions based on both individually and socially acquired information. Using the bumblebee model, an efficient channel sensing and selection system has been developed that can rapidly and adaptively respond to changes in multi-channel environments. The key component of this system is channel memory, which will enable the optimum point between switching to the better quality channel, and the channel switching cost. Although the proposed mechanism is specified for accessing DTV spectrum in this dissertation, it can be adapted to any spectrum band.

5.2.1 Why Bumblebees?

There have been several practical approaches proposed in the open literature that leverage distributed optimization techniques employed in nature, such as ant colonies, honeybees, and other insects, that perform swarm optimization of available resources [219]. However, these techniques require that each node within the network is dependent on the social interaction with all other nodes within the network, which is not the case in applications such as connected vehicle networks.

Consequently, we explore the bumblebee as a suitable social insect model for studying distribution optimization of channel resources. Unlike ants and honeybees, bumblebees socially share information with others but independently solve optimization problems within the distributed network. The behavior of colony-based animals often involves duty sharing, such as a queen, a scout, and a worker bee. Therefore, the social dependence of each individual does not cover all possible connected vehicle networking scenarios. For example, if a vehicle is in a rural area, it may lose connectivity with a centralized database or other neighboring vehicles. In such a scenario,

any optimization mechanism relying on this form of communication may potentially not work properly.

In a honey bee colony, the scout bee finds a food source, comes back to the hive, performs a “dance” to guide the worker bees to the food source [220]. If the nectar level decreases at the food source, the worker bees are informed of a better food source when they all return to the hive and decode the dance. The scouting process and the need for worker bees to return to the hive in order to be informed about a better food source can incur a delay with respect to accessing a better food source. By considering the highly dynamic characteristics of a vehicular environment, the honeybee colony behavior is not an efficient mechanism for such a highly time-varying environment. Similarly, ant colony behavior is based on the tracking the pheromones that primer ants have left [221]. Although ant colonies are very efficient for routing scheduling and organization, this mechanism also cannot deal with highly time-varying vehicular networking environment.

As an alternative to colony behavior, reinforcement learning mechanisms have been presented in the existing literature. Genetic algorithms provide a reliable optimization technique but at the expense of a large computation latency with respect to converging to the optimum value [116]. Partial swarm optimization is a very fast optimization technique since it jointly solves the fitness function based on a multiobjective formulation [222]. However, it is highly dependent on the initial information about the swarm structure, which is not realistic for connected vehicle networks.

Bumblebee foraging behavior is mainly based on individual decision mechanisms and fed by collaborative decisions when available to make a decision more reliable. Since there is no need to access any centralized system or wait for information from others, the decision and adaptation to change that can occur as rapidly as their highly efficient neural processing system allows. Thus, the proposed approach to translate bumblebee distributed optimization to connected vehicle networks and their access to wireless spectrum is efficient.

5.2.2 Translation Between Two Worlds

Matching the terminology between bumblebee foraging and vehicular communications is the first step in transiting bumblebee behavior to the vehicular optimization problem. In-band interference is an unwanted phenomenon in the channel bandwidth. The equivalent of this phenomenon are the pheromones produced by other bees in around a flower. Pheromones from other bees may

Table 5.2: Several Definitions in Connected Vehicular Communications and Their Equivalent Definitions in Bumblebees.

Vehicles	Bumblebees
In-band Interference	Pheromone by other bees
Out-of-Band Interference	Pheromone from the adjacent flowers
Minimum Channel Energy Level	Maximum Nectar Level
Computation/Process Time	Handling/Searching Time
Latency vs. Reliability	Speed vs. Accuracy
Switching Cost/ Time between channels	Switching Cost/Time between flowers
Channel activity over time	Flower occupancy over time
Channel-user distribution	Ideal free distribution

cause the incorrect detection of nectar levels by the bumblebee. Out-of-band interference is a form of interference produced by co-channels that is similar to the pheromones produced by the bees foraging at adjacent flowers.

Channel energy levels is a key feature with respect to channel access and is similar to nectar levels of the flowers for the foraging bees. However, there is an inverse relationship between these two features. In vehicular communications, it is desired to access the channel with as low energy level as possible since low energy level means there is no other user in the channel, which also means low noise levels and interference effects. On the other hand, bumblebees desire to access the flower with the highest nectar levels since they can collect more nectar as well as more energy.

Computation/process time of the algorithms used by connected vehicles corresponds to the handling/searching time of bees. Many algorithms have been proposed for connected vehicles that provide the perfect channel access scheme. However, if the algorithm gives the result across a longer time interval than the coherence time, the environment conditions change and the output of the algorithm does not match. Similarly, if the foraging process time for bumblebees to find the best food source is relatively long, this causes longer searching times as well as spending more energy. In other words, the trade-off between latency and reliability is mirrored with respect to the bumblebees in terms of speed versus accuracy.

Switching cost/time between channels should be considered although switching operations



Figure 5.4: Representation of mixed floral array used to assay learning, memory, and decision-making in foragers. Various patch colors present the nectar levels of flowers. Bumblebee uses the nectar levels to decide whether fly to the another flower with higher nectar level although it will spend energy to fly there.

provide the access to the channel with higher quality. Similarly, bumblebees switch to the flower with the higher nectar level in order to gain more energy. However, they also loose energy and time for switching to another flower.

Channel activity over time helps to understand channel behavior as well as design a prediction mechanism. Similarly, flower occupancy over time provide some input for modeling the foraging behavior. In the literature, foraging animals distribute themselves among several patches of re-sources, which is called *Ideal Free Distribution* [223]. As a result, these similarities between the two worlds help us to leverage these mechanisms from nature. The relation between these two disciplines is summarized in Table 5.2.

5.2.3 Foraging Theory

Bumblebees provide a robust biological framework for building and implementing cognitive algorithms for DSA in vehicular networks. Bumblebees are social insects that form colonies comprised of a single queen and up to several hundred workers. A small subset of workers called “for-agers” have the sole task of finding and collecting food for the colony in the form of floral nectar

and pollen rewards [224]. Foragers routinely encounter a wide array of flowers with reward levels that rapidly change over time and space (see Figure 5.4) [225]. Foragers are not pre-programmed with information on the reward level associated with different flowers [226]. Rather, they learn and remember the reward level and sensory cues (color, odor, shape) associated with each flower types and then decide which ones to visit [227]. Importantly, bumblebee foragers do not depend on "scout" bees such as honeybees or pheromone trails left by others such as ants. Consequently, each individual has the capacity to learn, remember, and track changes in floral rewards on its own. This system has evolved to enable maximal reward intake to the colony across complex and highly variable floral conditions. While searching for flowers containing the greatest reward, foragers implement a number of adaptive behavioral processes that are comparable to those processes needed for vehicles to function independently and effectively in a connected network environment. First, foragers (vehicles) evaluate the available flower types (channels) and then select the type (channel) that yields the greatest reward (channel quality). Second, foragers (vehicles) track and respond to changes in floral reward levels (channel quality) in a flexible manner. Finally, foragers (vehicles) make floral (channel) decisions that maximize the rate of nectar delivery to the colony (constant utilization of a high quality channel by the vehicle). For example, the decision on whether or not to switch to a new flower type (channel) is based on a trade-off between the rewards gained by visiting a new type types (channel quality) and the time costs incurred when switching to that type (channel; also referred to as a "switch cost"). Although they primarily use their personal experiences to make floral decisions, they can also enhance their knowledge of floral environments by gaining information from other foragers. For example, individuals can passively acquire information about reward quality from cuticular hydrocarbon "footprints" left on flowers by previous foragers: low hydrocarbon levels signal high likelihood of reward and high hydrocarbon levels signal low likelihood of reward. In this way, individual bumblebee foragers can use the experiences of others (use memory of other vehicles) to increase their efficiency of flower (channel) selection by minimizing the amount of time spent (cost) on empty flowers (low quality channels). By incorporating this agent-based approach into our empirical studies of forager behavior, we greatly accelerate the subsequent development and implementation of cognitive algorithms for optimal channel selection by vehicles in connected network environments.

5.2.4 Proposed Switching Decision Mechanism

To leverage the potential of bumblebee foraging behavior in connected vehicle environments, we propose to translate evolutionarily optimized bumblebee forager memory strategies to DSA decision making for connected vehicle networks. One of the major challenges faced by vehicles in a connected network environment is that they must accurately estimate channel quality from power levels that significantly vary over both time and space. The incorporation of an individual memory component into the algorithm design would overcome this challenge by enabling individual vehicles to derive estimates of local channel quality, which could then be shared throughout the vehicular network. Equipping vehicles with an unlimited memory capacity would provide the most accurate estimate of channel quality. However, unlimited memory would also generate additional costs, *e.g.*, information processing speed, time lag in reacting to environmental changes. Thus, determination of an optimal decision-making strategy requires consideration of memory capacity, dynamics, and associated costs. Bumblebees face identical constraints in choosing the optimal foraging strategy in variable floral environments.

Once the SU vehicles occupy the channel that is available, \mathbf{H}_0 , they need to periodically check whether they may switch to a better channel. The key parameter associated with the channel switching decision is the switch threshold, which decides whether the users should continue to use the same channel or search for another. However, the fixed switch threshold does not work for a highly dynamic connected vehicle environment. For example, the noise level may be low while the vehicle drives across a highway during a time step, and then it can drive into an urban area possessing a high noise floor during the next time step. In this example, switching to another channel may not be the best decision since all of the channels could potentially be noisy. To overcome this issue, we borrow the control mechanism employed in optimal foraging theory [224]:

$$\text{Switching Decision} = \begin{cases} \text{“Switch”}, & \frac{D_i}{\mathbf{h}_i} \leq \frac{\sum_{k \neq i} \lambda_k \mathbf{D}_k}{1 + \sum_{k \neq i} \lambda_k \mathbf{h}_k} \\ \text{“Stay”}, & \text{otherwise} \end{cases}, \quad (5.13)$$

where $D_x = \max_j(\mathbf{E}_j) - \mathbf{E}_x$ the subscript i refers to the channel which is currently used, while k refers to the other ones than Channel i , and j refers to the channel which has the highest energy

level. The duration of searching for and switching to Channel k is defined as λ_k and the other cost to switch Channel k such as energy consumption and computation is defined as the parameter of h_k . Without loss of generality, we assume the switching time and cost are the same for all channels since the network devices and capabilities are the same for all vehicles.

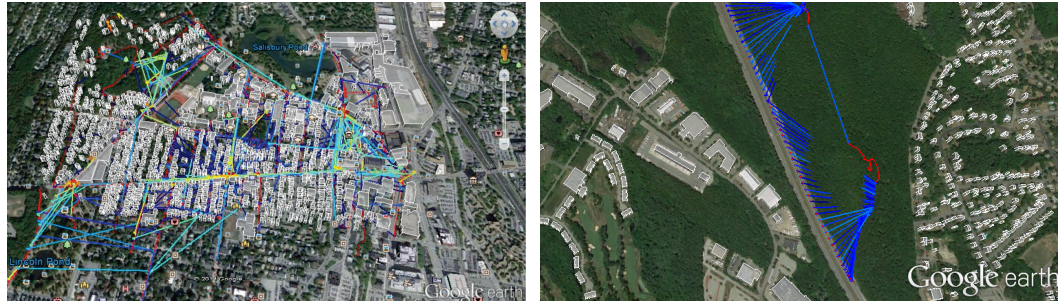
The fraction in Equation (5.13) formalizes the *Benefit/Cost* rate of the switching operation. The benefit is defined as the lowest energy level since SUs are searching for the available channels and if available, the least noisy one. Therefore, the benefit is the difference between the energy level channel, which has the highest one, and the energy level of the current channel. A larger difference between the highest energy level and the current noise floor implies a more beneficial channel. In case the current benefit/cost rate is less than the others, it means there is a less noisy channel worth switching to despite the switching cost.

5.2.5 Memory Structures

Our proposed mechanism includes an individual memory structure to store the energy levels of the channel during each energy detection period. By using the stored energy values, the proposed channel access technique provides long term understanding of channel behaviors. For example, the individual responses for changing channel energy values without memory. However, in case there is an instantaneous change in a channel energy level, the individual should not need to respond to that change. The output of the memory structure helps to eliminate this effect of instantaneous changing.

We use the mean value of the stored energy values for each channel. However, the weighting of the memory stacks needs to be defined differently, even adaptively. In the proposed mechanism, the individual vehicle stores the channel energy values during the defined memory length, computes its mean, and uses this mean energy values to perform in switching decision in Equation (5.13). The memory structure Equation (5.13) transforms as:

$$\text{Switching Decision} = \begin{cases} \text{“Switch”}, & \frac{\bar{D}_i}{\mathbf{h}_i} \leq \frac{\sum_{k \neq i} \lambda_k \bar{D}_k}{1 + \sum_{k \neq i} \lambda_k \mathbf{h}_k} \\ \text{“Stay”}, & \text{otherwise} \end{cases}, \quad (5.14)$$



(a) Dense urban traffic

(b) Light highway traffic

Figure 5.5: The artificial vehicle traffic data in Worcester, MA for numerical results.

where \bar{D}_x is computed by using the mean of the stored channel energy values in the memory. The memory length directly affects the output of the memory mechanism as well as the switching decision. For highly varying vehicular environments, it is not efficient to use a large memory length since the energy values will change and the next energy value will be uncorrelated relative to the stored energy values. On the other hand, large memory lengths help to decrease the switching costs and make the channel access efficient for stable vehicular environment.

5.3 Numerical Results

We analyzed the performance of the proposed cooperative channel sensing algorithm within a CVN environment using the *GEMV*² Vehicle-to-Vehicle (V2V) propagation simulator and MATLAB [43]. *GEMV*² computes the propagation features of vehicular communication links for given vehicular traffic and environment map. The experiment regions are obtained in Open Street Map [201] as shown in Figure 5.5 for dense urban and sparse highway scenarios. Vehicle traffics are created on SUMO [200] for the given experiment regions for 100 sec. During the experiment, the vehicles are moving in the experiment region randomly. As the experiment time progresses on, the number of vehicles in the experiment region increases. The parameter setup implemented in *GEMV*² is summarized in Table 5.3.

Table 5.3: System Parameter Setup.

Parameter	Value
Communication Parameters	
Transmission Power (dBm)	23
Carrier Sense Threshold (dBm)	-90
Noise Floor (dBm)	-113
Number of Samples per detection	1024
Max Transmission Range (m)	500
Message Period (msec)	100
DTV Band (MHz)	509-605 & 617-698
Mobility Parameters	
Number of Lanes	2-6 (Depends on street)
Number of Vehicles	150 (Sparse)&1200 (Dense)
Size of Experiment Region (km ²)	2

5.3.1 Simulation Results

We show the results for proposed distributed cooperative spectrum sensing mechanism by comparing the existing solutions. In addition to better performance results, we prove that the proposed mechanism has less computational time than the channel coherence time. This feature makes the proposed algorithm more realistic. Lastly, we show the results for proposed channel switching decision mechanism. We provided a *Benefit/Cost* rate analysis and concluded the results with the process time analysis.

5.3.1.1 Channel Sensing Algorithm

In Figure 5.6, the probability of incorrect detection defined by Equation (5.3) is presented as a surface function. The optimization techniques defined in Section 5.1.2 can provide a global optima only for convex and concave functions. Since the probability of incorrect detection is convex, there is only one minimum point for each SNR value. Hence, the proposed mechanism is valid for any operating condition.

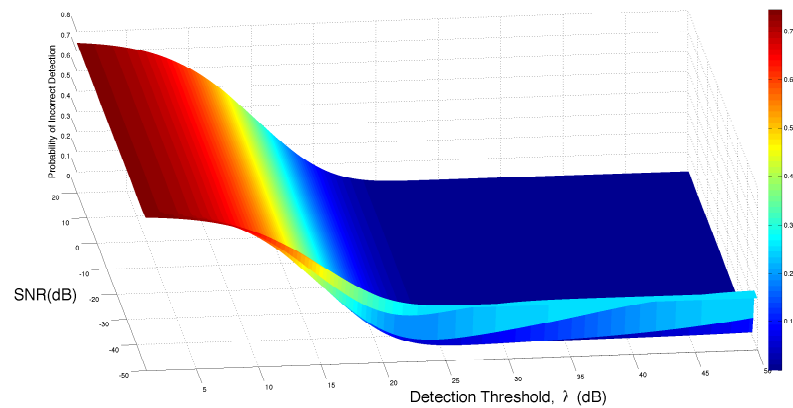


Figure 5.6: Probability of incorrect detection by changing the SNR and detection threshold. For each SNR value, there is only one minimum point since the function is convex.

In Figure 5.7, the probability of incorrect detection is derived in order to optimize the adaptive energy threshold for both Secant and Newton's methods, which is chosen as a reference numerical method for the literature, and also compared with the result of having no optimization of the energy detection threshold. The results show that adapting the detection threshold provides approximately a 20% decrease in incorrect detection around $\text{SNR} = 15$ dB. For other values of SNR, the optimization is more beneficial since it adapts the detection to the changing environment while the fixed threshold does not.

In Figure 5.8, the optimum threshold value is evaluated and compared for three results, namely: Actual value, Newton's method, and Secant method. The Newton's method is chosen as the reference numerical method. As observed in the results, both numerical methods give an accurate actual result for any SNR value. The benefit of the Secant method is that it provides the result in a shorter period of time since the process does not include the derivative operation.

In Figure 5.9, the convergence time of both Secant and Newton's methods are presented. The experiment is repeated 20 times and the worst performances are chosen to demonstrate. As observed in the results, both methods yield shorter times relative to the channel coherence time. This experiment is performed using low SNR values (5dB) since the algorithms converge to the optimum threshold more slowly in these scenarios. Therefore, the algorithms are sufficiently fast even in the worst case scenarios. The Secant method is relatively faster than the Newton's method since the Secant method does not need to compute a derivative operation. Since the coherence time is

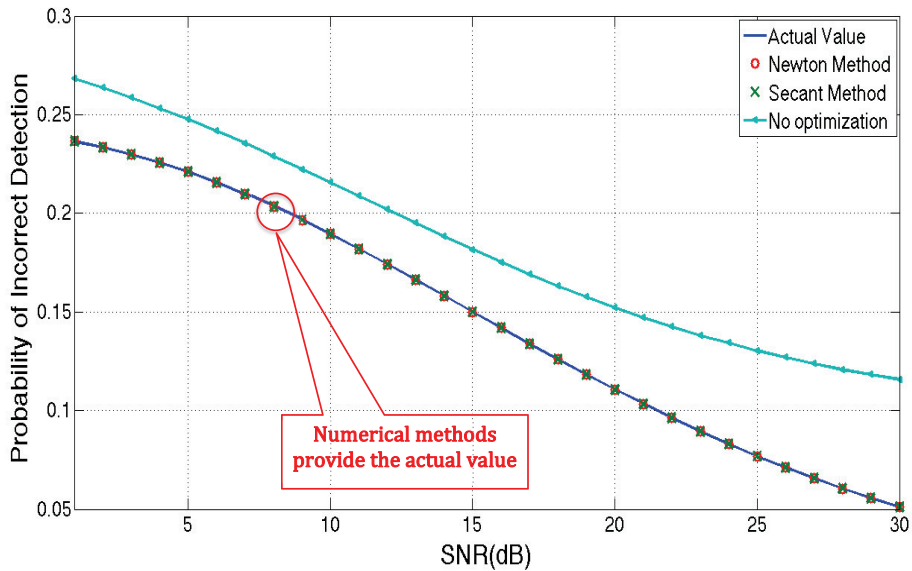


Figure 5.7: Probability of incorrect detection by the optimizing detection threshold. Comparing to a fixed threshold, the probability of incorrect detection is decreased by approximately 20%. Both iterative methods give the correct probability values.

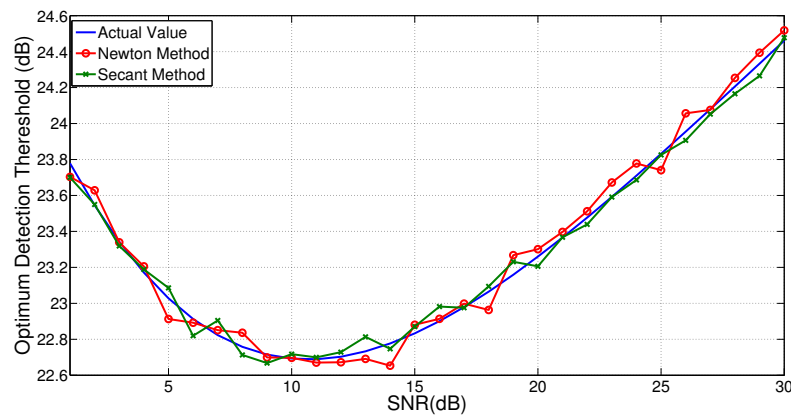


Figure 5.8: Optimum energy threshold for different SNR values. Both the Newton's method (as a reference numerical method) and the proposed Secant method are employed. The Secant method provides an accurate threshold value during a shorter process time.

relatively longer than the algorithm duration, the proposed method is capable of performing the detection before the channel values changes [152].

In Figure 5.10, the performance of the proposed fitness function in Equation (5.3) is compared with the fitness functions based on either only probability of missed detection or the probability

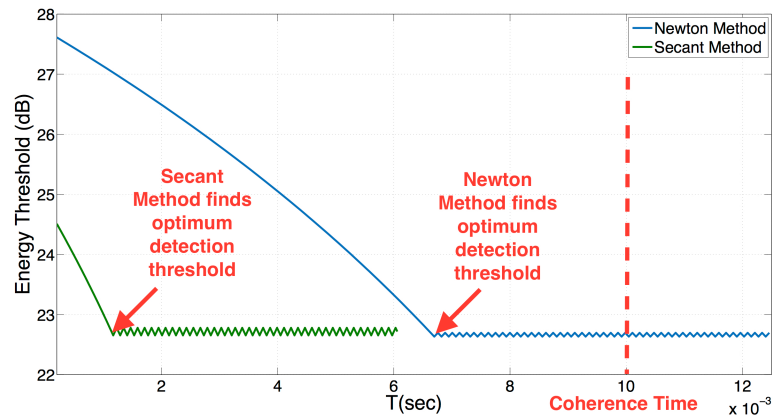


Figure 5.9: Convergence time of the iterative methods the optimum threshold is detected in less time relative to the coherence time. Therefore, the proposed approach would be suitable for time varying CVN operating conditions.

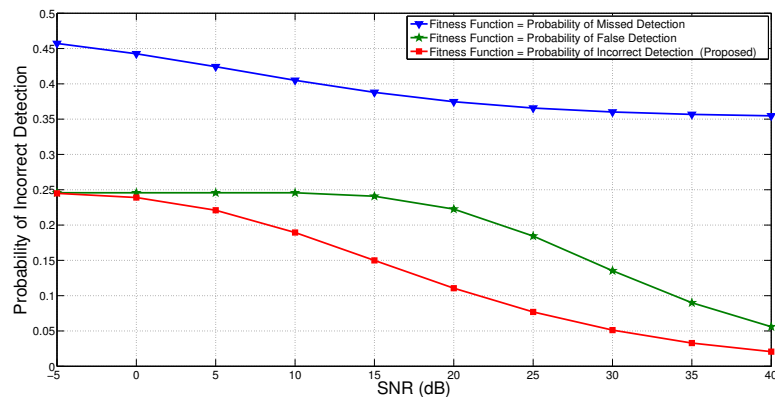


Figure 5.10: Probability of incorrect detection for different fitness functions for spectrum detection at the individual vehicle. If the fitness function is defined with respect to only probability of missed detection to find the optimum energy threshold, the chosen threshold may not be optimum for the probability of false detection, or vice versa. On the other hand, the proposed mechanism finds the optimum energy detection threshold by considering both probability of missed and false detection. Therefore, the incorrect detection is minimized.

of false detection. If the fitness function is defined with respect to only probability of missed detection to find the optimum energy threshold, the chosen threshold may not be optimum for the probability of false detection, or vice versa. On the other hand, the proposed mechanism finds the optimum energy detection by considering both probability of missed and false detection. Therefore the incorrect detection is minimized.

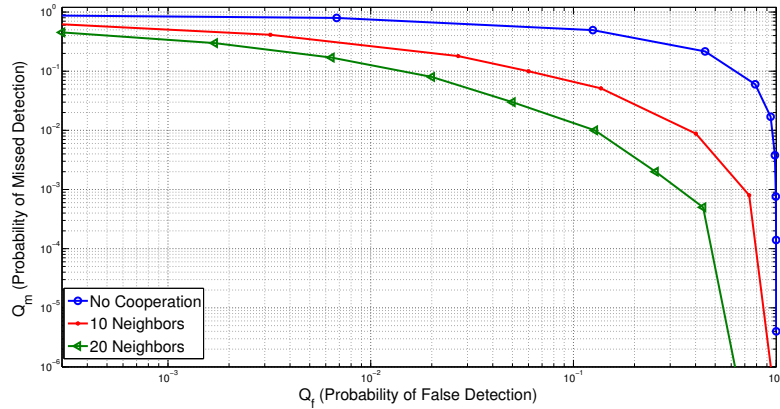


Figure 5.11: Receiver operating characteristics (ROC) curves for different numbers of attendees that join the cooperative channel sensing network. Notice how an increase in the number of neighbors provide a more robust sensing environment.

The performance of the proposed entropy-based weighted cooperative sensing approach is evaluated using the total probability of the missed detection and false alarm. We use the approach of Letaief *et al.* derived in [156] that computes the total error probabilities of M users by considering the transmission error on control message:

$$Q_i^f = 1 - \prod_{j=0}^M \left[(1 - P_j^f) (1 - P_{ij}^{te}) + P_j^f P_{ij}^{te} \right], \quad (5.15)$$

$$Q_i^m = \prod_{j=0}^M \left[P_j^m (1 - P_{ij}^{te}) + (1 - P_j^m) P_{ij}^{te} \right], \quad (5.16)$$

where the probability of transmission error on the control messages received from j^{th} neighbor is taken into account as P_{ij}^{te} . The transmission error for the ego node itself is set to zero, *i.e.*, $P_{i0}^{te} = 0$. In Figure 5.11, receiver operating characteristics (ROC) curve is shown for non-cooperative and cooperative scenarios with entropy-based voting mechanism for $M = 10$ and 20 users. The results show that increasing the amount of cooperation decreases the detection error and provides for a more reliable result despite the transmission errors during the control messaging.

In Figure 5.12, the entropy-based weighted voting scheme is compared with the non-cooperative sensing and equally-weighted voting technique in the current state-of-the-art for the sparse traffic condition. There are 150 vehicles employed in the selected experiment region that senses 10 DTV channels at each time step. The wrong detection percentage results show that the individual

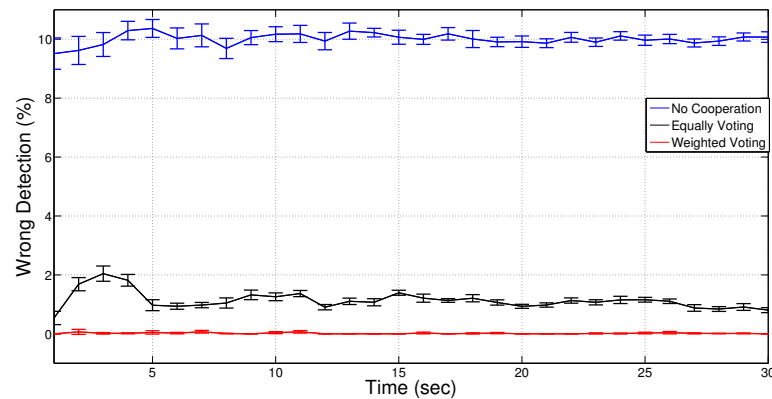


Figure 5.12: Comparison of only individual sensing, equally-weighted voting mechanism, and entropy-based weighted voting. Sparse traffic conditions of 150 vehicles were employed within the experiment region. Each vehicle senses the status of 10 channels at each time step.

spectrum sensing cannot handle the dynamic spectrum characteristics. Although the cooperative sensing scheme helps to decrease the wrong detection results, the equally-weighted voting still performs relatively poorly. Since the vehicle traffic environment is not dense, the distribution of the neighbors within the region varies more than the dense vehicle scenario. Since the ego node assigns the same credibility to all the neighbors without considering the variations for the path loss across the links, the cooperative sensing error occurs in the equally-weighted voting mechanism. Conversely, in the proposed entropy-based voting algorithm employing the adaptive energy detection threshold, each ego node defines the weight of each neighbor as well as itself. Therefore, even in the event that there are very few or no neighbors present, the ego node achieves an almost zero-error spectrum sensing performance unlike the other approaches.

In Figure 5.13, the entropy-based weighted voting scheme is compared with the current state-of-the-art employed in a high density traffic scenario. The performance of the individual spectrum sensing approach yields a spectrum detection error of around 10%. The detection of the equally-weighted voting cooperative sensing scheme converges to zero, as well as the entropy-based voting scheme. The equally-weighted approach converges to an errorless detection state at around 30 sec since it needs a sufficient number of neighbors in order to perform reliable voting mechanism. The proposed entropy-based mechanism is reliable with any number of neighbors. Therefore, the entropy-based approach converges to an errorless state more quicker than the equally-weighted

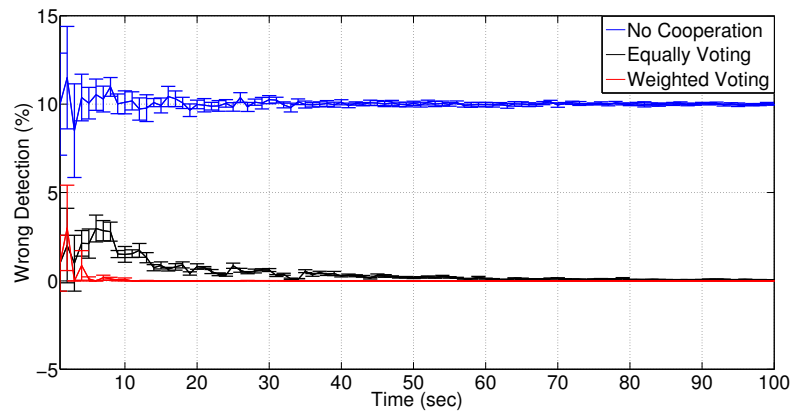


Figure 5.13: Comparison of only individual sensing, equally voting mechanism, and entropy-based weighted voting. High dense traffic conditions of 1200 vehicles were employed within the selected region. Each vehicles sense the status of 20 channels at each time step.

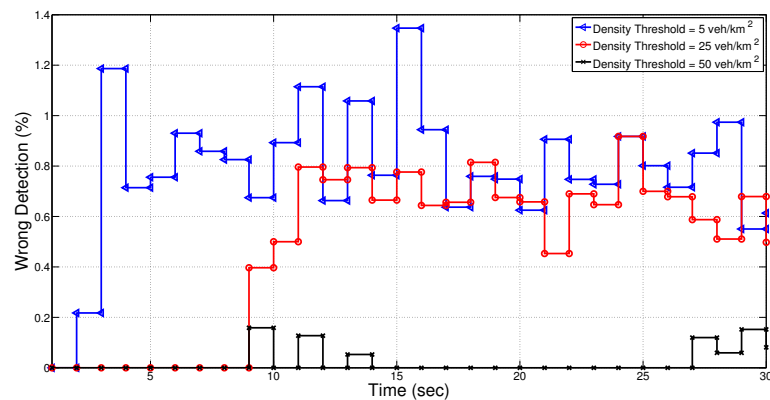


Figure 5.14: The effect of the threshold on the number of neighbors in sparse traffic conditions. The switching scheme decides on using the entropy-based weighted voting if the number of neighbors are less than the neighbor threshold. Otherwise, equally-weighted voting is performed.

approach without needing sufficient traffic density. Since the large amount of information being shared can compensate for the detection error caused by giving equal credibility to each neighbor, the equally-weighted voting approach can provide equivalently accurate detection performance as the proposed mechanism in case the ego vehicle has a large number of neighbors. Since the detection error converges to zero for both voting schemes, equally-weighted voting is chosen for dense traffic conditions due to its relatively low computational cost.

There exists a trade-off with respect to the proposed switching mechanism. The equally-

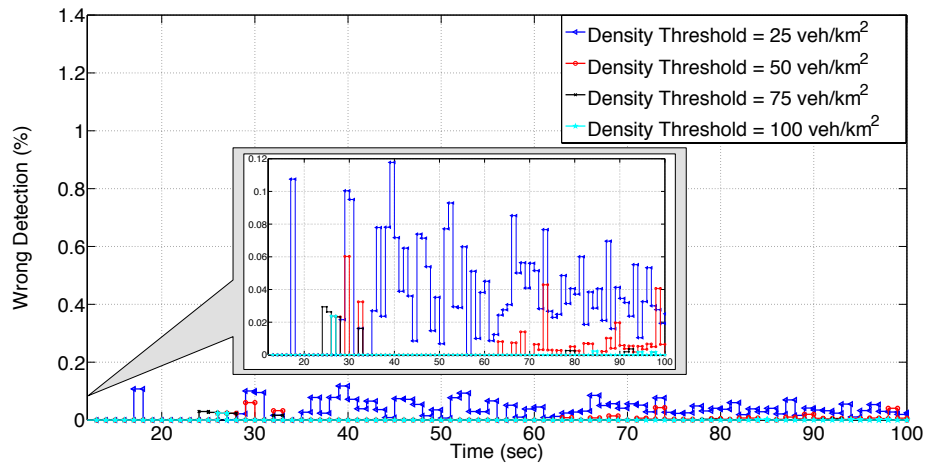


Figure 5.15: The effect of the threshold of number on the neighbors in dense traffic conditions. The cognitive scheme decides on using the entropy-based weighted voting if the number of neighbors are less than the threshold. Otherwise, equally-weighted voting is performed.

weighted voting mechanism is desirable since the computational cost is relatively lower to other techniques. However, the equally-weighted voting scheme cannot provide reliable voting results for sparse traffic conditions. On the other hand, the entropy-based weighted voting provides accurate detection results in any cases but it is computationally more expensive in high with the dense traffic. In Figure 5.14, the proposed switching mechanism between the entropy-based weighted and equally-weighted voting mechanisms is simulated in sparse traffic conditions. The detection results for 150 vehicles for 10 channels are computed during a 30 sec time interval. Although the general setup of the experiment is for sparse traffic, the individual vehicles may possess dense traffic characteristics due to the mobility and obstacle conditions at the current simulation time. In this experiment, different values for the traffic densities are chosen to represent the accuracy of both voting mechanisms. The blue line in Figure 5.14 shows that the ego vehicle uses equally-weighted voting if the current density is more than the density of $5 \text{ vehicle}/\text{km}^2$, which means equally-weighted voting is used for very sparse traffic condition according to the definition of sparse traffic in the standards [73]. Otherwise, it uses entropy-based weighted voting. As shown in the results, using the equally-weighted voting scheme in the sparse traffic causes detection error. Similarly, for the red line, if the ego vehicle uses the equally-weighted voting more than the density of $25 \text{ vehicle}/\text{km}^2$ which is still very sparse traffic, significant detection error occurs. For

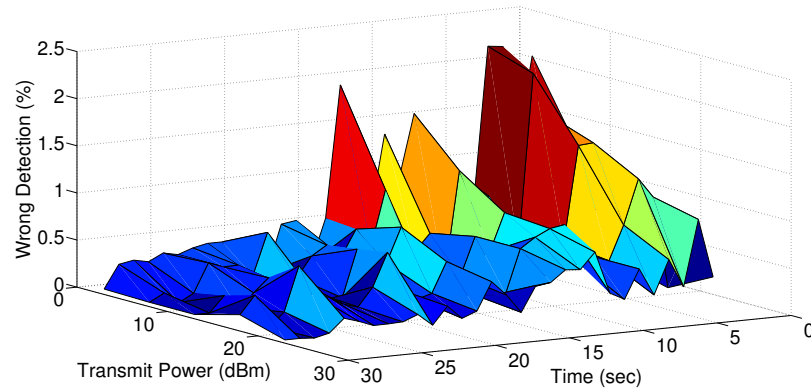


Figure 5.16: Detection performance changes with transmit power for sparse traffic conditions.

the black line, the switching mechanism uses the equally-weighted voting if the current traffic density is more than the density of $50 \text{ vehicle}/\text{km}^2$. Since the entropy-based weighted voting is used up to the density of $50 \text{ vehicle}/\text{km}^2$ and it provides an accurate detection although the small number of neighbors, it provides almost error-free mechanism.

In Figure 5.15, the switching mechanism between the entropy-based weighted and equally-weighted voting mechanisms is simulated in dense traffic conditions. Similar to sparse traffic, different values for the traffic densities are chosen to represent the accuracy of both voting mechanisms. For the different threshold values, the ego vehicle uses entropy-based weighted voting less often than the threshold mentioned in the legend and equally voting more often than the threshold. Since the ego vehicle has a large number of neighbors for reliable spectrum detection most of the time in the dense scenario, the equally voting can provide almost error-free detection. As a result, the proposed switching mechanism due to the sparse and dense traffic classes is consistent with the definition of traffic classes defined in standards [73].

In Figure 5.16, the same sparse traffic experiment is simulated for different transmit power values for the proposed distributed cooperative sensing mechanism. Transmit power values affect the SNR level and the detection performance, which are important to observe since the standards have not been finalized yet regarding the transmit power [73]. Furthermore, recent research activities propose adaptive transmit power techniques which changes in the interval from 10 to 23 dBm based on the environment and application requirements e.g., Chapter 4. The results show

that transmit power can cause incorrect detection up to 2.5%.

5.3.1.2 Computational Complexity and Process Latency

One major consideration with respect to connected vehicles is process latency. In this subsection, we evaluate computational complexity and process the latency of proposed mechanism². In Table 5.4, the computational complexity of both the entropy-based weighted voting and equally-weighted voting schemes are compared with respect to the amount of mathematical operations they each perform. The operations of Equations (5.10) and (5.11) are listed in the first two lines of the table. These operations are performed $M + 1$ times, which is obtained from the M number of neighbors as well as the ego vehicle itself. Once the weights are obtained, voting is performed by summing the weights of the M neighbors and the ego vehicles for each channel. Defining the total number of channels to be equal to N , the $M + 1$ adding operations are performed N times. For the equally voting scheme, only the binary decisions of the neighbors and the ego vehicle are summed up for N channels. As a result, the proposed entropy-based weighted voting scheme has a higher computational complexity relative to the equally-weighted voting mechanism. Therefore, the switching mechanism is used to leverage the benefit of the robustness associated with the entropy-based weighted voting scheme and the low computational load associated with the equally-weighted voting scheme.

In Table 5.5, the process time is shown for both sparse (150 vehicles) and dense (1200 vehicles) traffic scenarios within the experiment region. Although the complexity of the proposed algorithm is higher than the equally-weighted voting algorithm, the latency levels do not violate the coherence time limitations, *e.g.*, 1 – 10 msec depends on the vehicle speed, as Kremo *et al.* explained in [152]. These results prove that proposed algorithm provide an accurate spectrum detection for any environment conditions without violating the latency limitations.

5.3.1.3 Channel Switching Decision Mechanism

The channel characteristic is shown in Figure 5.17. Vehicles switch between channels in order to find the most powerful available channel of a given time instant. The adaptive behavioral

²Experiment is run with Intel Core i7 and 2.2 GHz processor. The processing time is tested by using *tic – toc* comments on *MATLAB*.

Table 5.4: Computational complexity analysis based on the number of mathematical operations at each voting scheme. Total number of mathematical operations that are noted at the last two lines show that equally-weighted voting has relatively lower complexity than entropy-based weighted voting.

	Operation	\times	$+/-$	\log_2	\div
Entropy-Based Weighting	Eq. (5.10)	$2 \cdot (M + 1)$	$(M + 1)$	$2 \cdot (M + 1)$	
	Eq. (5.11)		$2 \cdot (M + 1)$		$M + 1$
	$Ch_n = \sum_{j=0}^M w_j \quad n = 1 \dots N$		$N \cdot (M + 1)$		
Equally Voting	$Ch_n = \sum_{j=0}^M \mathbb{1}_j \quad n = 1 \dots N$		$N \cdot (M + 1)$		
Entropy-Based Total		$O(2 \cdot (M + 1))$	$O((3 + N)(M + 1))$	$O(2 \cdot (M + 1))$	$O(M + 1)$
Equally Total			$O(N \cdot (M + 1))$		

Table 5.5: Process latency caused by cooperative sensing mechanism. Results show that the operation duration of both voting mechanisms is lower than channel coherence time that makes the proposed approach practical.

	150 Vehicles	1200 Vehicles
Entropy-Based Weighted Voting (Min-Max μsec)	401.38 – 418.64	271 – 790.416
Equally Voting (Min-Max μsec)	13 – 26.23	9 – 135

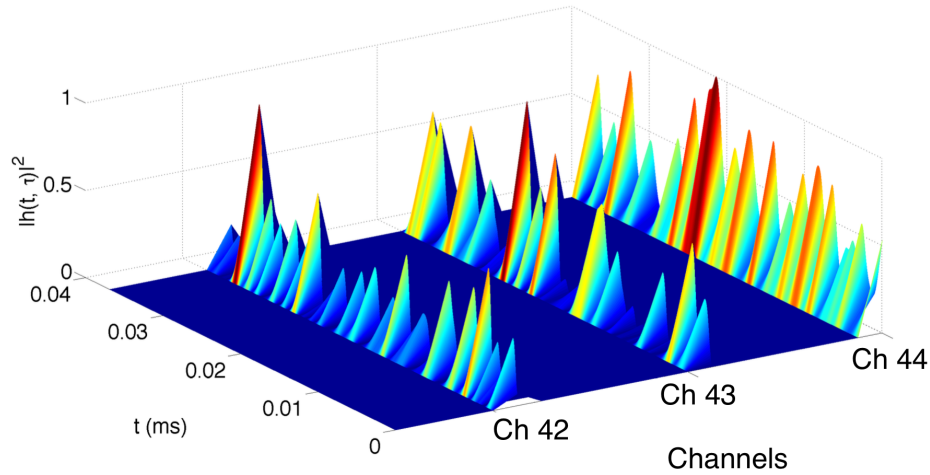


Figure 5.17: Normalized squared magnitude of the channel impulse response: t refers to the time variation on a channel. Three representative channels are visualized to indicate the environment changes on time.

response mechanism is needed to decide whether the channel is worth switching to despite the switching cost. The individual memory will provide a solid decision on the channel switching. For example, a vehicle chooses to be on Channel 42, if available, by using its individual memory since Channel 42 is more powerful based on its long term behavior. Therefore, the unwanted switching

cost, which is caused by instantaneous decisions, will be avoided.

In Figure 5.18 and Figure 5.19, the sparse traffic conditions, $12 \text{ vehicles}/\text{km}^2$, are tested without and with the proposed switching mechanism for various memory lengths. The simulation is performed for 100 sec. The number of randomly moving vehicles increases at each time step from 0 to 1200 vehicles. In Figure 5.18, the number of vehicles that can access the best possible channel at each time step. "Best possible channel" means the available channel to be used by the SU is the least noisy DTV channel. In Figure 5.19, the number of vehicles that performs the switching operation is counted to compute the switching cost. Without a switching decision, vehicles randomly access a DTV channel and stay in the same channel until the connection is lost. The switching cost is always zero for this case since the switching operation is never performed. The proposed switching decision with a memoryless mechanism checks the requirement for the switching operation by using Equation (5.13) at each time step. Therefore, the vehicles can access the best possible channel at each time if they are not already using a good quality channel. However, the switching cost is higher than the memory mechanisms since they check the switching decision at each time step. For the memory systems, the energy detection is performed at each second and stored in the memory. When the memory length is 3 sec, the memory stores the energy values for 3 sec, performs the switching decision, and then waits for the next 3 sec to store the new energy levels to perform another switching decision. By increasing the memory length, the number of best vehicles accesses of the best available channels decrease since the waiting time for the switching decision increases. However, the switching cost also decreases since the number of switching operation decreases. In Figure 5.20 and Figure 5.21, the experiment is run for dense urban traffic conditions, *i.e.*, $150 \text{ vehicles}/\text{km}^2$. In this scenario, the number of vehicles increases from 0 to 900 vehicles at each time step. Unlike sparse highway scenario, the channel qualities quite change every time step due to dense traffic, reflection and scatterers by the obstacles. The memory mechanism waits for new energy values are stored the memory. Therefore, the longer memory lengths wait longer than the shorter memory lengths to perform the switching decision. Since the energy values change immediately, the number of vehicles that uses the best available channel significantly decrease at the next time step when performing the switching. Therefore, although there is a decrease on switching cost, using a longer memory length in dense urban scenarios may not be practical.

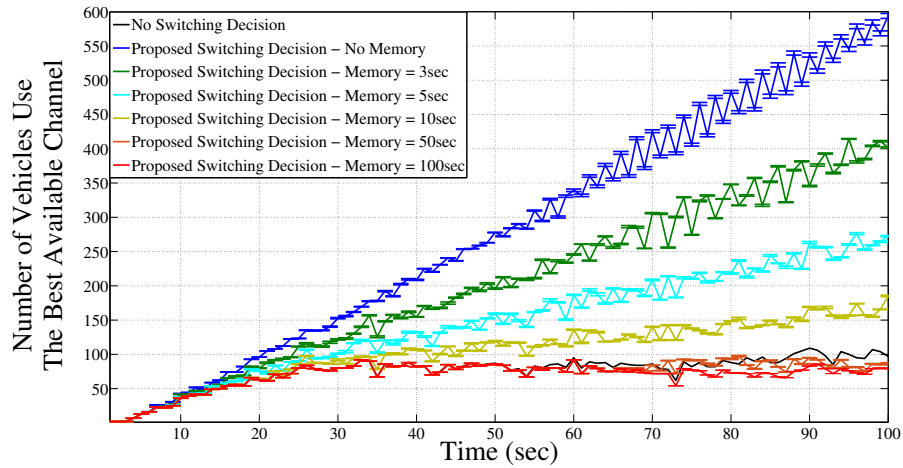


Figure 5.18: Sparse highway traffic: The best number of vehicles that can access the best possible channel at the corresponding time step.

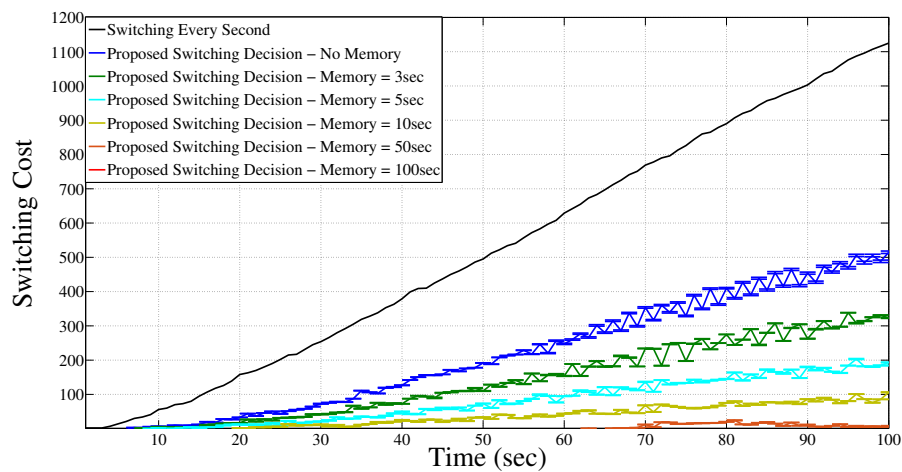


Figure 5.19: Sparse highway traffic: Switching cost at the corresponding time step.

The previous results show the trade-off between accessing the best available channel and switching costs. In Figure 5.22 shows the *Benefit/Cost* rate to decide which memory length to choose. For sparse highway traffic, 10 *sec* memory length provides the optimum point of trade-off while 5 *sec* is the best for dense urban traffic. For highly dynamic environment, lower memory length is preferred since the mean of channel values are different than the instant channel values that may cause wrong detection. For less dynamic environments, large memory length is pre-

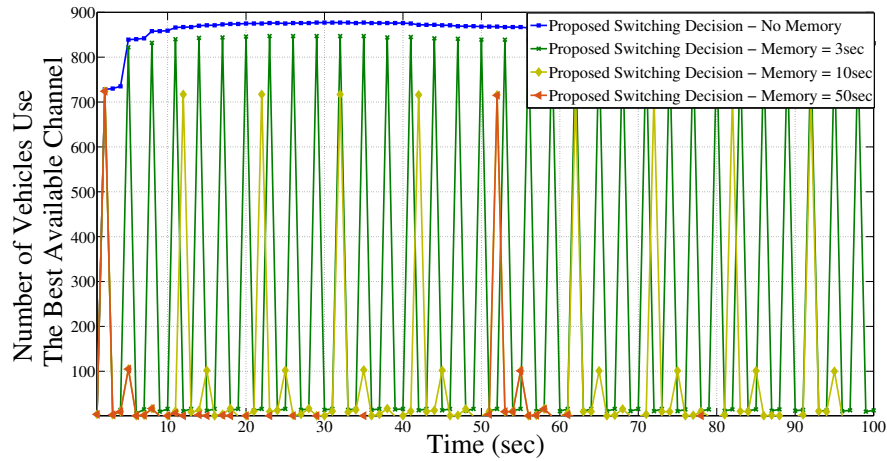


Figure 5.20: Dense urban traffic: The number of vehicles that can access the best possible channel at the corresponding time step.

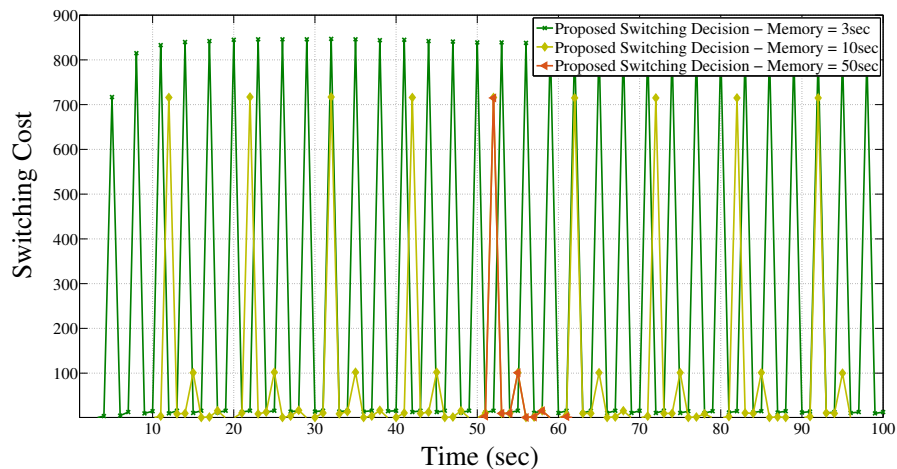


Figure 5.21: Dense urban traffic: Switching cost at the corresponding time step.

ferred since the average of channel values in the memory is close to the instant values that helps to decrease channel switching operation as well as switching cost.

In Figure 5.23, the proposed approach is compared with the existing works, *i.e.*, optimal modified deflection coefficient (OPT-MDC), parallel artificial bee colony (PABC), genetic algorithms (GA), partial swarm optimization (PSO), memory enable genetic algorithms (MEGA). Since the proposed switching mechanism is based on individual decision process and uses the energy val-

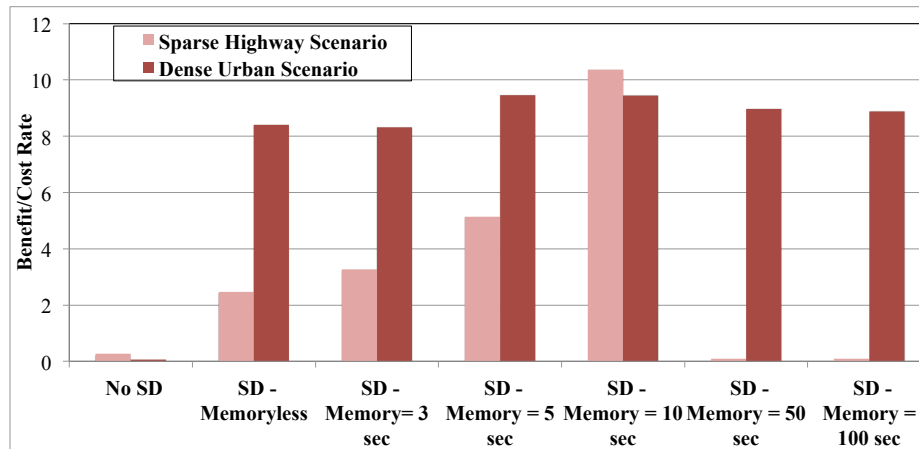


Figure 5.22: Sparse highway traffic: Benefit / Cost Rate for various memory lengths. For sparse highway traffic, 10 sec memory length provides the optimum point of trade-off while 5 sec is the best for dense urban traffic.

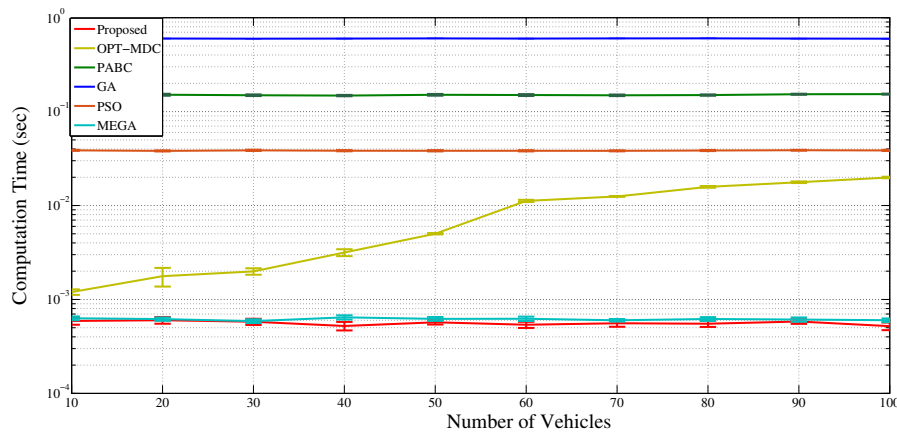


Figure 5.23: Benchmark on computation time: the proposed approach, optimal modified deflection coefficient (OPT-MDC), parallel artificial bee colony (PABC), genetic algorithms (GA), partial swarm optimization (PSO), memory enable genetic algorithms (MEGA). Since the proposed switching mechanism is based on individual decision process and uses the energy values in the memory without performing any complicated mathematical operation, the proposed approach possesses a low computation time.

ues in the memory without performing any complicated mathematical operation, the proposed approach possesses a lower computation time than existing solutions [116, 228].

As a result, bumblebee foraging behavior provides a potentially efficient solution with respect to channel accessing requirements in vehicular communications. Individual adaptive switching

decisions provide a fast computation, while obtaining the optimum point between switching to the better quality channel and the switching cost by memory structure.

5.4 Chapter Summary

In this chapter, we propose a voting-based distributed dynamic spectrum access solutions for CVNs. We first proposed a voting based cooperative channel sensing algorithm for connected vehicles. We adapted the energy detection threshold based on minimizing the probability of incorrect detection using a fast numerical method and employed the optimum energy detection threshold to sense the available channels. The individual decision per available channel is shared between one-hop neighbors. The ego vehicle uses entropy-based weighted voting mechanism to derive its neighbors' credibility as well as its own. The weights are used for voting on the available channel and the channel that has the highest votes is selected to be used by the SU vehicle. The proposed mechanism employs a tradeoff between robustness and computational load. To achieve a suitable tradeoff, we proposed a switching algorithm between the entropy-based weighted voting mechanism applied to sparse traffic conditions and an equally-weighted voting mechanism for dense traffic conditions. Once SU vehicles access the DTV channel, we proposed a distributed channel switching decision mechanism. Channel energy levels are compared to decide whether there is a better quality channel than currently used one, that is worth to switch despite of its switching cost. With this decision mechanism, the optimum trade-off point between switching cost and benefits is provided with memory structure.

Chapter 6

Conclusion and Future Work

In this dissertation, we proposed distributed adaptation techniques for connected vehicles to have reliable communications in any environmental condition. We first identify the channel characteristics to enable the research approaches. Next, we proposed a distributed congestion control algorithm for defined channel characteristics that increases the environmental awareness and achieves the application requirements. While the proposed DCC algorithm provides a robust mechanism for high priority messaging in DSRC band, we proposed a distributed DSA mechanism to access the DTV channels for low priority messaging. The solutions defined in this dissertation are practical and compatible with the communication standards.

6.1 Research Achievements

In this dissertation, several contributions have been made in the area of CVNs. The research achievements of this thesis are the following:

- Channel models for CVNs with large and small scale fadings. The system limitations of P2P and multi-hop CVNs. A novel selective message relaying mechanism, which decreases the message congestion due to the redundant messages received by relay vehicles without any assumption on network architecture.
- A novel environment- and context- aware combined power and rate adaptation algorithm for decentralized V2V communications. The proposed algorithm jointly controls the message

rate and transmission power as well as achieves the target awareness rate, target message rate, and target awareness distance requirements of each vehicle for any environment and context.

- A novel voting based distributed cooperative VDSA mechanism with an adaptive optimization of the energy detection threshold by considering process time limits. The optimum point of the trade-off between the computational cost and robust spectrum sensing is achieved. The spectrum detection error of the proposed mechanism converges to zero in any environmental condition without violating process time constraints.
- A bumblebee-inspired distributed adaptive channel switching mechanism to decide if the unlicensed user should stay in the same channel or switch to better channel. The proposed mechanism uses memory structure to obtain the optimum point between switching to the better quality channel and the switching cost. Hence, the increase is observed on the *Benefit/Cost* rate.

6.2 Lessons Learned

The summary of the discoveries from this dissertation are listed below:

- Large scale fading characteristics vary due to LOS and NLOS links. NLOS links possess various attenuation model due to the different obstacle types on the links
- There are two small scale fading models for multi-hopping connected vehicles: Geometrical and SoS models. Geometrical model computes the channel impulse responses based on geometrical parameters of scatterers. However, this model assumes the number and location of scatterers are known which may not be practical for dynamic CVN environment. On the other hand, SoS model assigns the location of the scatterers statistically as well as considers the time delay between multipaths. These features make SoS model more practical and more accurate.
- Multi-hop CVNs have better performance than P2P regarding to channel capacity and propagation error. However, rebroadcasting each received message at the relay vehicle causes

message storm. Clustering messages helps to detect the redundant information and rebroadcast only unique incidents. Thus, the same environment awareness is satisfied by rebroadcasting less number of messages.

- Distributed congestion control technique improves environment awareness and provides the context requirements. Existing techniques can be classified under three main categories: only transmit power adaptation, only message rate adaptation, combined power and rate adaptation.
- For transmit power adaptation, estimation of the current path loss exponent makes the system adjust itself to the current environment conditions. As using the current path loss exponent, the transmit power at the next time step can be found to reach the target awareness distance.
- Message rate adaptation keeps the channel utilization under the limits defines by standards.
- Combined power and rate adaptation approach needs to proactively consider the effect of next power value decided by the mechanism on the next message rate performance or *vice versa*.
- VDSA techniques needs adaptive energy detection threshold due to the dynamic environment characteristics. For an accurate adaptive sensing, the adapted energy threshold should minimize both false detection and missed detection errors.
- Cooperative sensing needs an accurate definition of neighbor credibility. Entropy as a definition of uncertainty of the information provides a reliable definition of credibility.
- Channel switching decision mechanism needs to be adaptive and simple. Bumblebees foraging behavior helps to deal with these requirements.

6.3 Future Works

The future work of this PhD research can be classified in two main categories. In the first category, we will be extending the proposed solutions to the further steps. The channel capacity

analysis for connected vehicles will be derived for frequency selective fading characteristics as an extension of block fading analysis in this dissertation. Another future work will be on bumblebee-inspired channel switching decision mechanism. Various weight functions will be defined for memory structure alternative to average the stored values in the memory as defined in this dissertation. Furthermore, we will be working on adaptive weighting on memory stacks that changes the weights each time by learning about the current environment conditions.

Second category of the future works is to combine the connected vehicles including the proposed solutions in this dissertation with the various architectures such as the sensory system of the vehicle. In addition, the combination of DSRC system and cellular networks is still an open research topic since using cellular networks for vehicular communications enables to have the benefits of both systems. Another practical consideration for future works is to bridge the DSRC standards with other standards since the improving technology leans to have all existing structures in one main frame. However, this approach needs to link the structures properly.

Bibliography

- [1] U.S. Department of Transportation Announces Decision to Move Forward with Vehicle-to-Vehicle Communication Technology for Light Vehicles. [Online]. Available: <http://www.nhtsa.gov/About+NHTSA/Press+Releases/2014/USDOT+to+Move+Forward+with+Vehicle-to-Vehicle+Communication+Technology+for+Light+Vehicles>
- [2] “Amendment of the Commission’s Rules Regarding Dedicated Short-Range Communication Services,” Federal Communications Commission, Tech. Rep. FCC 03-3240, Feb. 2004.
- [3] H. Hartenstein and K. L. Laberteaux, *VANET: Vehicular Applications and Inter-networking Technologies*. Wiley: 1st Ed, 2010.
- [4] Manifesto of the Car-to-Car Communication Consortium. [Online]. Available: www.car-to-car.org
- [5] “Vehicle-to-Vehicle Communications: Readiness of V2V Technology for Application,” U.S. Department of Transportation National Highway Traffic Safety Administration, Tech. Rep. DOT HS 812 014, 2014.
- [6] “Vehicle Safety Communications – Applications (VSC-A),” U.S. Department of Transportation National Highway Traffic Safety Administration, Tech. Rep. DOT HS 811 492A, 2011.
- [7] “Human Factors for Connected Vehicles: Effective Warning Interface Research Findings,” U.S. Department of Transportation National Highway Traffic Safety Administration, Tech. Rep. DOT HS 812 068, 2014.
- [8] Ertico Partners, Cooperative Mobility Services Plugtests. [Online]. Available: http://www.etsi.org/plugtests/ITS_CMS/Home.htm

- [9] R. D. Strickland, M. Yuan, S. Bai, D. Webber, and R. Miucic, "Vehicle to Pedestrian Communication System and Method," Patent US 20 150 035 685A1, Feb 5, 2015. [Online]. Available: <http://www.google.com/patents/US20150035685>
- [10] M. Dozza, M. Idegren, T. Andersson, and A. Fernandez, "Platform Enabling Intelligent Safety Applications for Vulnerable Road Users," *IET Intelligent Transport Systems*, vol. 8, no. 4, pp. 368–376, June 2014.
- [11] TMC Develops Mutual Power Supply System for Electric Vehicles and Homes. [Online]. Available: <http://www2.toyota.co.jp/en/news/12/06/0604.pdf>
- [12] 2015 FHWA Vehicle to Infrastructure Deployment Guidance and Products. [Online]. Available: http://www.its.dot.gov/meetings/pdf/V2I_DeploymentGuidanceDraftv9.pdf
- [13] ETSI TC ITS, "Intelligent Transport Systems (ITS); Vehicular Communications; Basic Set of Applications; Part 1: Functional Requirements," Tech. Rep. ETSI TR 102 637-1 V1.1.1, Sep. 2010.
- [14] Cooperative ITS Corridor Joint Deployment. [Online]. Available: https://www.bmvi.de/SharedDocs/EN/Anlagen/VerkehrUndMobilitaet/Strasse/cooperative-its-corridor.pdf?__blob=publicationFile
- [15] Tesla Autopilot Crash Exposes Industry Divide. [Online]. Available: <http://spectrum.ieee.org/cars-that-think/transportation/self-driving/what-next-for-teslas-autopilot>
- [16] U.S. Proposes Spending \$4 Billion to Encourage Driverless Cars. [Online]. Available: <http://www.wsj.com/articles/obama-administration-proposes-spending-4-billion-on-driverless-car-guidelines-1452798787>
- [17] GM, Toyota Make Big Investments –like \$1 billion big– in Autonomous Car Startups. [Online]. Available: <http://arstechnica.co.uk/cars/2016/03/gm-toyota-invest-self-driving-car-startups>
- [18] Kia is Thinking of Creating a Self-Driving Car. [Online]. Available: <http://technologyinformation12345.blogspot.com/2016/01/kia-is-thinking-of-creating-self.html>

- [19] 30 Corporations Working On Autonomous Vehicles. [Online]. Available: <https://www.cbinsights.com/blog/autonomous-driverless-vehicles-corporations-list/>
- [20] Honda Supports Smart Columbus for Electric Connected Cars and V2X. [Online]. Available: <http://www.autoconnectedcar.com/2016/06/honda-supports-smart-columbus-for-electric-connected-cars-v2x/>
- [21] Toyota Invests \$50M in Artificial Intelligence. [Online]. Available: <http://www.freep.com/story/money/cars/2015/09/04/intelligent-cars-robots-focus-toyota-research-plans/71702672/>
- [22] Apple's Tim Cook Sees 'Massive' Tech-led Upheaval in Car Industry. [Online]. Available: <http://www.ft.com/cms/s/0/153d2d62-76e8-11e5-933d-efcdc3c11c89.html#axzz4AxKIRsXV>
- [23] "IEEE Standard for Information technology– Local and metropolitan area networks– Specific requirements– Part 11: Wireless LAN Medium Access Control (MAC) and Physical Layer (PHY) Specifications," *IEEE Std 802.11p-2010*, pp. 1–51, July 2010.
- [24] J. B. Kenney, "Dedicated Short-Range Communications (DSRC) Standards in the United States," *Proceedings of the IEEE*, vol. 99, no. 7, pp. 1162–1182, July 2011.
- [25] "IEEE Standard for Wireless Access in Vehicular Environments (WAVE) – Multi-Channel Operation," *IEEE Std 1609.4-2016 (Revision of IEEE Std 1609.4-2010)*, pp. 1–94, March 2016.
- [26] "IEEE Standard for Wireless Access in Vehicular Environments (WAVE) – Networking Services," *IEEE Std 1609.3-2016 (Revision of IEEE Std 1609.3-2010)*, pp. 1–160, April 2016.
- [27] "IEEE Standard for Wireless Access in Vehicular Environments–Security Services for Applications and Management Messages," *IEEE Std 1609.2-2016 (Revision of IEEE Std 1609.2-2013)*, pp. 1–240, March 2016.
- [28] C. F. Mecklenbrauker, A. F. Molisch, J. Karedal, F. Tufvesson, A. Paier, L. Bernado, T. Zemen, O. Klemp, and N. Czink, "Vehicular Channel Characterization and Its Implications for Wireless System Design and Performance," *Proceedings of the IEEE*, vol. 99, no. 7, pp. 1189–1212, July 2011.

- [29] P. Bello, "Characterization of Randomly Time-Variant Linear Channels," *IEEE Transactions on Communications Systems*, vol. 11, no. 4, pp. 360–393, Dec. 1963.
- [30] B. Aygun, M. Boban, and A. M. Wyglinski, "ECPR: Environment- and Context-aware Combined Power and Rate Distributed Congestion Control for Vehicular Communications," *Computer Communications*, vol. abs/1502.00054, 2016. [Online]. Available: <http://arxiv.org/abs/1502.00054>
- [31] B. Aygun, R. J. Gegear, E. F. Ryder, and A. M. Wyglinski, "Adaptive Behavioral Responses for Dynamic Spectrum Access-Based Connected Vehicle Networks," *IEEE Comsoc Technical Committee on Cognitive Networks*, vol. 1, no. 1, pp. 45 – 48, Dec. 2015.
- [32] B. Aygun, M. E. Gamal, and A. M. Wyglinski, "Performance Analysis for High-Velocity Connected Vehicles," in *IEEE 81st Vehicular Technology Conference (VTC Spring)*, May 2015, pp. 1–5.
- [33] B. Aygun and A. Wyglinski, "Channel Modeling of Decode-and-Forward Relaying VANETs," in *IEEE 80th Vehicular Technology Conference (VTC Fall)*, Sept 2014, pp. 1–5.
- [34] B. Aygun, A. Soysal, and A. Wyglinski, "Short paper: Performance Analysis of MIMO-Based Decode-and-Forward Relaying VANETs," in *IEEE Vehicular Networking Conference (VNC)*, Dec 2013, pp. 222–225.
- [35] P. Papadimitratos, A. La Fortelle, K. Evenssen, R. Brignolo, and S. Cosenza, "Vehicular Communication Systems: Enabling Technologies, Applications, and Future Outlook on Intelligent Transportation," *IEEE Communications Magazine*, vol. 47, no. 11, pp. 84–95, Nov. 2009.
- [36] W. C. Jakes and D. C. Cox, Eds., *Microwave Mobile Communications*. Wiley-IEEE Press, 1994.
- [37] A. Akki and F. Haber, "A Statistical Model of Mobile-to-Mobile Land Communication Channel," *IEEE Transactions on Vehicular Technology*, vol. 35, no. 1, pp. 2–7, Feb 1986.
- [38] Y. Zheng and C. Xiao, "Simulation Models with Correct Statistical Properties for Rayleigh Fading Channels," *IEEE Transactions on Communications*, vol. 51, no. 6, pp. 920–928, June 2003.

- [39] C. Patel, G. Stuber, and T. Pratt, "Simulation of Rayleigh-Faded Mobile-to-Mobile Communication Channels," *IEEE Transactions on Communications*, vol. 53, no. 10, pp. 1773–1773, Oct 2005.
- [40] A. G. Zajic and G. L. Stuber, "Efficient Simulation of Rayleigh Fading with Enhanced Decorrelation Properties," *IEEE Transactions on Wireless Communications*, vol. 5, no. 7, pp. 1866–1875, 2006.
- [41] C. Xiao, Y. Zheng, and N. Beaulieu, "Novel Sum-of-Sinusoids Simulation Models for Rayleigh and Rician Fading Channels," *IEEE Transactions on Wireless Communications*, vol. 5, no. 12, pp. 3667–3679, Dec 2006.
- [42] J. Ortiz, *Mobile Networks (1st ed)*. Intech, 2012.
- [43] M. Boban, J. Barros, and O. K. Tonguz, "Geometry-Based Vehicle-to-Vehicle Channel Modeling for Large-Scale Simulation," *IEEE Transactions on Vehicular Technology*, vol. 63, no. 9, pp. 4146–4164, Nov 2014.
- [44] J. Karedal, F. Tufvesson, N. Czink, A. Paier, C. Dumard, T. Zemen, C. Mecklenbrauker, and A. Molisch, "A Geometry-Based Stochastic MIMO Model for Vehicle-to-Vehicle Communications," *IEEE Transactions on Wireless Communications*, vol. 8, no. 7, pp. 3646–3657, July 2009.
- [45] H. Kremo, I. Seskar, and P. Spasojevic, "Experimental Modeling of the Effect of Adjacent Lane Traffic on the Vehicular Channel," in *IEEE Vehicular Networking Conference (VNC)*, Oct 2009, pp. 1–8.
- [46] M. Boban and P. d'Orey, "Measurement-based Evaluation of Cooperative Awareness for V2V and V2I Communication," in *IEEE Vehicular Networking Conference (VNC 2014)*. IEEE, December 2014, pp. 1–8.
- [47] Information Society Technologies, "Final Report on Link Level and System Level Channel Models," Tech. Rep. IST-2003-507581 WINNER I, D5.4., 2005.

- [48] J. Gozalvez, M. Sepulcre, and R. Bauza, "IEEE 802.11p Vehicle to Infrastructure Communications in Urban Environments," *IEEE Communications Magazine*, vol. 50, no. 5, pp. 176–183, May 2012.
- [49] V. Shivaldova, A. Winkelbauer, and C. Mecklenbrauker, "Vehicular Link Performance: From Real-World Experiments to Reliability Models and Performance Analysis," *Proceedings of IEEE Vehicular Technology Magazine*, vol. 8, no. 4, pp. 35–44, Dec 2013.
- [50] V. Shivaldova, A. Paier, D. Smely, and C. Mecklenbrauker, "On Roadside Unit Antenna Measurements for Vehicle-to-Infrastructure Communications," in *Proceedings of IEEE International Symposium on Personal, Indoor and Mobile Communications (PIMRC)*, Sydney, Australia, September 2012, pp. 1–5.
- [51] G. Maier, A. Paier, and C. Mecklenbrauker, "Performance Evaluation of IEEE 802.11p Infrastructure-to-Vehicle Real-World Measurements with Receive Diversity," in *Proceedings of the 8th International Wireless Communications and Mobile Computing Conference (IWCMC)*, Limassol, Cyprus, August 2012.
- [52] V. Shivaldova, G. Maier, D. Smely, N. Czink, A. Alonso, A. Winkelbauer, A. Paier, and C. Mecklenbrauker, "Performance Evaluation of IEEE 802.11p Infrastructure-to-Vehicle Tunnel Measurements," in *Proceedings of International Wireless Communications and Mobile Computing Conference (IWCMC)*, Istanbul, Turkey, July 2011, pp. 1–5.
- [53] T. Paulin and S. Bessler, "Controlled Probing - A System for Targeted Floating Car Data Collection," in *IEEE Intelligent Transportation Systems (ITSC)*, Oct 2013, pp. 1095–1100.
- [54] NS-3. [Online]. Available: <http://www.nsnam.org/>
- [55] O. Altintas, F. Dressler, F. Hagenauer, M. Matsumoto, M. Sepulcre, and C. Sommer, "Making Cars a Main ICT Resource in Smart Cities," in *Proceedings of First International Workshop on Smart Cities and Urban Informatics*, Hong Kong, China, April 2015.
- [56] M. Pan, P. Li, and Y. Fang, "Cooperative Communication Aware Link Scheduling for Cognitive Vehicular Networks," *IEEE Journal on Selected Areas in Communications*, vol. 30, no. 4, pp. 760–768, May 2012.

- [57] S. Dietzel, J. Petit, F. Kargl, and B. Scheuermann, "In-Network Aggregation for Vehicular Ad Hoc Networks," *IEEE Communications Surveys Tutorials*, vol. 16, no. 4, pp. 1909–1932, Nov. 2014.
- [58] H. Ilhan, M. Uysal, and I. Altunbas, "Cooperative Diversity for Intervehicular Communication: Performance Analysis and Optimization," *IEEE Transactions on Vehicular Technology*, vol. 58, no. 7, pp. 3301–3310, Sept 2009.
- [59] A. El-Keyi, T. ElBatt, F. Bai, and C. Saraydar, "MIMO VANETs: Research Challenges and Opportunities," in *International Conference on Computing, Networking and Communications (ICNC)*, Jan 2012, pp. 670–676.
- [60] A. Paier, L. Bernado, J. Karedal, O. Klemp, and A. Kwoczek, "Overview of Vehicle-to-Vehicle Radio Channel Measurements for Collision Avoidance Applications," in *IEEE 71st Vehicular Technology Conference (VTC 2010-Spring)*, May 2010, pp. 1–5.
- [61] A. Zajic and G. Stuber, "Simulation Models for MIMO Mobile-to-Mobile Channels," in *IEEE Military Communications Conference (MILCOM)*, Oct 2006, pp. 1–7.
- [62] M. Patzold, B. Hogstad, N. Youssef, and D. Kim, "A MIMO Mobile-To-Mobile Channel Model: Part I - The Reference Model," in *IEEE 16th International Symposium on Personal, Indoor and Mobile Radio Communications (PIMRC)*, vol. 1, Sept 2005, pp. 573–578.
- [63] B. Hogstad, M. Patzold, N. Youssef, and D. Kim, "A MIMO Mobile-To-Mobile Channel Model: Part II - The Simulation Model," in *IEEE 16th International Symposium on Personal, Indoor and Mobile Radio Communications (PIMRC)*, vol. 1, Sept 2005, pp. 562–567.
- [64] H. Zhang, D. Yuan, M. Patzold, Y. Wu, and V.-D. Nguyen, "A Novel Wideband Space-Time Channel Simulator Based on the Geometrical One-Ring Model with Applications in MIMO-OFDM Systems," *Wireless Communications and Mobile Computing*, pp. 758–771, 2010.
- [65] B. Talha and M. Patzold, "A Geometrical Three-Ring-Based Model for MIMO Mobile-to-Mobile Fading Channels in Cooperative Networks," *EURASIP J. Adv. Sig. Proc.*, pp. 1–1, 2011.

- [66] A. Alonso, A. Paier, T. Zemen, N. Czink, and F. Tufvesson, "Capacity Evaluation of Measured Vehicle-to-Vehicle Radio Channels at 5.2 GHz," in *IEEE International Conference on Communications Workshops (ICC)*, May 2010, pp. 1–5.
- [67] G. M. T. Abdalla, M. A. Abu-Rgheff, and S.-M. Senouci, "An Adaptive Channel Model for VBLAST in Vehicular Networks," *EURASIP J. Wireless Comm. and Networking*, pp. –1–1, 2009.
- [68] A. Borhani and M. Patzold, "Modeling of Vehicle-to-Vehicle Channels in the Presence of Moving Scatterers," in *IEEE Vehicular Technology Conference (VTC)*, Sept 2012, pp. 1–5.
- [69] M. Barradi, A. S. Hafid, and S. Aljahdali, "Highway Multihop Broadcast Protocols for Vehicular Networks," in *IEEE International Conference on Communications (ICC)*, Jun. 2012, pp. 5296–5300.
- [70] F. Hoque and S. Kwon, "An Emergency Packet Forwarding Scheme for V2V Communication Networks," *The Scientific World Journal*, vol. 2014, pp. 1–7, Jun. 2014.
- [71] Q. Xiang, X. Chen, L. Kong, L. Rao, and X. Liu, "Data preference matters: A new perspective of safety data dissemination in vehicular ad hoc networks," in *IEEE Conference on Computer Communications (INFOCOM)*, Apr. 2015, pp. 1149–1157.
- [72] ETSI TC ITS, "Intelligent Transport Systems (ITS); Vehicular Communications; Basic Set of Applications; Definitions," Tech. Rep. ETSI TR 102 638 V1.1.1, June 2009.
- [73] "Intelligent Transportation System (ITS); Cross Layer DCC Management Entity for Operation in the ITS G5A and ITS G5B Medium; Report on Cross layer DCC Algorithms and Performance Evaluation," European Telecommunications Standards Institute (ETSI), Tech. Rep. ETSI TR 101 612, 2014.
- [74] D. Puthal, Z. Mir, F. Filali, and H. Menouar, "Cross-layer Architecture for Congestion Control in Vehicular Ad-hoc Networks," in *International Conference on Connected Vehicles and Expo (ICCVE)*, Dec 2013, pp. 887–892.

- [75] S. Zemouri, S. Djahel, and J. Murphy, "Smart Adaptation of Beacons Transmission Rate and Power for Enhanced Vehicular Awareness in VANETs," in *IEEE International Conference on Intelligent Transportation Systems (ITSC)*, Oct 2014, pp. 739–746.
- [76] O. Shagdar, "Evaluation of Synchronous and Asynchronous Reactive Distributed Congestion Control Algorithms for the ITS G5 Vehicular Systems," Tech. Rep., 2015. [Online]. Available: <http://arxiv.org/abs/1506.07674>
- [77] M. Sepulcre, J. Mittag, P. Santi, H. Hartenstein, and J. Gozalvez, "Congestion and Awareness Control in Cooperative Vehicular Systems," *Proceedings of the IEEE*, vol. 99, no. 7, pp. 1260–1279, July 2011.
- [78] G. Bansal, K. Rohrs, B. John, and E. Charles, "LIMERIC: A Linear Adaptive Message Rate Algorithm for DSRC Congestion Control," *IEEE Transactions on Vehicular Technology*, vol. 62, no. 9, pp. 4182–4197, Nov. 2013.
- [79] T. Tielert, D. Jiang, Q. Chen, L. Delgrossi, and H. Hartenstein, "Design Methodology and Evaluation of Rate Adaptation Based Congestion Control for Vehicle Safety Communications," in *IEEE Vehicular Networking Conference (VNC)*, 2011, pp. 116 –123.
- [80] P. Shankar, T. Nadeem, J. Rosca, and L. Iftode, "CARS: Context-Aware Rate Selection for Vehicular Networks," in *Proceedings of the IEEE International Conference on Network Protocols (ICNP)*, October 2008.
- [81] E. Egea-Lopez and P. Pavon-Mariño, "Distributed and Fair Beaconing Congestion Control Schemes for Vehicular Networks," *arXiv preprint arXiv:1407.6965*, 2014.
- [82] S. Joerer, B. Bloessl, M. Segata, C. Sommer, R. Lo Cigno, A. Jamalipour, and F. Dressler, "Enabling Situation Awareness at Intersections for IVC Congestion Control Mechanisms," *IEEE Transactions on Mobile Computing*, vol. PP, no. 99, pp. 1–1, 2015.
- [83] M. Torrent-Moreno, J. Mittag, P. Santi, and H. Hartenstein, "Vehicle-to-Vehicle Communication: Fair Transmit Power Control for Safety-Critical Information," *IEEE Transactions on Vehicular Technology*, vol. 58, no. 7, pp. 3684–3703, Sept. 2009.

- [84] J. Mittag, F. Schmidt-Eisenlohr, M. Killat, J. Harri, and H. Hartenstein, "Analysis and Design of Effective and Low-overhead Transmission Power Control for VANETs," in *Proceedings of the Fifth ACM International Workshop on Vehicular Inter-NETworking*, ser. VANET '08, 2008, pp. 39–48.
- [85] G. Caizzone, P. Giacomazzi, L. Musumeci, and G. Verticale, "A Power Control Algorithm With High Channel Availability for Vehicular Ad Hoc Networks," 2005, pp. 3171 – 3176.
- [86] L. Le, R. Baldessari, P. Salvador, A. Festag, and W. Zhang, "Performance Evaluation of Beacon Congestion Control Algorithms for Vanets," in *IEEE Global Telecommunications Conference (GLOBECOM)*, 2011, pp. 1–6.
- [87] Kloiber, B. and Harri, J. and Strang, T. and Sand, S. and Garcia, C.R., "Random Transmit Power Control for DSRC and its Application to Cooperative Safety," *IEEE Transactions on Dependable and Secure Computing*, vol. 13, no. 1, pp. 18–31, Jan 2016.
- [88] A. Alonso Gomez and C. Mecklenbraeuer, "Dependability of Decentralized Congestion Control for Varying VANET Density," *IEEE Transactions on Vehicular Technology*, vol. PP, no. 99, pp. 1–1, 2016.
- [89] C. Math, A. Ozgur, S. de Groot, and H. Li, "Data Rate Based Congestion Control in V2V Communication for Traffic Safety Applications," in *IEEE Symposium on Communications and Vehicular Technology in the Benelux (SCVT)*, Nov 2015, pp. 1–6.
- [90] F. Marzouk, R. Zagrouba, A. Laouiti, and P. Muhlethaler, "An Empirical Study of Unfairness and Oscillation in ETSI DCC," 2015. [Online]. Available: <http://arxiv.org/abs/1510.01125>
- [91] C. Khorakhun, H. Busche, and H. Rohling, "Congestion Control for VANETs Based on Power or Rate Adaptation," in *Proceedings of the 5th International Workshop on Intelligent Transportation (WIT)*, 2008.
- [92] T. Tielert, D. Jiang, H. Hartenstein, and L. Delgrossi, "Joint Power/Rate Congestion Control Optimizing Packet Reception in Vehicle Safety Communications," in *Proceeding of the Tenth ACM International Workshop on Vehicular Inter-networking, Systems, and Applications*, ser. VANET '13, 2013, pp. 51–60.

- [93] R. K. Schmidt, B. Kloiber, F. Schuttler, and T. Strang, "Degradation of Communication Range in VANETs Caused by Interference 2.0 - Real-world Experiment," in *Proceedings of the International Conference on Communication Technologies for Vehicles*, 2011, pp. 176–188.
- [94] A. Kovacs and G. Efkou, "Resource Sharing Principles for Vehicular Communications," in *IEEE Global Telecommunications Conference (GLOBECOM)*, Dec. 2008, pp. 1–10.
- [95] J. Gozalvez and M. Sepulcre, "Channel Efficiency of Adaptive Transmission Techniques for Wireless Vehicular Communications," in *Proceedings of the International World Congress on ITS*, 2008.
- [96] B. Kloiber, J. Harri, and T. Strang, "Dice the TX Power – Improving Awareness Quality in VANETs by Random Transmit Power Selection," in *Vehicular Networking Conference (VNC), 2012 IEEE*, Nov 2012, pp. 56–63.
- [97] C.-L. Huang, Y. Fallah, R. Sengupta, and H. Krishnan, "Adaptive Intervehicle Communication Control for Cooperative Safety Systems," *IEEE Network*, vol. 24, no. 1, pp. 6–13, Jan 2010.
- [98] M. Sepulcre, J. Gozalvez, O. Altintas, and H. Kremo, "Integration of Congestion and Awareness Control in Vehicular Networks," *Ad Hoc Networks*, vol. 37, no. 1, pp. 29 – 43, Feb. 2016.
- [99] M. Frigau, "Fair Decentralized Congestion and Awareness Control for Vehicular Networks," in *IEEE 21st International Conference on Parallel and Distributed Systems (ICPADS)*, Dec 2015, pp. 172–180.
- [100] N. Nasiriani, Y. Fallah, and H. Krishnan, "Stability Analysis of Congestion Control Schemes in Vehicular Ad Hoc Networks," in *IEEE Consumer Communications and Networking Conference (CCNC)*, Jan 2013, pp. 358–363.
- [101] J. Jose, C. Li, X. Wu, L. Ying, and K. Zhu, "Distributed Rate and Power Control in DSRC," in *Information Theory (ISIT), 2015 IEEE International Symposium on*, June 2015, pp. 2822–2826.
- [102] S. Zemouri, S. Djahel, and J. Murphy, "Smart Adaptation of Beacons Transmission Rate and Power for Enhanced Vehicular Awareness in VANETs," in *Intelligent Transportation Systems (ITSC), 2014 IEEE 17th International Conference on*, Oct 2014, pp. 739–746.

- [103] R. A. Saeed and S. J. Shellhammer, *TV White Space Spectrum Technologies: Regulations, Standards, and Applications*, 1st ed. Boca Raton, FL, USA: CRC Press, Inc., 2011.
- [104] K. D. Singh, P. Rawat, and J.-M. Bonnin, "Cognitive Radio for Vehicular Ad Hoc Networks (CR-VANETs): Approaches and Challenges," *EURASIP J. Wireless Comm. and Networking*, pp. 1–22, 2014.
- [105] N. Lu, N. Cheng, N. Zhang, X. Shen, and J. Mark, "Connected Vehicles: Solutions and Challenges," *IEEE Internet of Things Journal*, vol. 1, no. 4, pp. 289–299, Aug 2014.
- [106] N. Meghanathan and Y. B. Reddy, *Cognitive Radio Technology Applications for Wireless and Mobile Ad Hoc Networks*. IGI Global, 2013.
- [107] M. Di Felice, R. Doost-Mohammady, K. Chowdhury, and L. Bononi, "Smart Radios for Smart Vehicles: Cognitive Vehicular Networks," *IEEE Vehicular Technology Magazine*, vol. 7, no. 2, pp. 26–33, June 2012.
- [108] S. Chen, R. Vuyyuru, O. Altintas, and A. M. Wyglinski, "Learning in Vehicular Dynamic Spectrum Access Networks: Opportunities and Challenges," in *International Symposium on Intelligent Signal Processing and Communications Systems*, Dec 2011, pp. 1–6.
- [109] R. Abeywardana, K. Sowerby, and S. Berber, "Spectrum Sensing in Cognitive Radio Enabled Vehicular Ad Hoc Networks: A Review," in *7th International Conference on Information and Automation for Sustainability*, Dec 2014, pp. 1–6.
- [110] A. S. Cacciapuoti, M. Caleffi, and L. Paura, "Optimal Strategy Design for Enabling the Co-existence of Heterogeneous Networks in TV White Space," *IEEE Transactions on Vehicular Technology*, vol. PP, no. 99, pp. 1–1, 2015.
- [111] S. Pagadarai, B. A. Lessard, A. M. Wyglinski, R. Vuyyuru, and O. Altintas, "Vehicular Communication: Enhanced Networking Through Dynamic Spectrum Access," *IEEE Vehicular Technology Magazine*, vol. 8, no. 3, pp. 93–103, Sept 2013.
- [112] A. J. Ghandour, K. Fawaz, H. Artail, M. Di Felice, and L. Bononi, "Improving Vehicular Safety Message Delivery Through the Implementation of a Cognitive Vehicular Network," *Ad Hoc Networks*, vol. 11, no. 8, pp. 2408–2422, Nov. 2013.

- [113] N. Cheng and X. S. Shen, *Opportunistic Spectrum Utilization in Vehicular Communication Networks*, 1st ed. New York, NY: Springer, 2015.
- [114] S. Chen and A. M. Wyglinski, "Cognitive Radio-Enabled Distributed Cross-Layer Optimization via Genetic Algorithms," in *4th International Conference on Cognitive Radio Oriented Wireless Networks and Communications*, June 2009, pp. 1–6.
- [115] S. Chen, T. Newman, J. Evans, and A. M. Wyglinski, "Genetic Algorithm-Based Optimization for Cognitive Radio Networks," in *IEEE Sarnoff Symposium*, April 2010, pp. 1–6.
- [116] F. Riaz, S. Ahmed, I. Shafi, M. Imran, N. Ratyal, and M. Sajid, "White Space Optimization Using Memory Enabled Genetic Algorithm in Vehicular Cognitive Radio," in *IEEE 11th International Conference on Cybernetic Intelligent Systems*, Aug 2012, pp. 133–140.
- [117] I. AlQerm and B. Shihada, "Adaptive Multi-Objective Optimization Scheme for Cognitive Radio Resource Management," in *IEEE Global Communications Conference*, Dec 2014, pp. 857–863.
- [118] S. Chen, R. Vuyyuru, O. Altintas, and A. M. Wyglinski, "On Optimizing Vehicular Dynamic Spectrum Access Networks: Automation and Learning in Mobile Wireless Environments," in *IEEE Vehicular Networking Conference (VNC)*, Nov 2011, pp. 39–46.
- [119] S. Chen, A. M. Wyglinski, R. Vuyyuru, and O. Altintas, "Feasibility Analysis of Vehicular Dynamic Spectrum Access via Queueing Theory Model," in *IEEE Vehicular Networking Conference (VNC)*, Dec 2010, pp. 223–230.
- [120] S. Chen, A. M. Wyglinski, S. Pagadarai, R. Vuyyuru, and O. Altintas, "Feasibility Analysis of Vehicular Dynamic Spectrum Access via Queueing Theory Model," *IEEE Communications Magazine*, vol. 49, no. 11, pp. 156–163, November 2011.
- [121] Elif Bozkaya and Berk Canberk, "Robust and Continuous Connectivity Maintenance for Vehicular Dynamic Spectrum Access Networks," *Ad Hoc Networks*, vol. 25, Part A, no. 0, pp. 72 – 83, 2015.

- [122] N. Cheng, N. Zhang, N. Lu, X. Shen, J. Mark, and F. Liu, "Opportunistic Spectrum Access for CR-VANETs: A Game-Theoretic Approach," *IEEE Transactions on Vehicular Technology*, vol. 63, no. 1, pp. 237–251, Jan 2014.
- [123] T. Wang, L. Song, and Z. Han, "Coalitional Graph Games for Popular Content Distribution in Cognitive Radio VANETs," *IEEE Transactions on Vehicular Technology*, vol. 62, no. 8, pp. 4010–4019, Oct 2013.
- [124] A. Min, X. Zhang, J. Choi, and K. Shin, "Exploiting Spectrum Heterogeneity in Dynamic Spectrum Market," *IEEE Transactions on Mobile Computing*, vol. 11, no. 12, pp. 2020–2032, Dec 2012.
- [125] T. Wang, L. Song, and Z. Han, "Coalitional Graph Games for Popular Content Distribution in Cognitive Radio VANETs," *IEEE Transactions on Vehicular Technology*, vol. 62, no. 8, pp. 4010–4019, Oct 2013.
- [126] H. Kremo, O. Altintas, H. Tanaka, M. Kitamura, K. Inage, and T. Fujii, "Cooperative Spectrum Sensing in the Vehicular Environment: An Experimental Evaluation," in *IEEE 79th Vehicular Technology Conference*, May 2014, pp. 1–5.
- [127] T. Zhang, N. Leng, and S. Banerjee, "A Vehicle-based Measurement Framework for Enhancing Whitespace Spectrum Databases," in *Proceedings of the 20th Annual International Conference on Mobile Computing and Networking*, ser. MobiCom '14, 2014, pp. 17–28.
- [128] R. Schiphorst and C. H. Slump, "Evaluation of Spectrum Occupancy in Amsterdam Using Mobile Monitoring Vehicles," in *IEEE 71st Vehicular Technology Conference*, May 2010, pp. 1–5.
- [129] O. Altintas, Y. Ihara, H. Kremo, H. Tanaka, M. Ohtake, T. Fujii, C. Yoshimura, K. Ando, K. Tsukamoto, M. Tsuru, and Y. Oie, "Field Tests and Indoor Emulation of Distributed Autonomous Multi-hop Vehicle-to-vehicle Communications over TV White Space," in *Proceedings of the 18th Annual International Conference on Mobile Computing and Networking*, ser. Mobicom '12, 2012, pp. 439–442.

- [130] K. Tsukamoto, Y. Oie, H. Kremo, O. Altintas, H. Tanaka, and T. Fujii, "Implementation and Performance Evaluation of Distributed Autonomous Multi-Hop Vehicle-to-Vehicle Communications over TV White Space," *Mobile Network Applications*, vol. 20, no. 2, pp. 203–219, Apr 2015.
- [131] Y. Ihara, H. Kremo, O. Altintas, H. Tanaka, M. Ohtake, T. Fujii, C. Yoshimura, K. Ando, K. Tsukamoto, M. Tsuru, and Y. Oie, "Distributed Autonomous Multi-Hop Vehicle-to-Vehicle Communications over TV White Space," in *IEEE Consumer Communications and Networking Conference (CCNC)*, Jan. 2013, pp. 336–344.
- [132] T. Rzayev, Y. Shi, A. Vafeiadis, S. Pagadarai, and A. M. Wyglinski, "Implementation of a Vehicular Networking Architecture Supporting Dynamic Spectrum Access," in *IEEE Vehicular Networking Conference*, Nov 2011, pp. 33–38.
- [133] G. Marfia, M. Roccetti, A. Amoroso, M. Gerla, G. Pau, and J. Lim, "Cognitive Cars: Constructing A Cognitive Playground for VANET Research Testbeds," in *International Conference on Cognitive Radio and Advanced Spectrum Management*, pages = 29, year = 2011,.
- [134] T. Pham, I. McLoughlin, and S. Fahmy, "Shaping Spectral Leakage for IEEE 802.11p Vehicular Communications," in *IEEE 79th Vehicular Technology Conference (VTC)*, May 2014, pp. 1–5.
- [135] F. Riaz, I. Shafi, S. Hasan, W. Younas, and Y. Mehmood, "Vehicle-to-vehicle Communication Enhanced by Cognitive Approach and Multi-radio Technologies," in *International Conference on Emerging Technologies*, Oct 2012, pp. 1–6.
- [136] D. Rawat, Y. Zhao, G. Yan, and M. Song, "CRAVE: Cognitive Radio Enabled Vehicular Communications in Heterogeneous Networks," in *IEEE Radio and Wireless Symposium*, Jan 2013, pp. 190–192.
- [137] D. Pu, "Primary User Emulation Detection in Cognitive Radio Networks," Worcester Polytechnic Institute, Worcester, Massachusetts, USA, Tech. Rep., 2013.
- [138] J. Ma, G. Li, and B. H. Juang, "Signal Processing in Cognitive Radio," *Proceedings of the IEEE*, vol. 97, no. 5, pp. 805–823, May 2009.

- [139] J. Chen, B. Liu, H. Zhou, L. Gui, N. Liu, and Y. Wu, "Providing Vehicular Infotainment Service Using VHF/UHF TV Bands via Spatial Spectrum Reuse," *IEEE Transactions on Broadcasting*, vol. 61, no. 2, pp. 279–289, June 2015.
- [140] I. Souid, H. Ben Chikha, and R. Attia, "Blind Spectrum Sensing in Cognitive Vehicular Ad Hoc Networks over Nakagami-m Fading Channels," in *International Conference on Electrical Sciences and Technologies in Maghreb*, Nov 2014, pp. 1–5.
- [141] F. F. Digham, M. S. Alouini, and M. K. Simon, "On the Energy Detection of Unknown Signals Over Fading Channels," *IEEE Transactions on Communications*, vol. 55, no. 1, pp. 21–24, Jan 2007.
- [142] X. Qian and L. Hao, "Spectrum Sensing with Energy Detection in Cognitive Vehicular Ad hoc Networks," in *IEEE 6th International Symposium on Wireless Vehicular Communications*, Sept 2014, pp. 1–5.
- [143] D. Rawat and S. Shetty, "Enhancing Connectivity for Spectrum-Agile Vehicular Ad hoc NETWORKS in Fading Channels," in *IEEE Intelligent Vehicles Symposium Proceedings*, June 2014, pp. 957–962.
- [144] A. Paul, A. Daniel, A. Ahmad, and S. Rho, "Cooperative Cognitive Intelligence for Internet of Vehicles," *IEEE Systems Journal*, vol. PP, no. 99, pp. 1–10, April 2015.
- [145] H. Rasheed and N. Rajatheva, "Spectrum Sensing for Cognitive Vehicular Networks over Composite Fading," *International Journal of Vehicular Technology*, pp. 1–9, 2011.
- [146] H. Li, "Impact of Primary User Interruptions on Data Traffic in Cognitive Radio Networks: Phantom Jam on Highway," in *IEEE Global Telecommunications Conference*, Dec 2011, pp. 1–5.
- [147] A. Bhowmick, S. D. Roy, and S. Kundu, "Cooperative Spectrum Sensing in Multiple Antenna Based Cognitive Radio Network Using an Improved Energy Detector," *IEEE Communications Letters*, vol. 16, no. 1, pp. 64–67, January 2012.

- [148] X. Xu, A. Huang, J. Zhang, and L. Gu, "Cooperative Wideband Spectrum Detection Based on Maximum Likelihood Ratio for Cognitive VANET," in *International Conference on Automatic Control and Artificial Intelligence (ACAI 2012)*, March 2012, pp. 726–729.
- [149] T. Wang, L. Song, and Z. Han, "Collaborative Data Dissemination in Cognitive VANETs with Sensing-Throughput Tradeoff," in *IEEE International Conference on Communications in China (ICCC)*, Aug 2012, pp. 41–45.
- [150] S. Busanelli, M. Martalo, and G. Ferrari, "Clustered Vehicular Networks: Decentralized Detection on the Move," in *11th International Conference on ITS Telecommunications (ITST)*, Aug 2011, pp. 744–749.
- [151] G. Ministeri and L. Vangelista, "On the Performance of Channel Occupancy Detectors for Vehicular Ad-Hoc Networks," in *5th International Congress on Ultra Modern Telecommunications and Control Systems and Workshops (ICUMT)*, Sept 2013, pp. 1–6.
- [152] H. Kremo and O. Altintas, "On Detecting Spectrum Opportunities for Cognitive Vehicular Networks in the TV White Space," *Journal of Signal Processing Systems*, vol. 73, no. 3, pp. 243–254, 2013.
- [153] S. Cheng, G. Horng, and C. Chou, "Adaptive Vehicle to Vehicle Heterogeneous Transmission in Cooperative Cognitive Networks VANETs," *International Journal of Innovative Computing, Information and Control*, vol. 8, no. 2, pp. 1263–1274, 2012.
- [154] J. Kim and M. Krunz, "Spectrum-aware Beaconless Geographical Routing Protocol for Cognitive Radio Enabled Vehicular Networks," *Mob. Netw. Appl.*, vol. 18, no. 6, pp. 854–866, Dec. 2013.
- [155] D. Borota, G. Ivkovic, R. Vuyyuru, O. Altintas, I. Seskar, and P. Spasojevic, "On the Delay to Reliably Detect Channel Availability in Cooperative Vehicular Environments," in *IEEE 73rd Vehicular Technology Conference (VTC Spring)*, May 2011, pp. 1–5.
- [156] K. Letaief and W. Zhang, "Cooperative Communications for Cognitive Radio Networks," *Proceedings of the IEEE*, vol. 97, no. 5, pp. 878–893, May 2009.

- [157] M. Di Felice, K. Chowdhury, and L. Bononi, "Analyzing the Potential of Cooperative Cognitive Radio Technology on Inter-Vehicle Communication," in *Wireless Days (WD)*, Oct 2010, pp. 1–6.
- [158] D. Pu, B. Aygun, and A. M. Wyglinski, "Primary User Emulation Detection Algorithm Based on Distributed Sensor Networks," *International Journal of Wireless Information Networks (Submitted)*, 2014.
- [159] Z. Jin, J. P. Morgan, S. Anand, and K. P. Subbalakshmi, "NEAT: A NEighbor AssisTed spectrum decision protocol for resilience against PUEA," in *IEEE Conference on Communications and Network Security (CNS)*, Oct 2014, pp. 44–52.
- [160] H. Li and D. Irick, "Collaborative Spectrum Sensing in Cognitive Radio Vehicular Ad Hoc Networks: Belief Propagation on Highway," in *IEEE 71st Vehicular Technology Conference (VTC)*, May 2010, pp. 1–5.
- [161] M. D. Felice, K. R. Chowdhury, and L. Bononi, "Cooperative Spectrum Management in Cognitive Vehicular Ad Hoc Networks," in *IEEE Vehicular Networking Conference (VNC)*, Nov 2011, pp. 47–54.
- [162] D. Bharadia, E. McMillin, and S. Katti, "Full Duplex Radios," *Computer Communication Review*, vol. 43, no. 4, pp. 375–386, Oct 2013.
- [163] C. Campolo, A. Molinaro, and R. Scopign, *Vehicular Ad Hoc Networks: Standards, Solutions, and Research (1st edn)*. Springer, 2015.
- [164] M. Duarte, C. Dick, and A. Sabharwal, "Experiment-Driven Characterization of Full-Duplex Wireless Systems," *IEEE Transactions on Wireless Communications*, vol. 11, no. 12, pp. 4296–4307, Dec 2012.
- [165] E. Ahmed and A. Eltawil, "All-Digital Self-Interference Cancellation Technique for Full-Duplex Systems," *IEEE Transactions on Wireless Communications*, vol. 14, no. 7, pp. 3519–3532, July 2015.

- [166] A. Thangaraj, R. Ganti, and S. Bhashyam, "Self-interference Cancellation Models for Full-Duplex Wireless Communications," in *International Conference on Signal Processing and Communications (SPCOM)*, July 2012, pp. 1–5.
- [167] D. Korpi, L. Anttila, and M. Valkama, "Reference Receiver Based Digital Self-Interference Cancellation in MIMO Full-Duplex Transceivers," in *Globecom Workshops (GC Wkshps)*, Dec 2014, pp. 1001–1007.
- [168] A. Masmoudi and T. Le-Ngoc, "Self-Interference Cancellation for Full-Duplex MIMO Transceivers," in *IEEE Wireless Communications and Networking Conference (WCNC)*, March 2015, pp. 141–146.
- [169] T. Cover and A. Gamal, "Capacity Theorems for the Relay Channel," *IEEE Transactions on Information Theory*, vol. 25, no. 5, pp. 572–584, Sep 1979.
- [170] B. Sklar, "Rayleigh Fading Channels in Mobile Digital Communication Systems. I. Characterization," *IEEE Communications Magazine*, vol. 35, no. 9, pp. 136–146, Sep 1997.
- [171] T. S. Rappaport, *Wireless Communications: Principles and Practice*. Prentice Hall, 1996.
- [172] M. Boban, T. T. V. Vinhoza, M. Ferreira, J. Barros, and O. K. Tonguz, "Impact of Vehicles as Obstacles in Vehicular Ad Hoc Networks," *IEEE Journal on Selected Areas in Communications*, vol. 29, no. 1, pp. 15–28, January 2011.
- [173] J. Goldhirsh and W. J. Vogel, "Handbook of Propagation Effects for Vehicular and Personal Mobile Satellite Systems – Overview of Experimental and Modeling Results," The Johns Hopkins University, Tech. Rep. A2A-98-U-0-021 (APL), EERL-98-12A (EERL), December 1998.
- [174] B. Aygun and A. Soysal, "Capacity Bounds on MIMO Relay Channel With Covariance Feedback at the Transmitters," *IEEE T. Vehicular Technology*, pp. 2042–2051, 2013.
- [175] J. G. Proakis, *Digital Communications (5th Ed.)*. McGraw-Hill, 2007.
- [176] S. Cheng, G. Horng, and C. Chou, "Adaptive Vehicle to Vehicle Heterogeneous Transmission

- in Cooperative Cognitive Networks VANETs,” *International Journal of Innovative Computing, Information and Control (ICIC)*, vol. 8, no. 2, pp. 1263–1274, Feb 2012.
- [177] B. Wang, J. Zhang, and A. Host-Madsen, “On the Capacity of MIMO Relay Channels,” *IEEE Transactions on Information Theory*, vol. 51, no. 1, pp. 29–43, Jan 2005.
- [178] “A Comparison of Routing Strategies for Vehicular Ad-Hoc Networks,” Department of Computer Science, University of Mannheim, Tech. Rep. Technical Report TR-02-003, 2002.
- [179] H. Fussler, J. Widmer, M. Kasemann, M. Mauve, and H. Hartenstein, “Contention-Based Forwarding for Mobile Ad Hoc Networks,” *Ad Hoc Networks*, vol. 1, no. 4, pp. 351 – 369, 2003.
- [180] R. Patil, A. Damodaram, and R. Das, in *Fifth IEEE Conference on Wireless Communication and Sensor Networks (WCSN)*.
- [181] L. Kleinrock, *Queueing Systems: Volume 2: Computer Applications*. New York: John Wiley & Sons, 1976.
- [182] S. Chen, A. M. Wyglinski, S. Pagadarai, R. Vuyyuru, and O. Altintas, “Feasibility analysis of vehicular dynamic spectrum access via queueing theory model,” *IEEE Communications Magazine*, vol. 49, no. 11, pp. 156–163, Nov. 2011.
- [183] P.-N. Tan, M. Steinbach, and V. Kumar, *Introduction to Data Mining, (First Edition)*. Boston, MA, USA: Addison–Wesley Longman Publishing, 2005.
- [184] J. MacQueen, “Some Methods for Classification and Analysis of Multivariate Observations,” in *Proceedings of the Fifth Berkeley Symposium on Mathematical Statistics and Probability, Volume 1: Statistics*. University of California Press, 1967, pp. 281–297.
- [185] M. Ester, H.-P. Kriegel, J. Sander, and X. Xu, “A Density-Based Algorithm for Discovering Clusters in Large Spatial Databases with Noise,” in *Proc. of 2nd International Conference on Knowledge Discovery and Data Mining*, 1996, pp. 226–231.
- [186] S. C. Johnson, “Hierarchical Clustering Schemes,” *Psychometrika*, vol. 32, no. 3, pp. 241–254, 1967.

- [187] M. Barradi, A. S. Hafid, and J. R. Gallardo, "Establishing strict priorities in IEEE 802.11p WAVE vehicular networks," in *IEEE Global Telecommunications Conference (GLOBECOM)*, Dec. 2010, pp. 1–6.
- [188] S. Salvador and P. Chan, "Determining the number of clusters/segments in hierarchical clustering/segmentation algorithms," in *16th IEEE International Conference on Tools with Artificial Intelligence*, Nov. 2004, pp. 576–584.
- [189] W. Zhang, X. Li, S. Saxena, A. Strojwas, and R. Rutenbar, "Automatic clustering of wafer spatial signatures," in *Proceedings of the 50th Annual Design Automation Conference*, 2013, pp. 1–6.
- [190] M. Haklay and P. Weber, "Openstreetmap: User-generated street maps," *IEEE Pervasive Computing*, vol. 7, no. 4, pp. 12–18, Oct. 2008.
- [191] M. Behrisch, L. Bieker, J. Erdmann, and D. Krajzewicz, "SUMO — simulation of urban mobility: An overview," in *The Third International Conference on Advances in System Simulation (SIMUL)*, 2011, pp. 63–68.
- [192] A. Molisch, *Wireless Communications (2nd ed)*. Wiley, 2011.
- [193] P. Karadimas and D. Matolak, "Generic Stochastic Modeling of Vehicle-to-Vehicle Wireless Channels," *Vehicular Communications*, vol. 1, no. 4, pp. 153 – 167, 2014.
- [194] ETSI, "Intelligent Transport Systems (ITS); Cross Layer DCC Management Entity for Operation in the ITS G5A and ITS G5B Medium; Validation Set-up and Results," European Telecommunications Standards Institute, ETSI TR 101 613, 2015. [Online]. Available: https://www.etsi.org/deliver/etsi_tr/101600_101699/101613/01.01.01_60/tr_101613v010101p.pdf
- [195] W. Viriyasitavat, M. Boban, H.-M. Tsai, and A. Vasilakos, "Vehicular Communications: Survey and Challenges of Channel and Propagation Models," *IEEE Vehicular Technology Magazine*, vol. 10, no. 2, pp. 55–66, June 2015.
- [196] J. K. Taimoor Abbas, Katrin Sjoberg and F. Tufvesson, "A Measurement Based Shadow Fading Model for Vehicle-to-Vehicle Network Simulations," *International Journal of Antennas and Propagation*, pp. 1 – 12, 2015.

- [197] C. Sommer, S. Joerer, M. Segata, O. Tonguz, R. Cigno, and F. Dressler, "How Shadowing Hurts Vehicular Communications and How Dynamic Beaconing Can Help," in *Proceedings of IEEE INFOCOM*, April 2013, pp. 110–114.
- [198] "Intelligent Transportation System (ITS); Vehicular Communications; Basic Set of Applications; Part 1: Functional Requirements," Tech. Rep. ETSI TS 102 637-1, 2010.
- [199] X. Wang, E. Anderson, P. Steenkiste, and F. Bai, "Simulating Spatial Cross-Correlation in Vehicular Networks," in *IEEE Vehicular Networking Conference (VNC 2014)*. IEEE, December 2014, pp. 213–220.
- [200] Simulation of Urban MObility (SUMO). [Online]. Available: http://www.dlr.de/ts/en/desktopdefault.aspx/tabid-9883/16931_read-41000/
- [201] Open Street Map. [Online]. Available: <http://www.openstreetmap.org/#map=5/51.500/-0.100>
- [202] O. K. Tonguz, W. Viriyasitavat, and F. Bai, "Modeling Urban Traffic: A Cellular Automata Approach," *IEEE Communications Magazine*, vol. 47, no. 5, pp. 142–150, 2009.
- [203] S. Choi, J. del Prado, N. Sai Shankar, and S. Mangold, "IEEE 802.11 e Contention-based Channel Access (EDCF) Performance Evaluation," in *IEEE International Conference on Communications (ICC)*, vol. 2, May 2003, pp. 1151–1156.
- [204] S. M. Kay, *Fundamentals of Statistical Signal Processing: Detection theory*. Prentice-Hall PTR, 1998.
- [205] W. Chen, *Vehicular Communications and Networks: Architectures, Protocols, Operation and Deployment*. Woodhead, 2015.
- [206] S. Li, Z. Zheng, E. Ekici, and N. Shroff, "Maximizing System Throughput by Cooperative Sensing in Cognitive Radio Networks," in *Proceedings IEEE INFOCOM*, March 2012, pp. 1575–1583.

- [207] J. Misić and V. Misić, "Probability Distribution of Spectral Hole Duration in Cognitive Networks," in *IEEE International Conference on Computer Communications (INFOCOM)*, April 2014, pp. 2103–2111.
- [208] Q. Song and W. Hamouda, "Performance Analysis and Optimization of Multiselective Scheme for Cooperative Sensing in Fading Channels," *IEEE Transactions on Vehicular Technology*, vol. 65, no. 1, pp. 358–366, Jan 2016.
- [209] R. L. Burden and J. D. Faires, *Numerical Analysis: 4th Ed.* Boston, MA, USA: PWS Publishing Co., 1989.
- [210] T. M. Cover and J. A. Thomas, *Elements of Information Theory.* Wiley-Interscience, 2006.
- [211] P. Nakov, A. Popova, and P. Mateev, "Weight Functions Impact on LSA Performance," in *EuroConference Recent Advances in NLP (RANLP)*, 2001, pp. 187–193.
- [212] V. Anisimov and B. Sotskii, "Estimate of the Entropy of Radiation by Means of Weight Functions," *Theoretical and Mathematical Physics*, vol. 29, no. 1, pp. 971–973, 1976.
- [213] L.-C. Hsu, "A Hybrid Multiple Criteria Decision-Making Model for Investment Decision Making," *Journal of Business Economics and Management*, vol. 15, no. 3, pp. 509–529, 2014.
- [214] J. Harte, *Maximum Entropy and Ecology A Theory of Abundance, Distribution, and Energetics.*
- [215] Y. Ge, Y. Sun, S. Lu, and E. Dutkiewicz, "ADSD: An Automatic Distributed Spectrum Decision method in Cognitive Radio Networks," in *International Conference on Future Information Networks*, Oct 2009, pp. 253–258.
- [216] G. Patounas, Y. Zhang, and S. Gjessing, "Evaluating Defence Schemes Against Jamming in Vehicle Platoon Networks," in *IEEE International Conference on Intelligent Transportation Systems*, Sept 2015, pp. 2153–2158.
- [217] S. Zemouri, S. Djahel, and J. Murphy, "A Short-Term Vehicular Density Prediction Scheme for Enhanced Beaconing Control," in *IEEE Global Communications Conference (GLOBECOM)*, Dec 2015, pp. 1–7.

- [218] M. Ferreira, R. Fernandes, H. Conceição, W. Viriyasitavat, and O. K. Tonguz, “Self-organized Traffic Control,” in *Proceedings of the Seventh ACM International Workshop on Vehicular Internetworking*, 2010, pp. 85–90.
- [219] E. Bonabeau, M. Dorigo, and G. Theraulaz, *Swarm Intelligence: From Natural to Artificial Systems*. New York, NY, USA: Oxford University Press, Inc., 1999.
- [220] D. Karaboga, “An Idea Based On Honey Bee Swarm For Numerical Optimization,” Erciyes University, Kayseri, Turkey, Tech. Rep., 2005.
- [221] M. R. Jabbarpour, A. Jalooli, E. Shaghaghi, R. M. Noor, L. Rothkrantz, R. H. Khokhar, and N. B. Anuar, “Ant-based Vehicle Congestion Avoidance System Using Vehicular Networks,” *Engineering Applications of Artificial Intelligence*, vol. 36, no. 11, pp. 303–319, 2014.
- [222] R. Poli, J. Kennedy, and T. Blackwell, “Particle Swarm Optimization,” *Swarm Intelligence*, vol. 1, no. 1, pp. 33–57, 2007.
- [223] H. Hakoyamai, “The Ideal Free Distribution When the Resource Is Variable,” *Behavioral Ecology*, vol. 14, no. 1, pp. 109–115, 2003.
- [224] D. Stephens and J. Krebs, *Foraging Theory*, 1st ed. Princeton, NJ, USA: Princeton University Press, 1987.
- [225] R. J. Gegear, J. S. Manson, and J. D. Thomson, “Ecological context influences pollinator deterrence by alkaloids in floral nectar,” *Ecology Letters*, vol. 10, no. 5, pp. 375–382, 2007.
- [226] R. Gegear and T. Laverty, *The effect of variation among floral traits on the flower constancy of pollinators (Chapter 1)*. In *Cognitive Ecology of Pollination: Animal Behavior and Floral Evolution*. Cambridge, UK: Cambridge University Press, 2001.
- [227] D. Goulson, S. A. Hawson, and J. C. Stout, “Foraging bumblebees avoid flowers already visited by conspecifics or by other bumblebee species,” *Animal Behaviour*, vol. 55, no. 1, pp. 199–206, Jan. 1998.

- [228] Y. Hei, W. Li, W. Fu, and X. Li, "Efficient Parallel Artificial Bee Colony Algorithm for Cooperative Spectrum Sensing Optimization," *Circuits, Systems, and Signal Processing*, vol. 34, no. 11, pp. 3611–3629, 2015.